

Institut für Erd- und Umweltwissenschaften  
Lehrstuhl für Hydrologie und Klimatologie

---

**Analyzing and Modelling of Flow Transmission Processes in River-Systems  
with a Focus on Semi-Arid Conditions**

**Dissertation**  
zur Erlangung des akademischen Grades  
"doctor rerum naturalium"  
(Dr. rer. nat.)  
in der Wissenschaftsdisziplin Hydrologie

eingereicht an der  
**Mathematisch-Naturwissenschaftlichen Fakultät**  
der Universität Potsdam

von  
**Alexandre Cunha Costa**

**Potsdam, im Januar 2012**

Published online at the  
Institutional Repository of the University of Potsdam:  
URL <http://opus.kobv.de/ubp/volltexte/2012/5969/>  
URN <urn:nbn:de:kobv:517-opus-59694>  
<http://nbn-resolving.de/urn:nbn:de:kobv:517-opus-59694>

## Contents

Abstract .....	II
Zusammenfassung .....	IV
<b>Chapter I: Introduction .....</b>	<b>1</b>
1. Background and Overview .....	2
2. Objectives .....	4
3. Outline of the Thesis .....	4
<b>Chapter II Analysis of channel transmission losses in a dryland river reach in northeastern Brazil using streamflow series, groundwater level series and multi-temporal satellite data.....</b>	<b>6</b>
1. Introduction .....	7
2. Study Area .....	9
3. Hydrological Data .....	10
4. Results .....	13
5. Discussion and Conclusion .....	25
6. Acknowledgements .....	28
<b>Chapter III: A channel transmission losses model for different dryland rivers .....</b>	<b>29</b>
1. Introduction .....	30
2. Modelling of Channel Transmission Losses .....	32
3. Case Studies of the Channel Transmission Losses Model .....	41
4. Model Reliability .....	48
5. Discussion .....	63
6. Conclusions and Outlook .....	64
7. Acknowledgements .....	65
<b>Chapter IV: Probabilistic flood forecasting for a mountainous headwater catchment using a nonparametric stochastic dynamic approach.....</b>	<b>66</b>
1. Introduction .....	67
2. Nonparametric Modelling .....	68
3. Parametric Modelling .....	71
4. An Example for Probabilistic Flood Prediction .....	71
5. Discussion and Conclusions .....	82
6. Further Work .....	83
7. Acknowledgements .....	83
<b>Chapter V: Discussion and Conclusion.....</b>	<b>84</b>
1. Perceptual Model of Channel Transmission Losses .....	85
2. Modelling of Channel Transmission Losses .....	85
3. Optimized Forecasting of Streamflow .....	86
4. A Benchmark for Hydrological Research using Semi-Distributed Modelling .....	87
5. Conclusion.....	90
References .....	92
Acknowledgements .....	100

## Abstract

One of the major problems for the implementation of water resources planning and management in arid and semi-arid environments is the scarcity of hydrological data and, consequently, research studies. In this thesis, the hydrology of dryland river systems was analyzed and a semi-distributed hydrological model and a forecasting approach were developed for flow transmission processes in river-systems with a focus on semi-arid conditions.

Three different sources of hydrological data (streamflow series, groundwater level series and multi-temporal satellite data) were combined in order to analyze the channel transmission losses of a large reach of the Jaguaribe River in NE Brazil. A perceptual model of this reach was derived suggesting that the application of models, which were developed for sub-humid and temperate regions, may be more suitable for this reach than classical models, which were developed for arid and semi-arid regions. Summarily, it was shown that this river reach is hydraulically connected with groundwater and shifts from being a losing river at the dry and beginning of rainy seasons to become a losing/gaining (mostly losing) river at the middle and end of rainy seasons.

A new semi-distributed channel transmission losses model was developed, which was based primarily on the capability of simulation in very different dryland environments and flexible model structures for testing hypotheses on the dominant hydrological processes of rivers. This model was successfully tested in a large reach of the Jaguaribe River in NE Brazil and a small stream in the Walnut Gulch Experimental Watershed in the SW USA. Hypotheses on the dominant processes of the channel transmission losses (different model structures) in the Jaguaribe river were evaluated, showing that both lateral (stream-)aquifer water fluxes and groundwater flow in the underlying alluvium parallel to the river course are necessary to predict streamflow and channel transmis-

sion losses, the former process being more relevant than the latter. This procedure not only reduced model structure uncertainties, but also reported modelling *failures* rejecting model structure hypotheses, namely streamflow without river-aquifer interaction and stream-aquifer flow without groundwater flow parallel to the river course. The application of the model to different dryland environments enabled learning about the model itself from differences in channel reach responses. For example, the parameters related to the unsaturated part of the model, which were active for the small reach in the USA, presented a much greater variation in the sensitivity coefficients than those which drove the saturated part of the model, which were active for the large reach in Brazil.

Moreover, a nonparametric approach, which dealt with both deterministic evolution and inherent fluctuations in river discharge data, was developed based on a qualitative dynamical system-based criterion, which involved a learning process about the structure of the time series, instead of a fitting procedure only. This approach, which was based only on the discharge time series itself, was applied to a headwater catchment in Germany, in which runoff are induced by either convective rainfall during the summer or snow melt in the spring. The application showed the following important features:

- the differences between runoff measurements were more suitable than the actual runoff measurements when using regression models;
- the catchment runoff system shifted from being a possible dynamical system contaminated with noise to a linear random process when the interval time of the discharge time series increased;
- and runoff underestimation can be expected for rising limbs and overestimation for falling limbs.

This nonparametric approach was compared with a distributed hydrological model designed for real-time flood forecasting, with both presenting similar results on average.

Finally, a benchmark for hydrological research using semi-distributed modelling was proposed, based on the aforementioned analysis, modelling and forecasting of flow transmission processes. The aim of this benchmark was not to describe a blueprint for hydrological modelling design, but rather to propose a scientific method to improve hydrological knowledge using semi-distributed hydrological modelling. Following the application of the proposed benchmark to a case study, the actual state of its hydrological knowledge and its predictive uncertainty can be determined, primarily through rejected hypotheses on the dominant hydrological processes and differences in catchment/variables responses.

### Zusammenfassung

Die Bewirtschaftung von Wasserressourcen in ariden und semiariden Landschaften ist mit einer Reihe besonderer Probleme konfrontiert. Eines der größten Probleme für die Maßnahmenplanung und für das operationelle Management ist der Mangel an hydrologischen Daten und damit zusammenhängend auch die relativ kleine Zahl wissenschaftlicher Arbeiten zu dieser Thematik. In dieser Arbeit wurden

- 1) die grundlegenden hydrologischen Bedingungen von Trockenflusssystemen analysiert,
- 2) ein Modellsystem für Flüsse unter semiariden Bedingungen, und
- 3) ein nichtparametrisches Vorhersageverfahren für Abflussvorgänge in Flüssen entwickelt.

Der Wasserverlust in einem großen Abschnitt des Jaguaribe Flusses im nordöstlichen Brasilien wurde auf Basis von Daten zu Abflussraten, Grundwasserflurabstände und mit Hilfe multitemporaler Satellitendaten analysiert. Dafür wurde zuerst ein konzeptionelles hydrologisches Modell über die Mechanismen der Transferverluste in diesem Abschnitt des Trockenflusses erstellt. Dabei ergab sich, dass der Flussabschnitt mit dem Grundwasser hydraulisch verbunden ist. Der Flussabschnitt weist in der Trockenzeit und am Anfang der Regenzeit nur Wasserverlust (Sickerung) zum Grundwasser auf. Im Laufe der Regenzeit findet auch ein gegenseitiger Austausch vom Grundwasser mit dem Flusswasser statt. Aufgrund dieser hydraulischen Kopplung zwischen Flusswasser und Grundwasser sind für diesen Flussabschnitt hydrologische Modellansätze anzuwenden, die generell für gekoppelte Fluss-Grundwassersysteme, v.a. in feuchtgemäßigten Klimaten, entwickelt wurden.

Es wurde ein neuartiges hydrologisches Simulationsmodell für Transferverluste in Trockenflüssen entwickelt. Dieses Modell ist für unterschiedliche aride und semiaride Landschaften anwendbar und hat eine flexible Modellstruktur, wodurch unterschiedliche Hypothesen zur Relevanz ein-

zelner hydrologische Prozesse getestet werden können. Es wurde für den zuvor genannten großen Abschnitt des Jaguaribe Flusses im nordöstlichen Brasilien und für einen kleinen Flussabschnitt im „Walnut Gulch Experimental Watershed“ (WGEW) in Arizona, Südwest-USA, angewendet. Für die eine prozess-orientierte Simulation von Abflussbedingungen und Transferverlusten im Einzugsgebiet des Jaguaribe hat sich gezeigt, dass die am besten geeignete Modellstruktur sowohl den Austausch zwischen Flusswasser und Grundwasser (senkrecht zur Fließrichtung des Flusses) als auch die parallel zum Fluss verlaufende Grundwasserströmung enthält. Die Simulationsexperimente mit unterschiedlichen Modellstrukturen („Hypothesentest“) reduzierte nicht nur die Modellstrukturunsicherheit, sondern quantifizierte auch die Qualität der Modellergebnisse bei folgenden Varianten der Modellstruktur: a) Abfluss im Fluss ohne Interaktion mit dem Grundwasser (keine Transferverluste) und b) Interaktion zwischen Fluss und Grundwasser ohne parallelen Grundwasserstrom zum Flussstrom. Durch die Anwendung auf die beiden unterschiedlichen Trockenflusssysteme wurden neue Erkenntnisse über die Sensitivität des Modells unter verschiedenen Bedingungen erworben. Beispielsweise waren die Parameter der ungesättigten Zone, die von hoher Relevanz für den kleinen Flussabschnitt im WGEW waren, viel sensitiver als die Parameter der gesättigten Zone, die besonders relevant für den Jaguaribe Flussabschnitt in Brasilien waren. Die Ursache für diese sehr unterschiedliche Sensitivität liegt darin, dass beim WGEW das Flusswasser nur mit der ungesättigten Zone in Kontakt steht, da sich in diesem Gebiet, welche im Vergleich zur Jaguaribe-Region noch deutlich trockener ist, kein Grundwasserleiter bildet.

Letztlich wurde ein nicht-parametrisches Verfahren, zur Simulation der deterministischen Evolution und stochastischen Fluktuation der Abflussdynamik entwickelt. Im Unterschied zu prozess-basiertem Modellsystemen basiert

dieses Verfahren nicht auf Modellkalibrierung sondern auf einem Lernprozess, basierend auf Zeitreihendaten. Als Anwendungsbeispiel wurde ein mesoskaliges Einzugsgebiet im Erzgebirge, NO-Deutschland gewählt, in dem starke Abflussereignisse entweder durch konvektive Niederschlagsereignisse oder durch Schneeschmelze generiert werden. Die folgenden wichtigsten Ergebnisse wurden erzielt:

- Regressionsmodellansätze basierend auf den zeitlichen Änderungen der Abflüsse liefern bessere Ergebnisse gegenüber Ansätzen basierend auf direkten Abflussdaten;
- mit zunehmendem Vorhersagehorizont wandelt sich das hydrologische System von einem mit Zufallsanteilen veräuschten dynamischen System zu einem linearen probabilistischen Zufallsprozess;
- Bei zunehmendem Abfluss (ansteigenden Ganglinie) erfolgt meist eine Abflussunterschätzung, bei abnehmendem Abfluss (fallende Ganglinie) erfolgt meist eine Abflussüberschätzung.

Dieses nichtparametrische Verfahren ergibt im Vergleich mit einem prozessorientierten und flächenverteilten hydrologischen Hochwasservorhersagemodell bis zu einem Vorhersagezeitraum von 3 Stunden Ergebnisse von vergleichbar guter Qualität.

Letztendlich wurde ein Vorgehen bzgl. künftiger Forschungen zu hydrologischer Modellierung vorgeschlagen. Das Ziel dabei war ein wissenschaftliches Verfahren zur Verbesserung des hydrologischen Wissens über ein Einzugsgebiet. Diese Verfahren basiert auf einem Hypothesentest zu den relevanten hydrologischen Prozessen und der Untersuchung der Sensitivitäten der hydrologischen Variablen bei unterschiedlichen Einzugsgebieten.





## **Chapter I:**

### **Introduction**

## 1. Background and Overview

Phenomenological modelling has the ultimate goal of establishing mathematically the actions of the dominant mechanisms, which have been previously derived from measurements, of an underlying system (Kantz and Schreiber, 2004). In this view, distributed hydrological models may be considered (quasi-)phenomenological ones, since observed *signatures* of hydrological processes (e.g. runoff coefficients of hillslopes and channel transmission losses) are mimicked by (inter-)actions of conceptual lump components, but model assumptions, which are not based on measurements, are almost always inevitable.

The technological improvements in the past 30 years, such as the reduction of computation time to run numerical models and the availability of large data sets of land surface, enabled a big increase of the number of developers and users of distributed models. However, this kind of modelling is a task that involved uncertainties, which can arise from initial and boundary conditions, parameters, model structure and/or space-time scales effects (see e.g. Beven, 1989; Blöschl and Sivapalan, 1995; Bronstert, 1999; Sivapalan et al., 2003b; Montanari, 2007). Moreover, the induction procedure (the upward or bottom-up approach), which links much smaller scale conceptual hydrological models (e.g. Horton infiltration model) and is at the heart of distributed modelling, produces almost inevitably over-parameterization and associated identifiability problems (Beven, 1989; Young, 2003; Littlewood et al., 2003; Kirchner, 2006).

In order to lessen the uncertainties of distributed models, advances in data sampling/assimilation on/of initial and boundary conditions and parameters have been used (e.g. Bauer et al., 2006; Soulsby et al., 2008; Milzow et al., 2009). Also, in this way, model assessment of different simulated variables and for catchments with different governing hydrological processes (avoiding the one-case-study application) have been suggested (Bronstert, 2004; Ebel

and Loague, 2006; Kirchner, 2006; Andréassian et al., 2007, 2009, 2010). Furthermore, it has been recognized that hydrological models in general should primarily proceed from *perceptual* hydrological models, which describe (develop hypotheses) in a physically meaningful way (on) the dominant hydrological mechanisms based on experiments/measurements at different space-time scales and expert information/knowledge of related variables (e.g. soils, geology and land cover) (e.g. Sivapalan et al., 2003a; Chirico et al., 2003; Dunn et al., 2008; Gallart et al., 2008; Wenniger et al., 2008; Tetzlaff et al., 2008; Gupta et al., 2008; Hughes, 2010; McMillan et al., 2011). Nevertheless, perceptual hydrological models have rarely been combined to build process-based models of a comprehensive range of catchment processes (McMillan et al., 2011).

In order to overcome the over-parameterization and associated identifiability problems of distributed models, some authors have re-visited the downward or top-down approach (e.g. Jothiyangkoon et al., 2001; Sivapalan et al., 2003a; Littlewood et al., 2003; Fenicia et al., 2008a,b) introduced by Klemeš (1983), which means that one should start with the simplest model configuration at a large scale and then gradually increase the complexity of the model with decreasing scales (Klemeš, 1983; Jothiyangkoon et al., 2001). Furthermore, the *purely* distributed modelling has also been modified for hybrid or semi-distributed modelling (e.g. Jothiyangkoon et al., 2001; Güntner and Bronstert, 2004), which combines the upward approach with the downward one. Semi-distributed modelling may be considered as a compromise between downward and upward approaches, trying to decrease the over-parameterization and associated identifiability problems of upward modelling (Young, 2003; Littlewood et al., 2003) and to surmount the lack or poor representation of the hydrological processes of downward modelling (e.g.

*purely* empirical models) (Littlewood et al., 2003).

Another emerging modelling approach has been made by assuming hydrological modelling as a tool for testing hypotheses on the dominant hydrological mechanisms (Graeff et al., 2009; Savenije, 2009; Andréassian et al., 2010; Buytaert and Beven, 2011; McMillian et al., 2011; Clark et al., 2011a,b), in which the feedbacks between experimentalists and modellers are indispensable for model development and assessment. In this context, the experimental challenge is to choose/develop a monitoring system or an experimental procedure, given natural and financial constraints, in order to quantify/qualify the (possible) dominant hydrological processes (perceptual hydrological model). On the other hand, the modelling challenge is to develop flexible model structures, in order to test hypotheses on the dominant hydrological mechanisms and to convert the *final* model applicable to the time and spatial scales of interest (based on Savenije, 2009; Andréassian et al., 2010; Buytaert and Beven, 2011; McMillian et al., 2011; Clark et al., 2011a).

Taken into account the synthesis proposed by Li et al. (2010) on comparative analysis in hydrology, that model strategy may be applied to a) just one catchment with a view to generating insights into catchment functioning through comparisons of model performance (inter-comparison studies), or b) a number of catchments in different hydro-climatic regions with a view to learning from differences in catchment responses (comparative diagnostic analysis). Finally, a compromise between model complexity, data availability and model accuracy/consistency with the observations should be achieved to find the *most suited* process-orientated model, which is able to simulate the long term dynamics of an underlying hydrological system.

However, optimised forecasting of an underlying hydrological system does not have to be designed for good reproduction of long term dynamics but may instead

focus on short time horizons into the future (based on Kantz and Schreiber, 2004). For this task, techniques, which are based almost entirely on time series data, often supersede the phenomenological models (Kantz and Schreiber, 2004). The first step of the time series approach consists in choosing an appropriate model equation containing free parameters, which in a second step are adapted to the observed series by some fitting procedure (Brockwell and Davis, 2003; Kantz and Schreiber, 2004). The application of such techniques to hydrological time series has become feasible through the increase in the number of monitoring networks and their long term functioning in the developed/developing world.

The application of time series models in hydrological sciences has been dominated by the assumption of a random nature of the hydrological data and then the use of nonparametric stochastic forecasting approaches. However, since the beginning of the 1990s, runoff series have been assumed to be responses of dynamical systems with a low-dimensional chaotic attractor resulting from the nonlinear coupling of precipitation and catchment state that depends on climatic condition and geo-patterns such as land cover, soils, river network and geology (Liu et al., 1998; Porporato and Ridolfi, 1997; Sivakumar et al., 2001). This nonlinear approach can provide accurate *one-discharge-value-per-time-step* forecasting, but it does not always offer insight into the probabilistic structure of the data resulting from the shortness of series and the inevitable presence of dynamical noise in open physical systems such as catchment hydrology (Porporato and Ridolfi, 2001; Kantz and Schreiber, 2004).

In this context, the challenge is to elaborate a model, which enables one to deal with both deterministic evolution and inherent fluctuations in river discharge data. There are a few examples in the literature which address this issue: Tamea et al. (2005) proposed a) an ensemble-based nonlinear prediction with parametric deterministic range similar to the GLUE

method (Beven and Binley, 1992) and b) a probabilistic prediction using global errors of a training set to “dress” the deterministic forecasts, which was also done by Chen and Yu (2007) using support vector machine background.

Even though the application of time series models are restricted by short-range dependence of the time series, i.e. its autocorrelation function has to reach approximately zero, and effects e.g. of man-made actions on landscape and water systems cannot be taken into account for forecasting, the time series models do not contain the inherent uncertainties of (semi-)distributed hydrological models arising from initial conditions, spatially distributed parameters, model structure and space-time scale effects. On the other hand, (semi-)distributed models can predict hydrological processes with some degree of certainty, when time series data are scarce (e.g. Lange et al., 1999; Gheith and Sultan, 2002). However, it would be desirable to combine the insight of a (quasi-)phenomenological approach with the statistical accuracy of a time series model (Kantz and Schreiber, 2004).

In this thesis, the hydrology of dryland river systems is analyzed and a semi-distributed hydrological model and a forecasting approach are developed for flow transmission processes in river-systems. A focus of this research will be on semi-arid environments, where scarcity of data and, consequently, of hydrological studies, due to financial constrains, low population density, remoteness of hydrological stations and inherent short duration of runoff, are one of the major problems for the implementation of water resources planning and management (El-Hames and Richards, 1998; Gaiser et al., 2003; Lange, 2005; Costelloe et al., 2006; Wheeler et al., 2008a; Morin et al., 2009).

## 2. Objectives

It is aimed to develop a process-orientated and semi-distributed channel transmission losses model which is able to cover a large variation in climate and hydro-geologic

controls, which are typically found in dryland regions of the Earth. The model is designed with a flexible structure in order to test hypotheses on the dominant hydrological processes of river reaches. Traditionally, channel transmission losses models have been developed for site specific conditions and fixed model structure.

For that task, the intention is also to quantify and qualify the channel transmission losses in a large river reach in NE Brazil, including the development of a concept of the dominant hydrological processes based on stream discharge series, groundwater series and multi-temporal satellite data.

Moreover, a new time series model based on stochastic dynamics theory (van Kampen, 1992; Anishenko et al., 2003; Kantz and Schreiber, 2004) is formulated to deal with both deterministic evolution and inherent fluctuations in river discharge data, in order to forecast real-time flood in headwater catchments. For this task, our formulation is compared with the standard nonparametric stochastic approach and a distributed hydrological model developed for real-time flood forecasting.

## 3. Outline of the Thesis

The observation and the analysis of the channel transmission losses in a large river reach in NE Brazil will be shown in Chapter II, which also deals with the perceptual model of the channel transmission losses and its implication for the hydrological modelling of that reach, whereas Chapter III is related to the development of the channel transmission losses model and its assessment for different dryland rivers located in NE Brazil (see also Chapter II) and the SW USA.

Chapter IV deals with the real-time probabilistic flood forecasting in a headwater catchment in Germany based on a new nonparametric approach. Chapter V discusses and brings together the main results of Chapters II to IV, presenting also a benchmark for hydrological research using semi-distributed hydrological modelling, which is a synthesis of those Chapters.

Chapter V also provides a general conclusion and implications of this work on real-world problems and hydrological research.

Chapters II to IV were written as stand-alone manuscripts that are either published or awaiting for publication in international peer-reviewed journals (for full references, see front pages of the respective chapters).

## Chapter II

# **Analysis of channel transmission losses in a dryland river reach in northeastern Brazil using streamflow series, groundwater level series and multi-temporal satellite data**

### **Abstract**

Scarcity of hydrological data, especially streamflow discharge and groundwater level series, restricts the understanding of channel transmission losses (TL) in drylands. Furthermore, the lack of information on spatial river dynamics encompasses high uncertainty on TL' analysis in large rivers. The objective of this study was to combine the information from streamflow and groundwater level series with multi-temporal satellite data to derive a hydrological concept of TL for a reach of the Middle Jaguaribe River (MJR) in semi-arid northeastern Brazil. Based on this analysis, we proposed strategies for its modelling and simulation. TL take place in an alluvium, where river and groundwater can be considered to be hydraulically connected. Most losses certainly infiltrated only through streambed and levees and not through the flood plains, as could be shown by satellite image analysis. TL events, whose input river flows were smaller than a threshold, did not reach the outlet of the MJR. TL events, whose input flows were higher than this threshold, reached the outlet losing on average 30% of their input. During the dry seasons (DS) and at the beginning of rainy seasons (DS/BRS), no river flow is expected for pre-events and events have vertical infiltration into the alluvium. At the middle and the end of the rainy seasons (MRS/ERS), river flow sustained by base flow occurs before/after events and lateral infiltration into the alluvium plays a major role. Thus, the MJR shifts from being a losing river at DS/BRS to become a losing/gaining (mostly losing) river at MRS/ERS. A model of this system has to include the coupling of river and groundwater flow processes linked by a leakage approach.

*Keywords: channel transmission losses; multi-temporal RapidEye satellite data; semi-arid hydrology; northeastern Brazil; dryland rivers; river-aquifer interaction*

Resubmitted to *Hydrological Processes* as

Costa, A.C., Foerster, S., de Araújo, J.C., and Bronstert, A.: Analysis of channel transmission losses in a different dryland river reach in northeastern Brazil using streamflow series, groundwater level series and multi-temporal satellite data, 2012.

## 1. Introduction

Channel transmission losses are a key factor for water and environmental planning and management in dryland environments, since they reduce not only surface flow volume, but also peak discharges, support riparian vegetation, and are a major source of potential groundwater recharge (Sharma and Murthy, 1994; Sharma et al., 1994; Lange, 2005; Dagès et al., 2008; Wheeler, 2008; Morin et al., 2009). Their dynamics have shown high nonlinearity in relation to streamflow magnitude:

a) Initial infiltration losses were smaller than during the main phase of the flood in a flash flood experiment in the southern Negev Desert, Israel (Lange et al., 1998).

b) Small to medium floods could travel considerable distances without substantial losses, whereas significant transmission losses occurred during high runoff peaks in a 150 km channel reach of the Kuiseb River, Namibia Desert. High runoff peaks were significantly diminished after the runoff had exceeded a certain threshold level (Lange, 2005).

c) Small floods did not usually traverse the full distance between stream gauges, whereas larger flows transmitted to the outlet about 20-50% of their discharge in a 420 km channel reach of the Cooper Creel River in Australia. Then, at a certain threshold level of input river flow, transmission losses increased again and flows transmitted to the outlet were about 10-20% of their discharge. Only during the largest floods did river flow transmission efficiency increase sharply (Knighton and Nanson, 1994).

For large river systems, that nonlinearity might be explained mainly by:

a) Pools, subsidiary channels and/or floodplain areas which act as sink areas of flows, but once they become fully saturated, the most direct floodways become fully active and river flow transmission efficiency increases

(Knighton and Nanson, 1994; Lange, 2005)

b) A clogging layer within or on the alluvial surface, which can act as a seal that is disrupted at higher discharge (Lange, 2005). Indeed, stratified alluviums with hydraulic conductivity heterogeneity were reported from point infiltration experiments (Parissopoulos and Wheeler, 1992) and local stratigraphies in dryland riverbeds (e.g. Lange, 2005).

Also, the subsurface water redistribution in the underlying alluvium may influence the infiltration rates from river to aquifer. The underlying alluvium saturation can be driven by local, intermediate or regional groundwater flow systems (Sophocleous, 2002), in which potential abstractions are through transpiration by (near-)river channel vegetation (Goodrich et al., 2004; Blasch et al., 2004) and groundwater pumping (Shentsis, 2003; Shentsis and Rosenthal, 2003).

Channel transmission losses take place in a) allogenic rivers, which are sourced almost entirely from upstream humid areas (e.g. the River Nile in Northern Sudan and Egypt) and commonly sustain perennial flow partly infiltrating in the alluvial system along the allogenic river, and b) endogenic rivers, which are sourced almost entirely within dryland environments and usually show an ephemeral (non-baseflow) or intermittent flow (Bull and Kirkby, 2002).

Dryland rivers can be hydraulically connected or disconnected to groundwater systems (Sophocleous, 2002). When hydraulically connected, the gradient between river and groundwater plays a major role in transmission losses, indicating whether they occur or not (see e.g. Lima et al., 2007).

Moreover, a fundamental physical principle which explains higher transmission losses at higher stream discharge is the increase in infiltration due to higher hydraulic head at the surface.

This assumption was taken into account for channel transmission losses modeling by Abdulrazzak and Morel-Seytoux (1983), Freyberg (1983), Illangasekare and Morel-Seytoux (1984), El-Hames and Richards (1998) and Xie and Yuan (2010).

However, the findings of Dahan et al. (2008) in the Kuiseb River, Namibia, suggested that the microlayering of the sandy alluvial sediments at the top of the vadose zone regulates the flux process through almost constant infiltration rates. This disagrees with the hypothesis of a flood-stage-based surface-groundwater flux process. Therefore, large transmission losses during high flood stages may be due to long duration of large floods (Dahan et al., 2008).

Scarcity of hydrological data, especially simultaneous streamflow discharge and groundwater level series, in dryland environments restricts the understanding of transmission losses processes. Furthermore, the lack of information on spatial river dynamics between stream gauges encompasses high uncertainty on transmission losses' analysis in large rivers.

In this paper, we address these problems by investigating channel transmission losses in a 60 km reach of the Middle Jaguaribe River in semi-arid northeastern Brazil. The river reach is located upstream of the 1940  $10^6 \text{ m}^3$  Orós reservoir (Fig. 1), one of the most important water resources for the whole Jaguaribe basin.

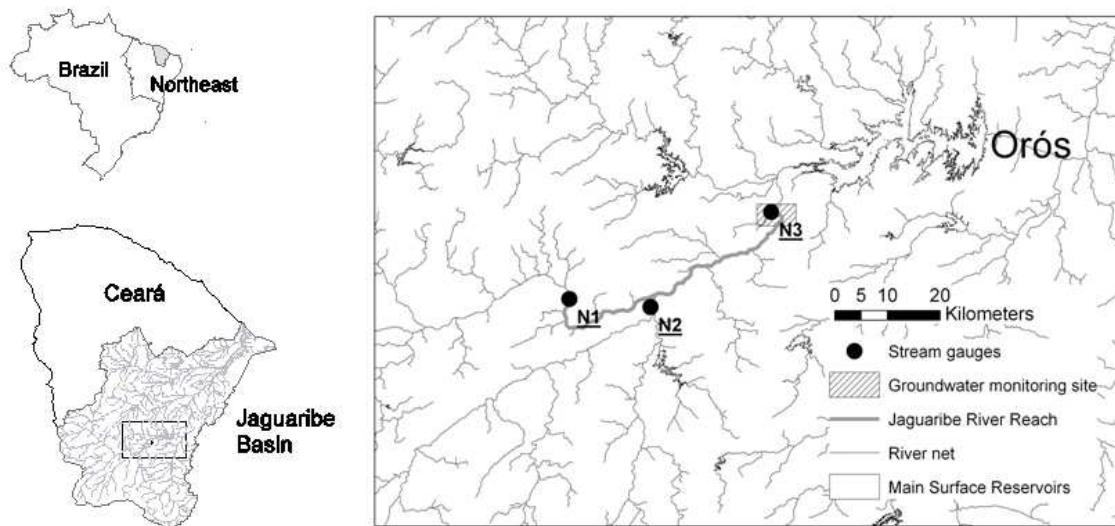


Figure 1. Location of the Middle Jaguaribe River reach under study in relation to the Orós reservoir.

The general objective of this study is to combine the information from streamflow and groundwater level series with multi-temporal satellite data to derive a hydrological concept of channel transmission losses for a large Jaguaribe River reach. Based on this analysis, we propose strategies for its hydrological modelling and simulation.

Using the streamflow series, we intend to a) quantify the event-based channel transmission losses and their impact on the flow volume and peak, b) verify the relationship between transmission losses and input flow magni-

tude, and c) identify the existence of runoff thresholds, which separate hydrological behaviours.

Analyzing the groundwater level series, we intend to a) determine whether the river-groundwater system is hydraulically connected or not, b) verify whether the recession limb of the outflow hydrograph is driven not only by the upstream boundary conditions, but also by the return flow originated from the previous transmission losses.

Assessment of channel transmission losses are traditionally carried out by streamflow water balance and compari-



son between streamflow and groundwater levels. Satellite data might contain complementary information as they have proved to be a valuable source to improve understanding of surface hydrological processes (van Dijk and Renzullo, 2011). They are particularly relevant in large remote catchments with restricted accessibility and therefore sparse hydrological measurements (Kite and Pietroniro, 2000). Satellite observations have been widely used for monitoring the extent of water bodies, e.g. in the context of flood monitoring, and mapping hydrological state variables, such as surface temperature, soil moisture and snow cover, to estimate hydrological fluxes, such as evapotranspiration and runoff (van Dijk and Renzullo, 2011; Schmugge et al., 2002). So far satellite observations have, however, hardly ever been used in the context of transmission losses.

For that purpose, particular satellite systems with a frequent coverage may provide information on seasonal, annual and long-term changes of surface water present in the riverbed or floodplain and of water surface connectivity along the river and its tributaries (see e.g. Costelloe et al, 2006). Water surface mapping and monitoring using optical satellite data are based on the spectral characteristics of water in the near infrared and visual region as compared to soils and vegetation.

The main scientific questions related to the use of satellite-based remote sensing data in this research are:

- a) Is the river confined within the streambed and levees or did it flow over the floodplain during flood events?
- b) Can river water volumes deriving from satellite data and river cross-sections indicate correctly whether channel transmission losses occur?
- c) Has there been any indication of spatial variability in transmission losses in MJR?

d) Even when the stream gauges register non-flow, is surface water observable in the river reach?

## 2. Study Area

The Jaguaribe River is 610 km long and the largest intermittent river in Brazil. Its basin covers an area of 76 thousand km<sup>2</sup> and is located within the institutional borders of the State of Ceará in the semi-arid northeastern Brazil (Fig. 1). The Orós reservoir, the second largest surface reservoir of the State of Ceará, is situated about 11 km downstream of the Middle Jaguaribe River reach (MJR) under study (Fig. 1).

The Jaguaribe River basin's hydrology is determined by an annual cycle of rainy and dry seasons, which are driven mainly by the position of the Intertropical Convergence Zone and secondarily by cold fronts from the South Atlantic (Xavier, 2001; Werner and Gerstengarbe, 2003). The rainy season lasts up to six months (December-May) on average.

The high water deficit can be derived from the difference between annual rainfall (400mm to 800mm depending on the location in the catchment) and the annual potential evaporation (about 2200mm). Together with the scarce, salty and spatially concentrated groundwater resources, this has led to the construction of many surface reservoirs during the last century (there is about one on-river reservoir every 6 km<sup>2</sup>: Malveira et al. (2011)). Furthermore, the large surface reservoirs have transformed large parts of the river network into perennial waterways in the Jaguaribe River basin.

The Middle Jaguaribe River reach (MJR), the focus of this research, is 60 km long and controlled by two upstream stream gauges (N1 and N2) and one downstream stream gauge (N3) (Fig. 2). N1 measures the discharge from the upstream Jaguaribe catchment while N2

measures the discharge from the only large tributary, Cariús River, into MJR.

These two upstream stream gauges control a catchment area of 20 thousand km<sup>2</sup> of the Jaguaribe basin. The additional drainage area between the up-

stream gauges and the downstream gauge is 1000 km<sup>2</sup>, which contains about 130 small surface reservoirs. Water has been released from upstream large reservoirs in the Jaguaribe River into MJR since the dry season of 2007.

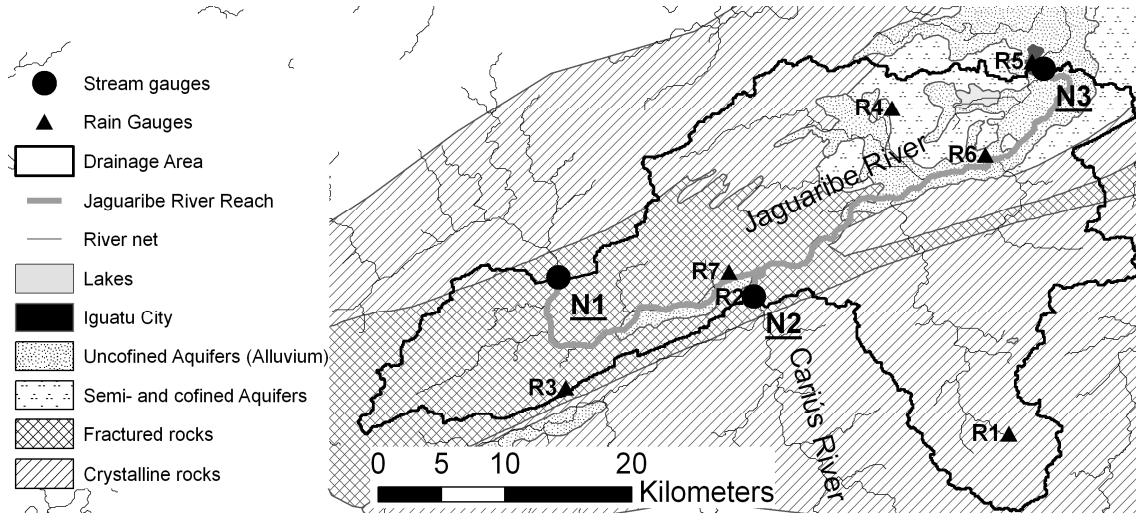


Figure 2. Middle Jaguaribe River reach (MJR) under study. The description of the hydrogeology was adapted from IBGE (2003).

Water consumption for agricultural purposes in the MJR is mainly supplied by tubular wells in an alluvium, which is characterized by unconfined aquifers, contiguous to the Jaguaribe River main stream (Fig. 2). This alluvial groundwater extraction occurs predominantly during the dry season and has an order of magnitude of 6000 m<sup>3</sup>/day (based on CPRM, 1998), whereas the continuous domestic supply for major towns and villages, including Iguatu City, is mainly provided by surface reservoirs or deep groundwater. This alluvium has a maximum thickness of 25 m with high permeability and overlays fractured rocks (IBGE, 2003). Its stratigraphy is composed of layers of fine and coarse sand, gravel and clay (IBGE, 2003). Moreover, the Orós reservoir is located over this same large alluvium-system (IBGE, 2003).

### 3. Hydrological Data

#### 3.1. Streamflow series

The Brazilian Geological Service (CPRM) has monitored the three stream gauges (N1, N2 and N3) in the MJR, measuring daily water level by rulers installed at the river sections and bi-monthly discharges. The time series data are made available by the Brazilian Water Agency (ANA), see <http://www.hidroweb.ana.gov.br>. Water levels at all three gauges have been measured simultaneously since 2001.

We used CPRM's flow discharge measurements to construct the rating curves. Then, we calculated an event-based water balance between input streamflow (N1 and N2) and output streamflow (N3), assuming the wave travel time from N1 and N2 to N3 equal to two days and one day, respectively. These travel times were estimated empirically from the differences between the days of peak flows at the stream gauges. We defined a runoff event ter-

minated if another one begins at the end of its recession limb or if the stream-flow ceases completely, i.e., the runoff volume of the recession limb is included in the calculation of the event-based water balance.

Furthermore, a transmission losses rate  $TL$  ( $10^6\text{m}^3/10^6\text{m}^3$ ) was calculated for every event

$$TL = \frac{\text{Output} - \text{Input}}{\text{Input}} \quad (1)$$

where  $\text{Output}$  ( $10^6\text{m}^3$ ) is the flow volume of the N3 stream gauge and  $\text{Input}$  ( $10^6\text{m}^3$ ) is the sum of flow volumes of the N1 and N2 stream gauges. We described every event according to  $TL$  as follows

- a) if  $TL \approx -1$ , all inflow (sum of the inflow from the upstream gauges N1 and N2) was lost through transmission losses. When river floods occur during the dry season the inflow from the direct drainage between the stream gauges can be neglected, because no significant rainfall over this area has been registered whatsoever;
- b) if  $-1 < TL < 0$ , then transmission losses were relevant and reduced the input flow from the upstream gauges (N1 and N2) and from the drainage area between the stream gauges;
- c) if  $TL \approx 0$ , then transmission losses were approaching zero or they were compensated by inflow from the direct drainage area between the stream gauges;
- d) if  $TL > 0$ , then inflow from the direct drainage area between the stream gauges was greater than possible transmission losses. However, situations with  $TL > 0$  mostly occur in the rainy season.

Rainfall time series of seven rain gauges within the MJR region, which are monitored daily by the Meteorological and Water Resources Foundation of the State of Ceará (FUNCEME) (see Fig. 2), were also taken into account to verify the possible influence on the MJR's water balance of the runoff

which might be generated within the drainage area between the stream gauges (items c) and d) mentioned above).

Moreover, we estimated the order of magnitude of the groundwater extraction during the events in the dry season, multiplying the daily groundwater pumping rate ( $6000\text{m}^3/\text{day}$ ) by the duration of the event.

In order to assess the channel transmission losses relating to the seasonal variation, the events have also been classified according to their seasonality based on the monthly river flow frequency through the years in the MJR. The dry season starts in July and lasts until January, the beginning of the rainy season from February to March, the middle of the rainy season from March to May and the end of the rainy season from May to July.

### ***3.2. The role of the inflow from the drainage area between the stream gauges***

The drainage area between the gauges is about 20 times smaller than the catchment area which the upper gauges drain. Moreover, it contains about 130 small surface reservoirs. However, the inflow from this direct drainage area (IDA) may influence the water balance and thus the channel transmission losses in the MJR for medium and large events during the rainy season. In those cases, Eq. (1) may underestimate the channel transmission losses and, consequently, does not yield reliable values of channel transmission losses for  $-1 < TL < 0$ .

In such cases it is necessary to estimate the inflow from the direct drainage area (IDA). Therefore, we tried to estimate the order of magnitude of IDA using a simple empirical approach.

First, we calculated an event-based runoff coefficient for the drainage area between the stream gauges, based on 1) the assumption that IDA for the events

with  $TL > 0$  is equal to the difference between the upstream inflow into and the outflow out of MJR, and 2) the average rainfall obtained from the rain gauges within the MJR (Fig. 2).

This procedure resulted in an event-based runoff coefficient of 4% on average. These numbers coincide with results from Cadier (1996), who found an annual runoff coefficient of about 6% for a catchment with similar geo-hydro-climatic controls and reservoirs' density in the Jaguaribe River. Using this average runoff coefficient and the estimated rainfall, we calculated IDA for all events within  $-1 < TL < 0$ .

We found that 3 of the 10 events (4, 13 and 26 in Table II) had IDA greater than 20% of the input flow upstream MJR (sum of flow at N1 and N2 stream gauges). Therefore we did not include these events in our investigation of the transmission losses using only Eq. (1).

On the other hand, the other events had on average IDA of 4% of the input flow upstream MJR, which permitted the assumption that IDA can be neglected for these events and, consequently, the use of Eq. (1) is applicable for the investigation of the corresponding channel transmission losses.

### 3.3. Groundwater level series

We have monitored the groundwater level at three observation wells (W1, W2 and W3) on a daily basis (see: groundwater monitoring site in Fig. 1). Fig. 3 details the location of the N3 stream gauge and the nearby observation wells. An approximated alluvial stratigraphy (Carneiro, 1993) of the site where these gauges are located is shown in Table I. Groundwater level in these wells has been measured since April 2010.



Figure 3. Location of the N3 stream gauge and observation wells W1, W2 and W3 (map basis: Google Earth).

**Table I. Approximated alluvial stratigraphy where the N3 stream gauge and the monitoring observation wells are located (adapted from Carneiro, 1993).**

Depth (m)	Texture
0 - 1	Loam
1 - 3	Loamy sand
3 - 9	Fine to coarse sand
9 - 29	Coarse gravel and very coarse sand

We compared the groundwater level series a) to the water level series of the N3 stream gauge during the rainy season of 2010 and b) to the streamflow series of the N1 and N2 stream gauges during the dry season of 2010, when no flow was registered in the N3 stream gauge. In addition, the groundwater level in MJR (W1, W2 and W3) and the water level of the downstream Orós reservoir has also been compared to assess eventual groundwater discharge to this surface reservoir. The water level of the Orós reservoir is monitored daily by the Water Resources Agency of the State of Ceará (COGERH).

### 3.4. Multi-temporal satellite data

Multi-temporal satellite data were used to assess the spatial river dynamics between stream gauges. For this task, we chose the RapidEye system, which includes a constellation of five optical satellites and therefore allows a frequent coverage that is particularly important in areas such as our study area that are often covered by clouds. RapidEye collects large-area image data with 5 m spatial resolution in five bands (blue, green, red, red edge and NIR) on a daily basis (RapidEye, 2010).

Multi-temporal RapidEye data were acquired a) in 2009 during the dry season, i.e. non-flow registration by stream gauges, b) on 20 April 2010, exactly one day after the peak flow during the rainy season of that year, and c) on 18 May 2010 during the flow recession limb.

The satellite data were atmospherically corrected using *ATCOR3* in ERDAS Image 2010 to correct the effect of different illumination conditions due to varying acquisition dates and the terrain (see <http://www.geosystems.de/atcor/>). After the atmospheric correction, satellite image mosaics were generated using *Mosaic pro* in ERDAS Image 2010 to get a consistent image data set for each sampling period for further analysis.

We also delineated the streambed geometry of MJR based on the satellite image mosaic of 2009, which was acquired during non-flow conditions. Furthermore, we mapped the water surface extent within MJR based on the ratio between red and near infrared bands of the satellite image mosaics acquired on 20 April and on 18 May 2010.

Finally, the river water volumes around the stream gauges N1, N2 and N3 (about 500 m radius) were calculated combining the river cross-sections and the water surface extent of the image mosaics acquired on 20 April and on 18 May 2010. These water volumes (Wetted area  $\times$  1000 m of river length) were compared to verify whether the upstream streamflow volume was reduced or not in the MJR's outlet. Since the river velocities may be estimated from the river geomorphologic characteristics, the results of the water volumes, which indicate or not transmission losses, were compared with those based on the combination between streamflow and groundwater level series.

## 4. Results

### 4.1. Streamflow series

Figures 4 and 5 show the cross-sections and the rating curves of the stream gauges at MJR, respectively, wherein water level is the difference between streamflow and streambed levels according to the rulers at the river sec-

tions. The number of discharge measurements varies between the gauges, not only because of their dates of installation, but also because of their conditions

of accessibility during the rainy season. Figure 6 shows, for example, hydrographs of the stream gauges in 2008.

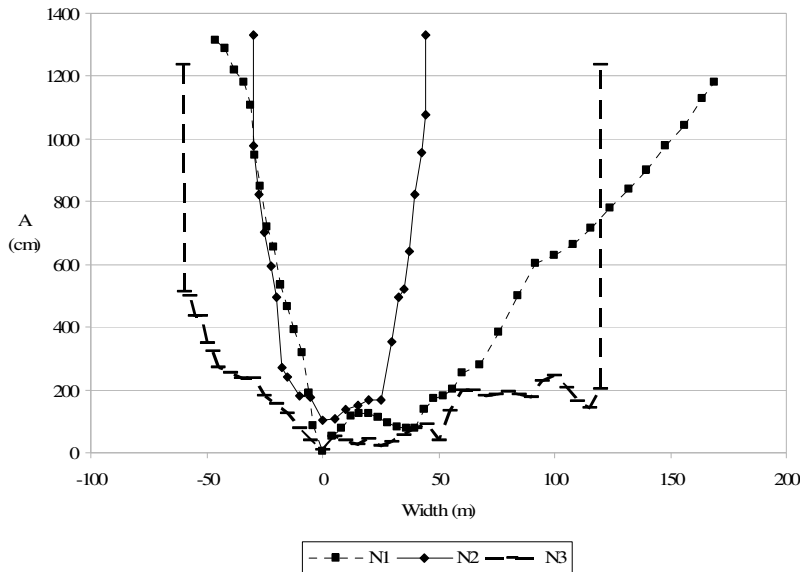


Figure 4. Cross-sections of N1, N2 and N3 stream gauges sampled in 2008 (made available by the Brazilian Geological Service), wherein A is altitude.

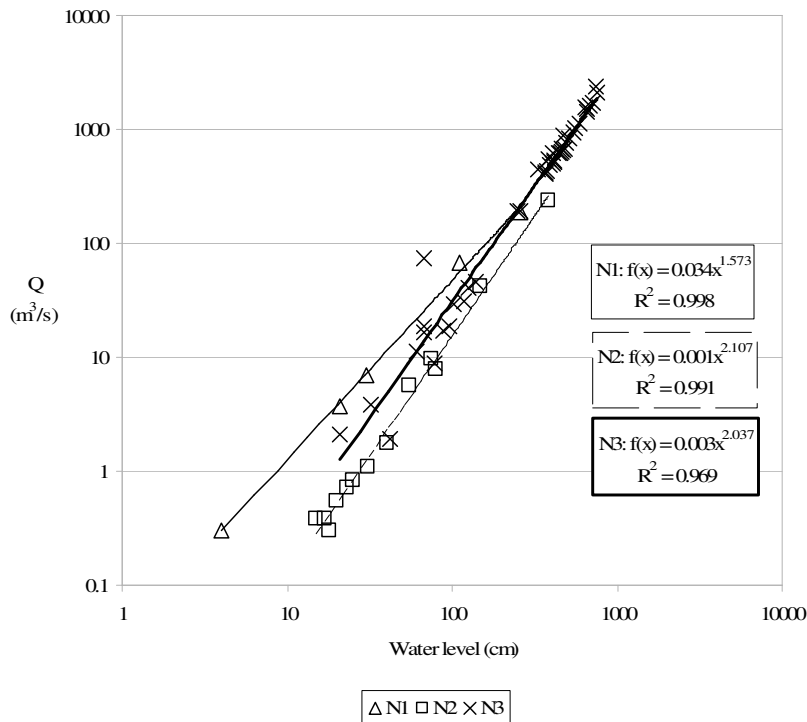
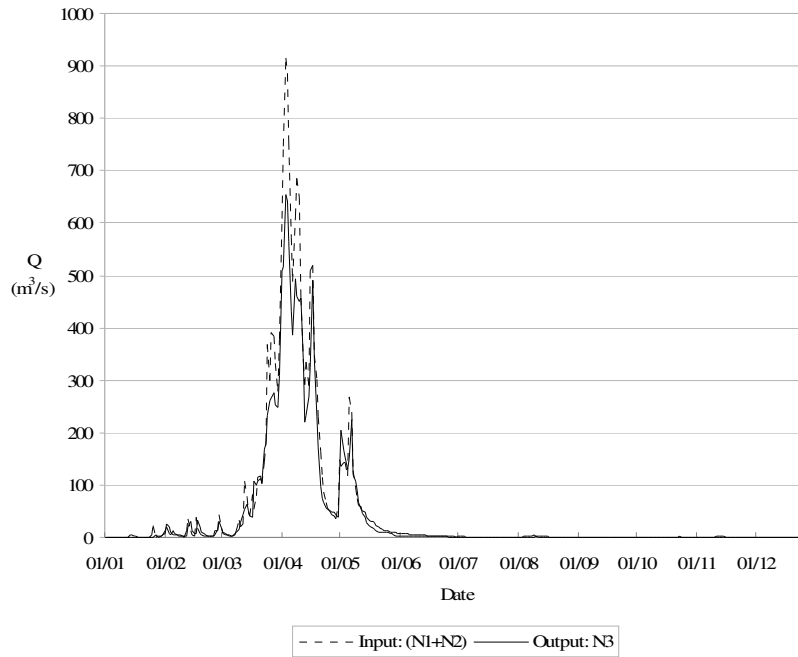


Figure 5. Rating curves of N1, N2 and N3 stream gauges, wherein water level is the difference between streamflow and streambed levels according to the rulers at the river section; and Q is discharge.



**Figure 6.** Hydrographs of N1, N2 and N3 stream gauges in 2008, wherein  $Q$  is discharge.

Table II shows the results of water balance analysis for 40 events monitored at MJR. The driest year was 2001, when no flow was registered by the N3 stream gauge, and the wettest year was

2004, when the N3 and N2 stream gauges were non-functioning due to very high floods. There were also minor gaps in the streamflow series in 2002 and 2007.

*Table II. Results of the water balance analysis for 40 events monitored at MJR, where N1 and N2 are the upstream gauges, N3 is the downstream gauge and the transmission losses  $TL = (O - I)/I$ , where  $O$  is output and  $I$  is input flow from the upstream stream gauges. The season of the event was classified as a) beginning of rainy season (BR), b) middle of rainy season (MR), c) end of rainy season (ER) and d) dry season (DS). We also included the order of magnitude of the groundwater extraction (GE), which occurs predominantly during the dry season.*

Date (m/y)	Event	PF <sup>I</sup> (N1+N2) (m <sup>3</sup> /s)	PF (N3) (m <sup>3</sup> /s)	Input (10 <sup>6</sup> m <sup>3</sup> )			Output (10 <sup>6</sup> m <sup>3</sup> )		O - I (10 <sup>6</sup> m <sup>3</sup> )	TL	Season	GE (10 <sup>6</sup> m <sup>3</sup> )
				N1	N2	N1+N2	N3					
4-5/01	1	8.7	0.0	3.1	0.0	3.1	0.0	-3.1	-1.0	DS	0.4	
12/01	2	5.9	0.0	0.0	1.8	1.8	0.0	-1.8	-1.0	DS	0.2	
1/02	3	18.0	0.0	0.0	6.9	6.9	0.0	-6.9	-1.0	DS	0.2	
3-6/02†	4	48.1	30.1	24.3	21.6	45.9	32.9	-13.0	-0.3	M-ER	na**	
1/03	5	24.8	0.0	0.0	3.6	3.6	0.0	-3.6	-1.0	DS	0.2	
2-3/03	6	77.9	83.2	23.9	21.6	45.5	59.5	13.9	0.3	BR	na	
3-4/03	7	444.5	272.7	211.3	83.4	294.7	232.3	-62.4	-0.2	MR	na	
4/03	8	23.3	34.0	3.7	7.1	10.8	17.4	6.6	0.6	MR	na	
4-5/03	9	22.3	30.8	4.5	1.1	5.6	10.3	4.6	0.8	M-ER	na	
5,6-7/03	10	97.8	67.4	21.9	8.4	30.3	30.6	0.2	0.0	ER	na	
1-2/05	11	15.0	0.0	2.1	0.0	2.1	0.0	-2.1	-1.0	DS	0.4	
3/05	12	6.3	0.0	0.0	3.5	3.5	0.0	-3.5	-1.0	BR	na	
3-4/05	13	41.2	36.0	5.3	28.3	33.6	22.8	-10.9	-0.3	MR	na	
5/05	14	3.9	0.0	1.0	6.1	7.1	0.0	-7.1	-1.0	ER	na	
2/06	15	18.7	0.0	0.0	3.8	3.8	0.0	-3.8	-1.0	BR	na	
2/06	16	46.8	36.0	0.0	20.3	20.3	18.6	-1.8	-0.1	BR	na	
3/06	17	6.3	10.1	0.0	3.8	3.8	6.1	2.3	0.6	MR	na	
3,4-5/06	18	328.0	63.7	28.4	370.3	398.7	175.5	-223.3	-0.6	M-ER	na	
4,5-6/07‡	19	175.4	50.9	52.2	40.4	92.6	55.4	-37.2	-0.4	M-ER	na	
8-12/07*	20	2.0	0.0	0.0	8.2	8.2	0.0	-8.2	-1.0	DS	0.9	
1/08	21	5.9	0.0	0.0	1.5	1.5	0.0	-1.5	-1.0	DS	0.2	
1-2/08	22	24.3	26.0	3.7	6.1	9.8	9.9	0.1	0.0	BR	na	
2/08	23	38.1	32.7	0.3	12.6	12.9	14.2	1.3	0.0	BR	na	
2-3/08	24	43.7	30.8	5.1	4.2	9.3	9.3	0.1	0.0	MR	na	
3-7/08	25	914.6	665.0	798.6	663.6	1462.2	1209.8	-252.4	-0.2	M-ER	na	
8/08	26	4.1	2.3	1.4	1.4	2.8	2.1	-0.8	-0.3	ER	na	
9-12/08*	27	1.6	0.0	0.7	7.3	8.0	0.0	-8.0	-1.0	DS	0.7	
1/09	28	2.8	0.0	0.0	0.7	0.7	0.0	-0.7	-1.0	DS	0.2	
2/09	29	0.3	2.7	0.0	0.2	0.2	0.9	0.7	4.2	BR	na	
2/09	30	4.1	10.1	0.0	2.1	2.1	3.3	1.1	0.5	BR	na	
2-3/09	31	120.0	96.7	7.2	19.3	26.5	32.7	6.2	0.2	MR	na	
3-4/09	32	11.5	18.3	1.3	3.4	4.7	6.6	1.8	0.4	MR	na	
4-8/09	33	788.3	728.3	556.8	542.0	1098.8	925.6	-173.3	-0.2	ER	na	
8-12/09*	34	1.7	0.7	0.3	3.9	4.2	0.0	-4.1	-1.0	DS	0.9	
1/10*	35	0.6	0.0	0.0	0.9	0.9	0.0	-0.9	-1.0	DS	0.2	
3-5/10	36	179.5	118.0	96.3	33.0	129.3	88.2	-41.0	-0.3	B-MR	na	
5/10	37	7.8	16.2	0.0	1.9	1.9	4.6	2.7	1.4	ER	na	
7-8/10*	38	2.6	0.0	0.3	0.8	1.1	0.0	-1.1	-1.0	DS	0.4	
8-9/10*	39	1.1	0.0	0.0	1.7	1.7	0.0	-1.7	-1.0	DS	0.4	
9-10/10*	40	2.1	0.0	0.0	1.8	1.8	0.0	-1.8	-1.0	DS	0.4	



<sup>1</sup>Peak flow.

†Third event in the rainy season of 2002: the second one has not been registered.

‡Second event in the rainy season of 2007: the first one has not been registered.

\*Event produced by release of water from upstream surface reservoirs during the dry season.

\*\*Not applicable.

Seven events were produced by release of water from upstream surface reservoirs into MJR during the dry season. These man-made events plus ten natural ones did not reach the N3 stream gauge (TL = -1.0). These events had maximum input flow (N1 + N2) equal to  $8.2 \cdot 10^6 \text{ m}^3$  and occurred mostly during the dry season.

However, the man-made events and two very small natural events (11 and 28 in Table II) had high probability to be partially abstracted by groundwater extraction for agricultural use (between 5% and 40% of input flow) (see Table II).

Moreover, one event with  $2.8 \cdot 10^6 \text{ m}^3$  input flow reached the N3 stream gauge in August 2008 (26 in Table II), at the end of the rainy season. This event lost about 30% of flow through the MJR only. The rainfall spatial distribution of the rain gauges inside the MJR's drainage area (Fig. 7) showed a rainfall just one day before this event, which might generate enough runoff to compensate for some of the channel transmission losses. Furthermore, this event occurred after a large one, whose infiltrated streamflow may be discharged during this small event.

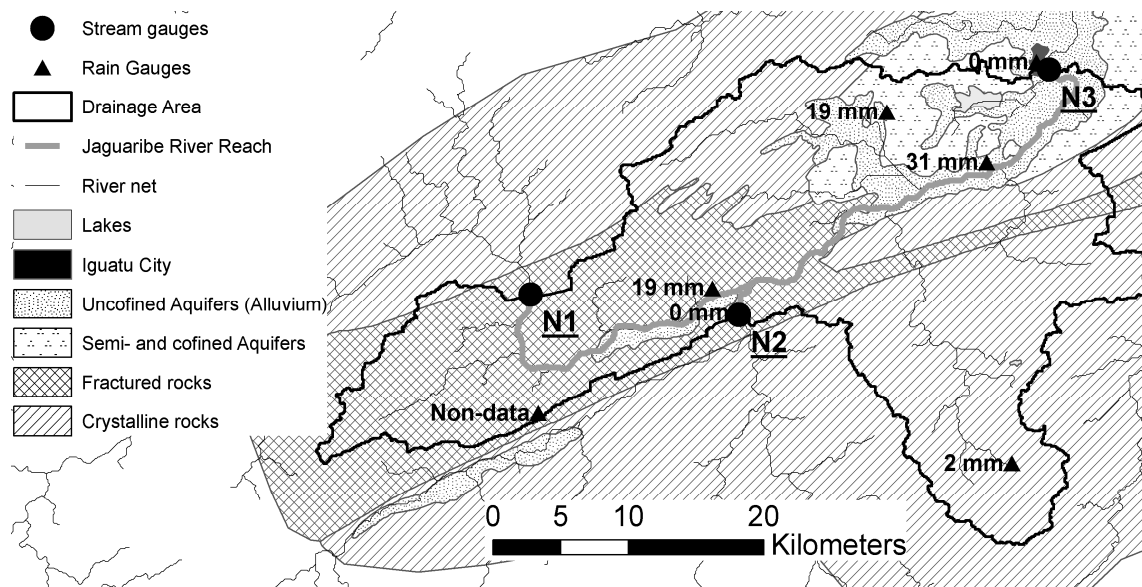


Figure 7. Rainfall spatial distribution on 8 August 2008.

Nine events between 20 and  $1460 \cdot 10^6 \text{ m}^3$  input flow at the middle and the end of the rainy seasons, including the largest ones, had relevant channel transmission losses ( $-1.0 < \text{TL} < 0.0$ ) and lost at least  $815 \cdot 10^6 \text{ m}^3$  of river flow. All these events resulted in a reduction in their peak flows (37% on average). However, 2 of these events (4 and 13 in Table II) had high probability of rele-

vant inflow from the direct drainage area between the gauges, more than 20% of the inflow from the upper gauges (see explanations in the previous paragraphs). On the other hand, inflow from this direct drainage area can be neglected for the other seven events, which had 30% of channel transmission losses on average. Therefore, a relationship between input flow and transmis-

sion losses may be estimated from these seven events (Fig. 8).

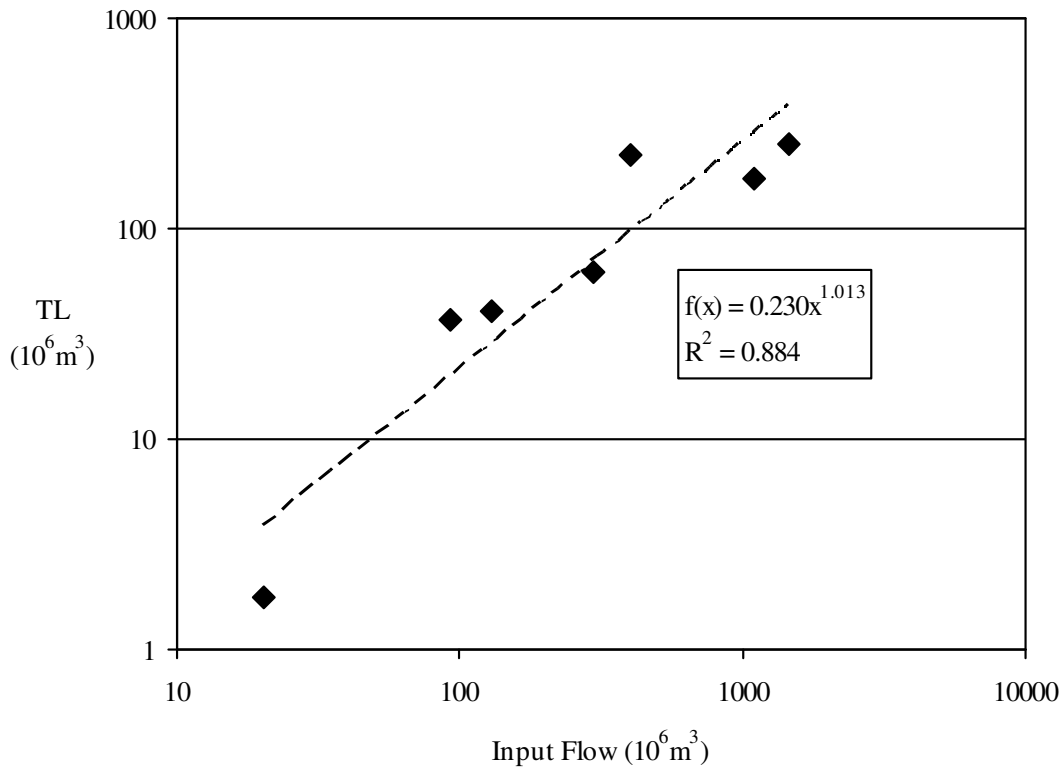
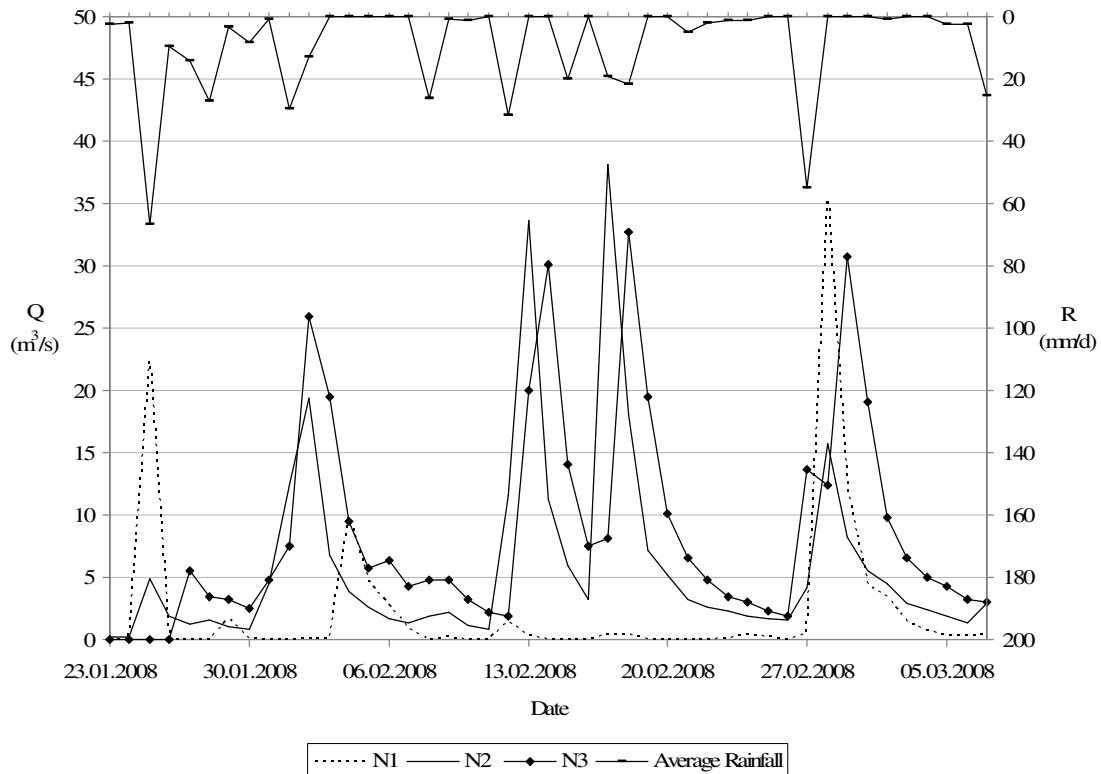


Figure 8. Input flow vs. channel transmission losses (TL) in MJR from seven events between 20 and 1460  $10^6 \text{ m}^3$  input flow at the middle and the end of the rainy seasons.

On one hand, 27 of the 40 observed events lost either completely or partially (30% on average) their input river flow (N1 + N2 stream gauges). Under these events, total channel transmission losses reached at least 880  $10^6 \text{ m}^3$  and peak flow was always reduced. On the other hand, channel transmission losses seemed to be compensated by or smaller than the runoff generated from the MJR's direct drainage area for 13 events between 0.9 and 60  $10^6 \text{ m}^3$  input flow (TL  $\approx$  0.0 or TL > 0.0, respectively), which could occur at the beginning, middle or end of the rainy seasons. Moreover, the events 8, 9, 10 and 37 in Table II, which occurred mainly at

the end of the rainy seasons, may be influenced by the contribution of the infiltrated streamflow of the previous large events at the middle of the rainy seasons.

For the nine events with TL > 0.0, the upstream peak flow always increased compared to the downstream one (Table II). This is only possible if another source of inflow, e.g. the runoff of the direct drainage area between the gauges, exists. For the other four events with TL  $\approx$  0.0, relevant rainfall over the MJR has always been measured during the events (e.g., see Fig. 9 for events in 2008 with TL  $\approx$  0.0).



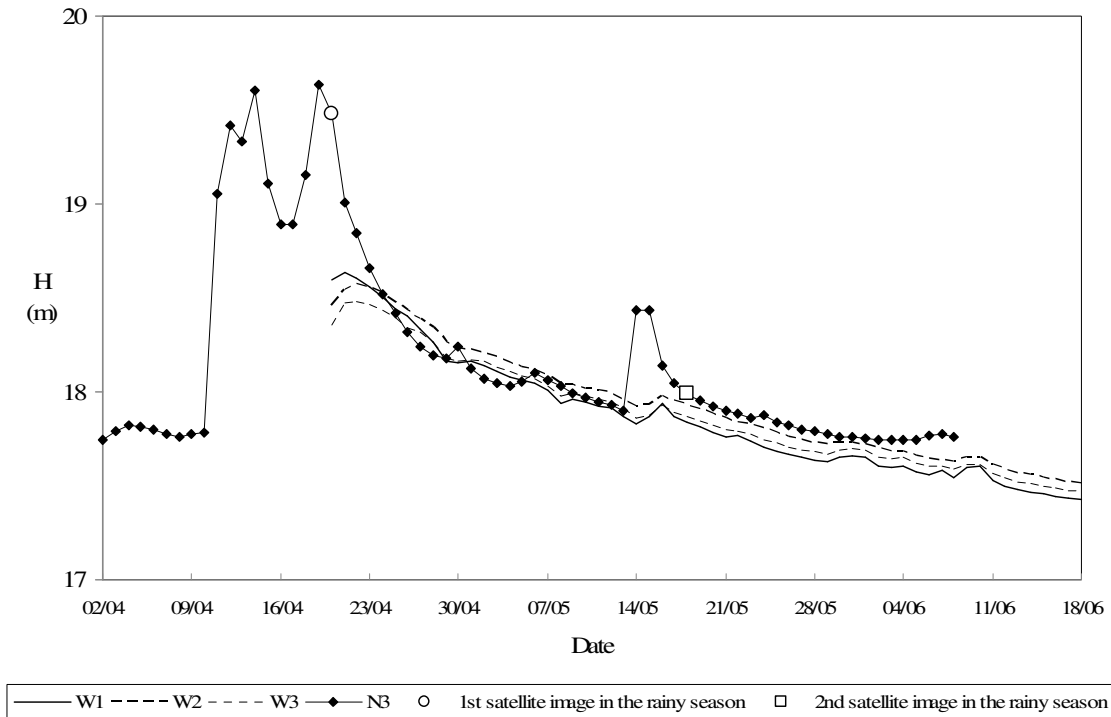
**Figure 9.** Streamflow ( $Q$ ) and average rainfall ( $R$ ) time series of events in the rainy season of 2008, whose channel transmission losses seemed to be compensated by the runoff generated from the MJR's drainage area ( $TL \approx 0.0$ ).

#### 4.2. Groundwater level series

The groundwater level monitoring started on 20 April 2010 just as the largest event in this year took place. Only two natural events occurred in 2010: a) the largest with  $129.3 \cdot 10^6 \text{m}^3$  input flow and losses of about 30% ( $TL = -0.3$ ) from March to May 2010, and b) the second largest with  $1.9 \cdot 10^6 \text{m}^3$  input and about 140% of gain ( $TL = 1.4$ ) in May 2010, which was caused by the runoff generated from the MJR's drain-

age area (see previous section). Moreover, three man-made events with losses of 100% were observed during the dry season of 2010 (see Table II) from June to October.

Figure 10 shows the groundwater level and the water level of the N3 stream gauge in relation to a reference level of 25 m depth from the terrain surface of W2 well during the rainy season of 2010. The water level series ends when the non-flow situation has been registered at the N3 stream gauge.



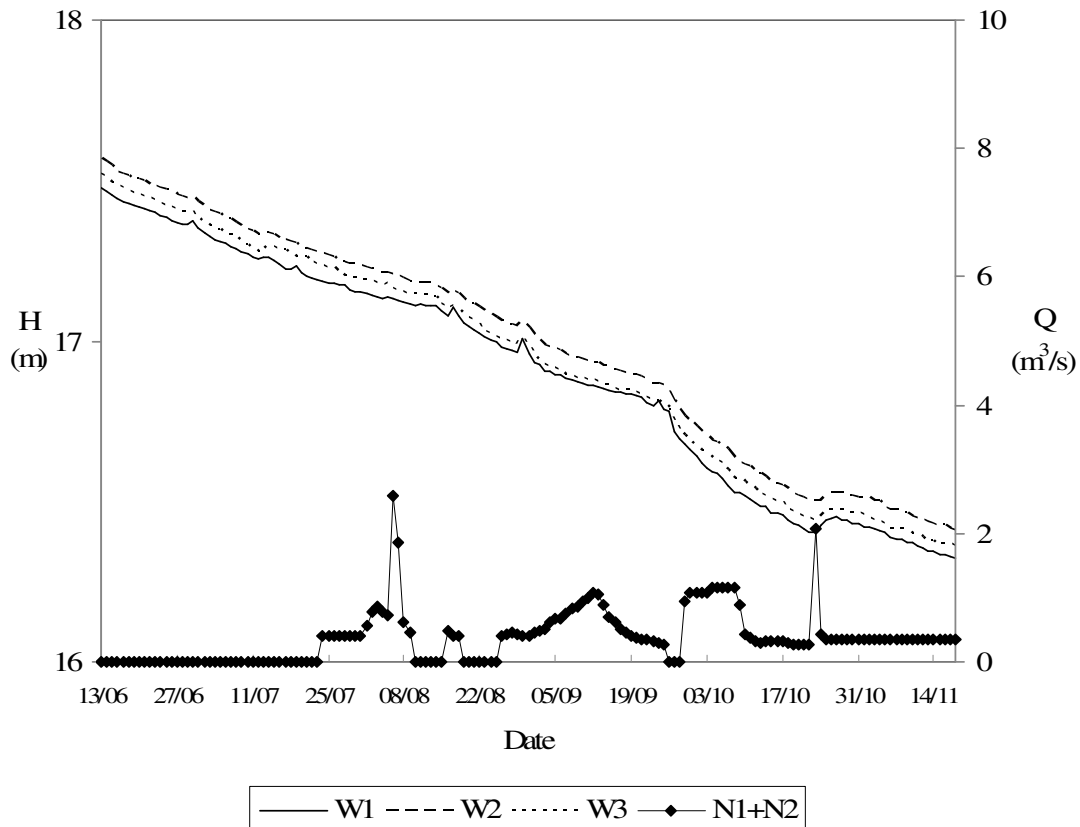
**Figure 10.** Groundwater level of three observation wells (W1, W2 and W3) and water level of the N3 stream gauge (H) in relation to a reference level of 25 m depth from the terrain surface of W2 well during the rainy season of 2010 (March-May). The groundwater level monitoring started on 20 April 2010. The water level series ended when the non-flow situation had been registered at the N3 stream gauge. The days of satellite image acquisition in the rainy season are also indicated.

Figure 10 shows that

- Water flow from the river to the groundwater, i.e. channel transmission losses, was observed in two events (9-22 April and 15 May, 2010), i.e. water level exceeded groundwater stages.
- The alluvium has shallow groundwater and the river-groundwater system can be considered to be hydraulically connected.
- Channel transmission losses stopped during the recession limb of the larger event from 24 April to 12 May 2010, when base flow occurred, i.e. the groundwater level was slightly higher than the river's water level.
- Different from the larger event, transmission losses occurred during all

smaller event, although the water balance pointed to a 140% gain in flow. The inflow from tributaries, which are closer to the N3 stream gauge and, therefore, have spatially smaller opportunity for channel transmission losses in the larger alluvial system (see Fig. 2), might compensate for these channel transmission losses.

Figure 11 shows the groundwater level and the summed upstream flow of the N1 and N2 stream gauges during the dry season of 2010. The water level series of the N3 stream gauge was not shown in Fig. 11 because no flow was registered at this gauge.



**Figure 11.** Groundwater level of three observation wells (W1, W2 and W3) ( $H$ ) in relation to a reference level of 25 m depth from the terrain surface of W2 well and the total upstream flows of N1 and N2 stream gauges ( $Q$ ) during the dry season of 2010 (June-October). The water level series of the N3 stream gauge was not shown here because no flow was registered at this gauge.

The man-made events (reservoir release), which resulted in 100% of channel transmission losses, had no significant influence on the evolution of the groundwater level series. Only a short peak on 23 October 2010 seemed to cause a rise in the groundwater level. Nevertheless, investigating the spatial

distribution of rainfall over MJR (Fig. 12), we found that a heavy rainfall on 23-24 October 2010 might be the reason for the sharp peak flow on 23 October 2010 during the man-made events and the dominant inflow for the groundwater recharge in the alluvial system.

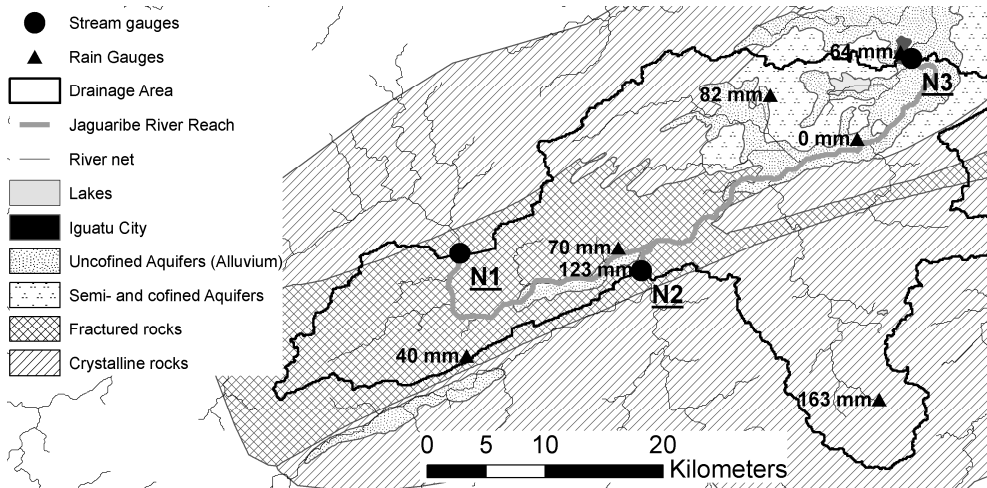


Figure 12. Rainfall spatial distribution on 23-24 October 2010.

The channel transmission losses in the large alluvial system seem to be transferred as groundwater flow to the downstream Orós reservoir, since the mean difference between groundwater level and Orós reservoir’s water level was 23 m in 2010. Considering that the distance between the groundwater at N3 stream gauge and the Orós reservoir is 11 km, groundwater from this gauge had a downwards gradient to this reservoir of 2.1 m/km in 2010.

are three overtopping weirs inside MJR (Fig. 13) from which water has been taken out for agricultural and domestic use, and b) that the Jaguaribe River character changes abruptly in the riverscape region displayed in Fig. 14: from (i) a moderate gradient and stable cross-section stream (a riffle-dominated channel type) (see cross-sections of N1 and N2 in Fig. 4) to (ii) a low gradient and unstable cross-section one (a meandering channel type) (see cross-section of N3 in Fig. 4).

### 4.3. Multi-temporal satellite data

It was identified in the satellite images and proved by field work: a) that there

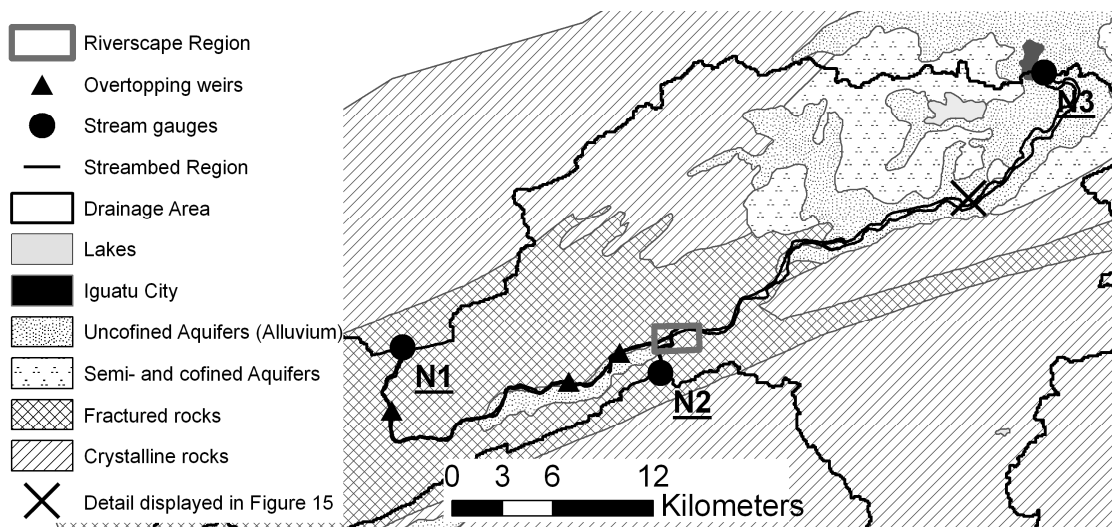
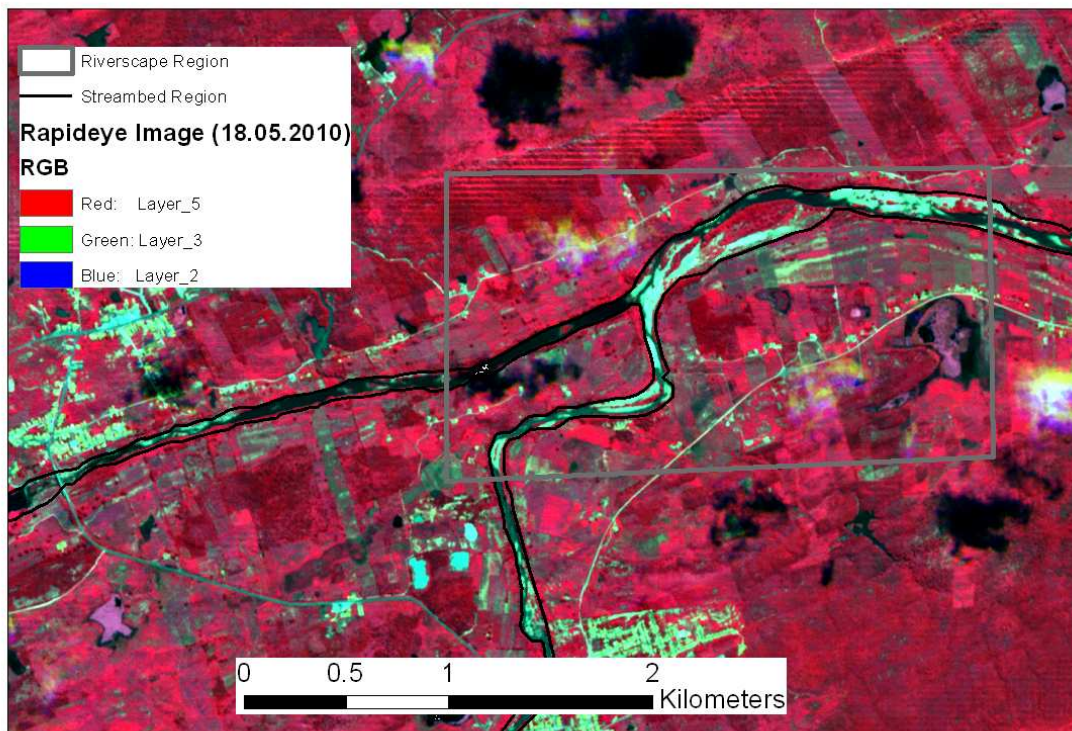


Figure 13. Location of the three overtopping weirs inside MJR.



*Figure 14. The riverscape region, where the characteristics of the MJR changes abruptly from (i) a moderate gradient and stable cross-section stream to (ii) a low gradient and unstable cross-section one. False colour composite image (Red= NIR, Green= red and Blue= green) collected on 18 May 2010.*

The existence of overtopping weirs, which have stored surface water for domestic and agricultural use during the dry seasons, suggested that channel transmission losses might not be relevant upstream of these weirs. Instead, the losses may occur mainly downstream of them, in the large alluvial system characterized by unconfined aquifers (see Fig. 13).

Moreover, we observed connected surface water throughout the whole MJR in the satellite image mosaic collected in 2009 during the dry season (not shown

here), when no flow was registered at the stream gauges. Upstream of the overtopping weirs, the surface water was clearly a result of water retention by them. Downstream of them, the surface water might percolate into the shallow groundwater in the alluvium system.

Water surface within the MJR from the images collected on 20 April 2010 (exactly one day after the peak flow during the rainy season) and on 18 May 2010 (during the flow recession limb) was restricted to the streambed of MJR (Fig. 15).

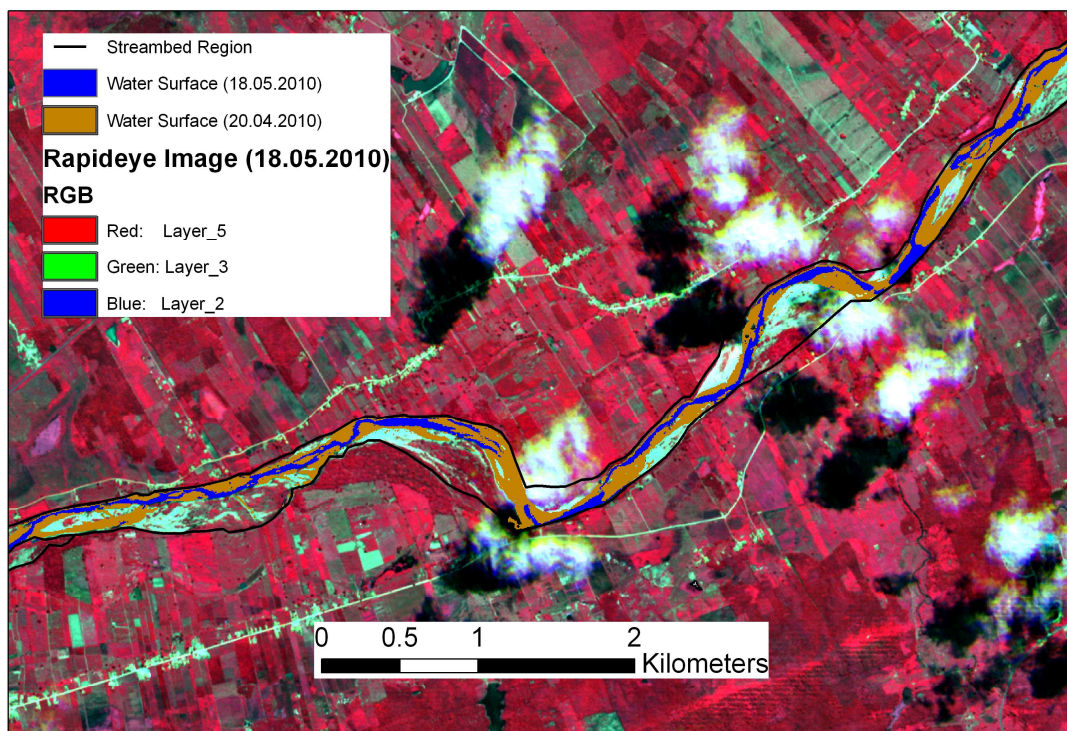


Figure 15. Details of water surface within the MJR from images collected on 20 April 2010 (exactly one day after the peak streamflow during the rainy season) and on 18 May 2010 (during the streamflow recession limb). False colour composite image (Red= NIR, Green= red and Blue= green) collected on 18 May 2010. The location of this Fig. in MJR was displayed in Fig. 13.

In this respect, river flows with a maximum of  $118 \text{ m}^3/\text{s}$  at the N3 stream gauge - the peak flow during the rainy season of 2010 - were certainly confined within the streambed and levees without inundating the floodplains. Hence, channel transmission losses of 24 out of the 27 events analysed previously, which lost their input river flow either completely or partially, infiltrated through streambed and levees only.

Furthermore, a discharge decrease at the N3 stream gauge from  $99.5 \text{ m}^3/\text{s}$  on 20 April 2010 to  $2.4 \text{ m}^3/\text{s}$  on 18 May 2010 (97.6 %) was equivalent to an areal reduction of water surface from 340 ha to 127 ha in the MJR between the overtopping weir furthest downstream and the N3 stream gauge (62.8 %) (see Fig. 13).

We also estimated the river water volumes by combining the image mosaics acquired on 20 April and on 18 May 2010 and the river cross-sections (Fig. 4). Con-



sidering a radius of 500 m centred on the stream gauges N1, N2 and N3, the water volumes (Wetted area  $\times$  1000 m of river length) on 20 April 2010 were  $90 \times 10^3 \text{ m}^3$ ,  $20 \times 10^3 \text{ m}^3$  and  $59 \times 10^3 \text{ m}^3$  for N1, N2 and N3, respectively. The water volumes on 18 May 2010 were  $54 \times 10^3 \text{ m}^3$ ,  $11 \times 10^3 \text{ m}^3$  and  $30 \times 10^3 \text{ m}^3$  for N1, N2 and N3, respectively.

The upstream water volumes (N1 + N2) were reduced in the MJR's outlet (N3) for both cases. Since this reach can be considered a riffle-dominated channel type upstream and a meandering channel type downstream, we assumed river velocity to be greater upstream than downstream. Therefore, these decreases in water volume were likely to lead to a decrease in river discharge, i.e. to channel transmission losses.

This finding agreed with the results presented previously that during the days when the satellite images were acquired, channel transmission losses were occurring (i.e. river water level was exceeding groundwater stages) (Fig. 10).

## 5. Discussion and Conclusion

### 5.1. Hydrological conceptualisation

Channel transmission losses in a 60 km long reach of the Jaguaribe River (MJR) have been analysed by streamflow series, groundwater level series and multi-temporal satellite data. Such losses occur through natural runoff events during the dry and rainy seasons and by man-made runoff events during the dry season, the latter caused by a release of water from upstream surface reservoirs into MJR. The transmission losses take place mainly in a large alluvial system with shallow groundwater extending about 30 km along the MJR. The river-groundwater system in this alluvium can be considered to be hydraulically connected.

The "flow paths" of transmission losses have been analysed. Most transmission losses infiltrated only through streambed and levees and not through the flood plains, as could be shown by satellite image analysis. Moreover, after upstream

discharge events, transmission losses may return to the channel as base flow when the groundwater level is higher than that of the water in the river, as also observed by Lima et al. (2007).

Seventeen natural and man-made runoff events during the dry seasons, whose input flows from the upper stream gauges were smaller than a runoff threshold of  $8.2 \times 10^6 \text{ m}^3$ , did not reach the outlet of MJR due mainly to infiltration into groundwater and secondly to groundwater abstraction. This is a similar finding to that reported by Knighton and Nanson (1994), who found a runoff threshold in the Cooper Creel River in Australia.

A clogging layer in the streambed, which is capable of allowing river flow transmission of small floods as hypothesised by Lange (2005), was not observed in the MJR. Man-made events (reservoir releases) during the dry season in 2010 had no significant influence on the evolution of the groundwater, which may be explained partially by the extraction of groundwater for agricultural use that abstracted roughly between 5% to 10% (maximum values 20% - 40%) of the input flow of these events.

Seven floods between 20 and  $1460 \times 10^6 \text{ m}^3$  at the middle and the end of the rainy seasons reached the outlet, losing on average 30% of their upstream (input) river flow. Input flows which achieve the outlet in the 420 km channel reach of the Cooper Creel River, Australia, lost about 75-80% on average (Knighton and Nanson, 1994) and 60% in the 150 km channel reach of the Kuiseb River, Namibia Desert, (estimated from Table II in Lange, 2005). The Jaguaribe River flows also suffered a reduction of 37% in their input peak flow.

Furthermore, we found that the higher the input river flow, the higher the channel transmission losses (linear behaviour on a log-log scale, see Fig. 8), underlining the major importance of high floods on channel transmission losses. This result is also supported by Knighton and Nanson (1994), Lange et al. (1998) and Lange (2005).

The influence of the floodplains and the effects of clogging layers on the channel transmission losses at the observed high discharges were not observed. However, we could not distinguish whether the hydraulic head at the surface and/or the micro-layering of the alluvial sediments at the streambed control the transmission losses during these high floods.

In total, we analyzed 27 transmission losses events in the MJR over 10 years, which amounts to at least  $880 \cdot 10^6 \text{m}^3$  of water losses. However, since the groundwater at the lower boundary of the MJR area had a slope towards the downstream Orós reservoir of 2.1 m/km (measured in 2010), which is located over the same large alluvium-system that MJR crosses, we hypothesise that the losses to the shallow groundwater system may return to the surface in this downstream reservoir. If this hypothesis is true, the groundwater fluxes to the Orós reservoir need to be considered when estimating its medium-term water budget.

### 5.2. Advantages of the use of remote sensing

The use of satellite data allows identifying the area of the MJR where channel transmission losses take place, hence reducing the spatial uncertainties of the streamflow water balance.

It also reduced the water balance's uncertainties related to the river stage, showing that the streamflow mainly infiltrates within the streambed and the levees.

Moreover, the results showed that channel transmission losses based on the satellite data, combined with the river cross-sections and geomorphologic characteristics, were similar to those derived by using streamflow and groundwater level series. Therefore, the former dataset may allow a rapid and rough estimation of channel transmission losses in ungauged dryland rivers.

### 5.3. Modelling and simulation strategies

Channel transmission losses in MJR can be conceptually described as sketched in Fig. 16:

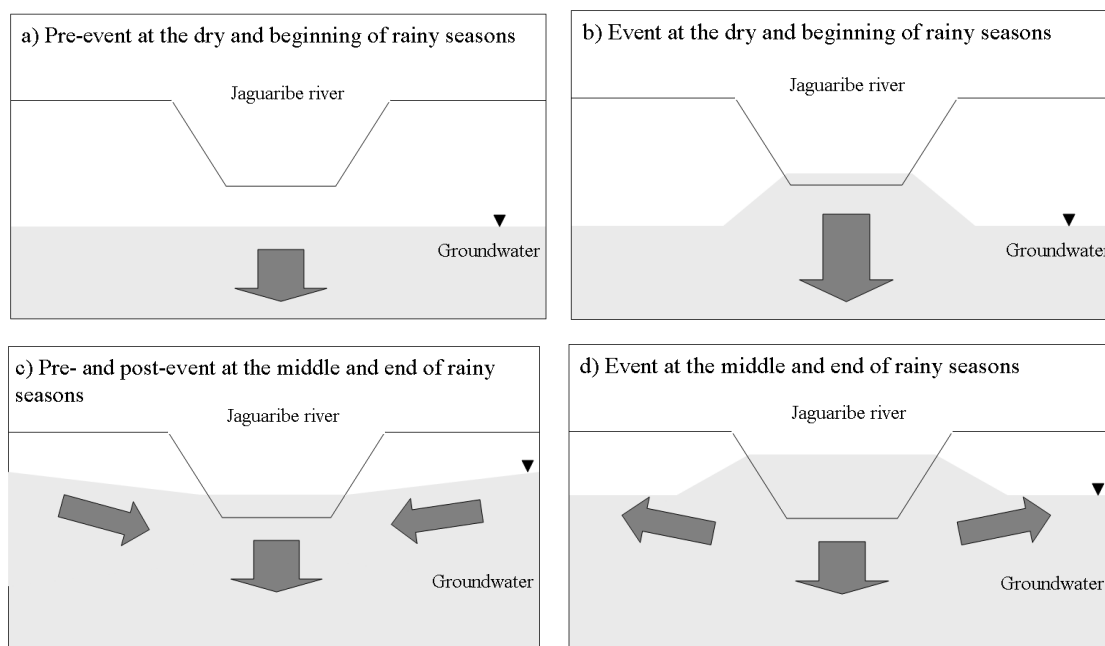


Figure 16. Conceptual description of channel transmission losses in the MJR.

During the dry and at the beginning of rainy seasons, no river flow is expected before a flood event (Fig. 16a) and events

lead to predominantly vertical infiltration into the alluvium (Fig. 16b). At the middle and end of the rainy seasons, river flow

sustained by base flow occurs before and after events (Fig. 16c) and lateral infiltration into the alluvium plays a major role during events (Fig. 16d). Thus, the hydraulically connected Jaguaribe River reach shifts from being a losing river at the dry and beginning of rainy seasons to become a losing/gaining (mostly losing) river at the middle and end of rainy seasons.

Due to this seasonal behaviour, we think that an adequate channel transmission losses model for this system should be based on the leakage approach for river-aquifer interaction (Rushton and Tomlinson, 1979), which allows modelling of connected losing/gaining rivers (see e.g. Xie and Yuan, 2010). The modelling of infiltration into unsaturated strata (e.g. a Green-Ampt approach, as carried out by Abdulrazzak and Morel-Seytoux (1983) and Illangasekare and Morel-Seytoux (1984)) is of minor relevance, because it applies only for hydraulically connected losing rivers, which is rather exceptional in the MJR.

In this way, a conceptual hydrological model based on the identified mechanisms of channel transmission losses in MJR needs to couple surface river water with groundwater, linked by a leakage approach, accounting for variable hydraulic heads at the surface and subsurface. This modelling strategy has been mostly undertaken in humid and temperate catchments (see e.g. Engeler et al., 2011; Krause and Bronstert, 2007) and more rarely in arid and semi-arid ones.

The data scarcity relating to the underlying alluvium and the groundwater extraction rates during the dry seasons might constrain the applicability of distributed groundwater flow models to MJR. Therefore, if more data for groundwater flow modelling are unobtainable, a simplified approach is more appropriate. For example, Niu et al. (2007) simplified the underlying unconfined aquifer as a reservoir, wherein the temporal variation of the water stored in this reservoir is equal to the water balance between recharge and discharge flows.

Partly based on this analysis, Costa et al. (2011) have developed a semi-distributed channel transmission losses model for different dryland rivers. They applied it to the studied Jaguaribe River reach using the conceptual model presented in this research and simulated streamflow volume and peak of selected runoff events.

They also tested different model structures derived from this conceptual model, in order to reduce structural model uncertainties and to guide future field campaigns for the more detailed elaboration of the dominant processes in the MJR. They found that both lateral stream-aquifer water fluxes and groundwater flow in the underlying alluvium parallel to the river course are necessary to predict streamflow and channel transmission losses, the former process being more relevant than the latter.

If a process-based model approach is not appropriate or feasible, an empirical approach, e.g., the relationship shown in Fig. 8, may be applied in order to obtain a rough estimate of transmission losses for the MJR. It may be applied for input river rates between 20 and 1460  $10^6\text{m}^3$  for event-based channel analysis:

$$V_{TL} = 0.230 \cdot V_{IF}^{1.013} \quad (2)$$

where  $V_{TL}$  is transmission losses ( $10^6\text{m}^3$ ) and  $V_{IF}$  is input river flow ( $10^6\text{m}^3$ ). It is clear that only the order of magnitude of  $V_{TL}$  can be expected from such an empirical relationship. Dividing the terms of Eq. (2) by the river reach extension contiguous with the alluvium, about 30 km, one may estimate roughly channel transmission losses per km for similar ungauged hydrogeologic areas.

#### 5.4. Possible further work

A more detailed assessment of subsurface flow conditions requires further groundwater level monitoring and the collection of more information on groundwater extraction from the alluvium, e.g. through interviews with locals and farmers. Another critical point is the derivation of parameters from the alluvium for groundwater

modelling in MJR, in particular the distribution of hydraulic conductivities in the alluvium and in its boundary, and the subsurface geometry of the alluvium.

Based on the depth and the texture information derived from borehole stratigraphies, one may apply an indicator geostatistical approach, as done by Carle and Fogg (1996; 1997) and Carle et al. (1998) for alluvial fans and fluvial deposits in California, USA. However, a rather costly number of new boreholes would have to be drilled in that area.

In this paper, we have shown how satellite images can support the understanding of channel transmission losses in large dryland rivers. The river reach studied has been monitored by stream gauges, however, most of dryland river reaches are ungauged. Therefore, further work may elaborate how far one can infer channel transmission losses in large ungauged dryland rivers based on remotely sensed data. For example, the combination of optical high resolution satellite images, e.g. as undertaken in this work, with high resolution digital elevation models (DEMs) of riverscapes may yield surface water area and volume maps of river reaches. DEM and satellite image based information about riverbed and floodplain may enable the application of Manning's equation to estimate the average flow velocities for different water levels. In that way, the combination of remote sensing based estimates on water volumes and velocities passing through two subsequent river cross sections may allow the estimation of the in-between losses.

Finally the question of how relevant the direct drainage area of a river reach is to the runoff in that river reach may be approached by a process-based hydrological catchment model, with a special emphasis on runoff generation conditions in drylands and possible runoff retention in small surface depressions and/or reservoirs, such as the WASA model, (Guentner and Bronstert, 2004; Guentner et al., 2004). However, this model does not yet include river transmission losses, which is why we plan

to extend its channel flow routine in this respect.

## **6. Acknowledgements**

The first author thanks the Brazilian National Council for Scientific and Technological Development (CNPq) for the PhD-scholarship. We thank the RapidEye Science Archive (RESA) of the German Aerospace Center (DLR) for providing the RapidEye images. We thank the Brazilian Geological Service (CPRM), the Brazilian Water Agency (ANA), the Meteorological and Water Resources Foundation of the State of Ceará (FUNCEME) and the Water Resources Agency of the State of Ceará (COGERH) for the data provided. We also thank the Federal Institute of Education, Science and Technology (IFCE) in Iguatu city for the facilities during the field work, especially Profa. Helba Araújo and student Junior Neto. We profoundly thank Jocasta Bezerra for the monitoring of the observation wells near Iguatu city. We also thank Profa. Eunice M. de Andrade for equipment support and valuable discussions. Finally, the authors are grateful to two anonymous reviewers for their valuable comments on a previous version of this manuscript.

## Chapter III:

# A channel transmission losses model for different dryland rivers

### Abstract

Channel transmission losses in drylands take place normally in extensive alluvial channels or streambeds underlain by fractured rocks. They can play an important role in streamflow rates, groundwater recharge, freshwater supply and channel-associated ecosystems. We aim to develop a process-oriented, semi-distributed channel transmission losses model, using process formulations which are suitable for data-scarce dryland environments and applicable to both hydraulically disconnected losing streams and hydraulically connected losing(/gaining) streams. This approach should be able to cover a large variation in climate and hydro-geologic controls, which are typically found in dryland regions of the Earth. Our model was first evaluated for a losing/gaining, hydraulically connected 30 km reach of the Middle Jaguaribe River (MJR), Ceará, Brazil, which drains a catchment area of 20 000 km<sup>2</sup>. Secondly, we applied it to a small losing, hydraulically disconnected 1.5 km channel reach in the Walnut Gulch Experimental Watershed (WGEW), Arizona, USA. The model was able to predict reliably the streamflow volume and peak for both case studies without using any parameter calibration procedure. We have shown that the evaluation of the hypotheses on the dominant hydrological processes was fundamental for reducing structural model uncertainties and improving the streamflow prediction. For instance, in the case of the large river reach (MJR), it was shown that both lateral stream-aquifer water fluxes and groundwater flow in the underlying alluvium parallel to the river course are necessary to predict streamflow volume and channel transmission losses, the former process being more relevant than the latter. Regarding model uncertainty, it was shown that the approaches, which were applied for the unsaturated zone processes (highly nonlinear with elaborate numerical solutions), are much more sensitive to parameter variability than those approaches which were used for the saturated zone (mathematically simple water budgeting in aquifer columns, including backwater effects). In case of the MJR-application, we have seen that structural uncertainties due to the limited knowledge of the subsurface saturated system interactions (i.e. groundwater coupling with channel water; possible groundwater flow parallel to the river) were more relevant than those related to the subsurface parameter variability. In case of the WEGW application we have seen that the non-linearity involved in the unsaturated flow processes in disconnected dryland river systems (controlled by the unsaturated zone) generally contain far more model uncertainties than do connected systems controlled by the saturated flow. Therefore, the degree of aridity of a dryland river may be an indicator of potential model uncertainty and subsequent attainable predictability of the system.

Resubmitted to *Hydrology and Earth Systems Sciences* as  
Costa, A.C., Bronstert, A., and de Araújo, J.C.: A channel transmission losses model for different dryland rivers, 2012.

## 1. Introduction

Dryland rivers can be classified into a) allogenic rivers, which are sourced almost entirely from upstream humid areas (e.g. the River Nile in Northern Sudan and Egypt) and commonly sustain perennial flow partly infiltrating in the alluvial system along the allogenic river, and b) endogenic rivers, which are sourced almost entirely within dryland environments and usually show an ephemeral (non-baseflow) or intermittent flow (Bull and Kirkby, 2002). Channel transmission losses in drylands occur in both types of dryland rivers. They take place normally in extensive alluvial channels (Renard et al., 2008) or streambeds underlain by fractured rocks (Hughes, 2008). They can play an important role in streamflow rates, groundwater recharge, freshwater supply and channel-associated ecosystems (Goodrich et al., 2004; Blasch et al., 2004; Lange, 2005; Dagès et al., 2008; Wheeler, 2008). The surface hydrological connectivity between dryland catchments and/or upstream and downstream reaches of dryland rivers occurs if and only if the runoff propagated into channels overcomes its transmission losses (based on Beven, 2002; Bracken and Croke, 2007). Consequently, runoff, sediment transport and channel morphology depend on how influential channel transmission losses are (Shannon et al., 2002).

When long time series of streamflow data are available, conceptual models and time series analysis may provide reliable prediction of channel transmission losses (Lane, 1983; Sharma and Murthy, 1994; Sharma et al., 1994; Hameed et al., 1996). However, monitoring of surface flow in dryland rivers is difficult in many regions, due to often low population density, the remoteness of hydrological stations and the inherent short duration of runoff (El-Hames and Richards, 1998). Moreover, extreme climatic variation from year to year, especially variation in annual precipitation, increases the problems of constructing probabilistic models (El-Hames and Richards, 1998). In this context, process-

oriented hydrological models parameterized from field measurements and geo-database maps may be the most suitable or indeed the inevitable tool to predict both streamflow and channel transmission losses (e.g. El-Hames and Richards, 1998; Lange et al., 1999; Gheith and Sultan, 2002; Lange, 2005; Costelloe et al., 2006; Morin et al., 2009).

Channel transmission losses can occur in streams which are hydraulically connected or disconnected with a groundwater system (Sophocleous, 2002; Ivkovic, 2009). Streams which only recharge groundwater are called losing (or influent) streams while those which both recharge and discharge groundwater are called losing/gaining (or effluent) streams (Ivkovic, 2009). Discussion on the hydrological processes involved in channel transmission losses can be found e.g. in Renard (1970), Abdulrazzak and Morel-Seytoux (1983), Knighton and Nanson (1994), Lange et al. (1998), Dunkerley and Brown (1999), Lange (2005), Konrad (2006), Dahan et al. (2007, 2008) and Dagès et al. (2008). From those studies, channel transmission losses may be seen to behave as follows: small sub-bank flows must firstly fill pool abstractions and channel filaments in order to propagate downstream; then bank-full flows infiltrate predominantly into bed and levees; and, at high stream discharges, overbank flows lose water for pools, subsidiary channels and floodplains, but once they become fully saturated, the most direct floodways become fully active and channel transmission losses decrease. However, this behaviour may vary depending on the seasonality, the underlying subsurface water flow and the (micro-)layered structure of alluvial and floodplain sediments.

If the groundwater level is too deep, i.e. below the level of the river bed, seepage flow may be predominantly vertical and unsaturated. In contrast, if there is shallow groundwater present, seepage may be primarily lateral and saturated, effecting the development of a groundwater mound. Depending on the interaction between

stream and groundwater and the variations of the groundwater level, the seepage may even shift from being vertical and unsaturated to being lateral and saturated in the same dryland stream-groundwater system. However, independently of the underlying groundwater, not every flood will result in deep infiltration and, consequently, groundwater recharge, because of lateral subsurface flow dispersion through the layered structure of alluvial sediments (Renard, 1970; Dahan et al., 2007). On the other hand, rapid deep infiltration may be driven by an active preferential flow mechanism that bypasses the porous matrix of the vadose zone (Dahan et al., 2007). Moreover, stream-aquifer exchanges may constitute hyporheic flow as in the case where a stream loses flow to a shallow aquifer that discharges back to the stream in a downstream reach due to decrease in aquifer thickness, aquifer narrowing and/or decrease in aquifer hydraulic conductivity (Konrad, 2006). In this way, the groundwater table rises due to the upstream groundwater recharge (Dahan et al., 2007).

Hydrological modelling of channel transmission losses for hydraulically (dis)connected losing/gaining streams has been based on the concept of leakage coefficient (Rushton and Tomlinson, 1979), which has been used to model the water fluxes between stream and (shallow) groundwater flows (see e.g. applications in Krause and Bronstert, 2007; Xie and Yuan, 2010; Engeler et al., 2011). This approach has been successfully applied to catchments and river reaches, especially in temperate and humid regions, linking distributed river and groundwater flow models. However, the leakage coefficient concept fails to model disconnected losing streams, because it neglects unsaturated flow through the alluvium (Brunner et al., 2010).

Hydraulically connected losing streams can also be modelled using the Green-and-Ampt infiltration approach (Abdulrazzak and Morel-Seytoux, 1983). However, the Green-and-Ampt infiltration approach turns on an equation without analytical

solution for disconnected streams, because in-channel ponding depth and gravitational terms are time-dependent (Freyberg et al., 1980). To overcome this difficulty, Freyberg (1983) proposed a numerical solution (trapezoidal quadrature) of the Green-and-Ampt equation for a uniform alluvium. His algorithm was initiated by the analytic solution to a non-gravity approximation due to the singularity in infiltration rate at time equal to zero and the inadequacy of the trapezoidal quadrature for rapid rate of change in infiltration rate at small time steps (Freyberg, 1983). Therefore, unsaturated flow through the alluvium, together with in-channel variable ponding depth, hampers a transmission losses model for disconnected losing streams. An extra difficulty might be the existence of an underlying stratified alluvium, which can often be found in dryland riverscapes (Parisopoulos and Wheeler, 1992; El-Hames and Richards, 1998).

Another approach for disconnected losing streams is the Smith-Parlange infiltration equation used in KINEROS2 model, which is based on an approximate solution of the basic equation of unsaturated flow (Smith et al., 1995; Semmens et al., 2008). The model requires basically three parameters (the integral capillary drive, the field effective saturated hydraulic conductivity and soil water content) to describe the infiltration behaviour, but the underlying soil profile can only be represented by two-layers with each layer allowed to have different infiltration parameters (Smith et al., 1995; Semmens et al., 2008).

Pressure-head-based Richards' equation enables us to model unsaturated flow through the alluvium considering both in-channel variable ponding depth and stratified alluvium as done by El-hames and Richards (1998). This might be the most physically comprehensive approach to model channel transmission losses for disconnected losing streams. However, its application can require a long processing time to simulate large- and meso-scale catchments (El-hames and Richards, 1998) and large sets of alluvium data, which are

usually not available, especially in dryland environments. Alternatively, some authors have used constant infiltration rates in the channels (Lange et al., 1999; Morin et al., 2009) neglecting both in-channel variable ponding depth and unsaturated flow.

In this paper, we present a process oriented and semi-distributed channel transmission losses model using process formulations which are suitable for data-scarce dryland environments, applicable for both hydraulically disconnected losing streams and hydraulically connected losing(/gaining) streams in dryland environments, considering a possible transition between the two states. Hence, this approach should be able to cover a large variation in climate and hydro-geologic controls, which are typically found in dryland regions of the Earth. We expect this new model to be able to predict the order of magnitude of the hydrograph volume and peak, both variables being relevant for water planning and management in arid and semi-arid environments. However, note that we do not focus specifically on the prediction of the timing of the hydrograph peak, i.e. this model is not aiming at flood forecasting in dryland regions.

Our channel transmission losses model is first evaluated for an intermittent 30 km reach of the Middle Jaguaribe River (MJR), Ceará, Brazil, which drains a catchment area of 20 000 km<sup>2</sup>. Secondly, we apply it to an ephemeral small 1.5 km channel reach in the Walnut Gulch Experimental Watershed (WGEW), Arizona, USA, which is well-known for its long-term database of semi-arid hydrology and studies on channel transmission losses (e.g. Renard, 1970; Renard et al., 2008; Stone et al., 2008). The MJR is a losing/gaining (mostly losing) river and hydraulically connected to the groundwater system; the small reach in the WGEW on the other hand is a losing stream and hydraulically disconnected to the groundwater system.

The application of the model to these channel reaches will be undertaken in order to evaluate the model capabilities in two rather different dryland environments.

Also, we will test hypotheses on the dominant hydrological processes with a view to generating insights into process functioning through comparisons of model performance (Savenije, 2009; Graeff et al. 2009, Buytaert and Beven, 2011; McMillan et al., 2011; Clark et al., 2011; Li et al., 2010).

Although increasing efforts have been made in the acquisition of remote sensing data, which have been used to derive e.g. precipitation data, soil moisture data, digital elevation models (DEMs), land-cover maps and river networks (see e.g. Milewski et al., 2009), the applicability of process-oriented, distributed hydrological models to arid and semi-arid catchments is still only feasible in exceptional cases due to generally sparse data, and high spatial variability, of surface and subsurface systems (see e.g. Al-Qurashi et al., 2008). Therefore, we want to analyse the applicability and predictive capability of our model by both individual parameter sensitivity analysis and an overall model parameter uncertainty analysis.

## **2. Modelling of Channel Transmission Losses**

Conceptually, we consider the following processes, which have been shown experimentally to be the most influential for channel transmission losses (see discussion in introduction):

- a) streamflow in natural rivers;
- b) unsaturated seepage under in-channel variable ponding depth through a stratified alluvium;
- c) vertical unsaturated subsurface water redistribution beneath the stream;
- d) lateral (stream-)aquifer interaction, which includes the development of a groundwater mound and;
- e) groundwater flow, parallel to the river course, in unconfined aquifers.

We establish possible in/outflow through the different boundaries of the modelled system, such as surface and subsurface inflow from the landscape adjacent to the river corridor, evapotranspiration from the streambed and groundwater ex-



traction by root water uptake. These fluxes might be external hydrological process models or prescribed as scenarios. The model structure is composed of five spatial components, which we consider to represent an appropriate spatial model scale for

the governing processes and which enables a spatial coupling of the sub-models of the processes, see Fig. 1 for a schematic overview.

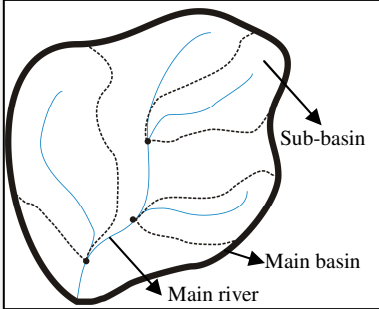
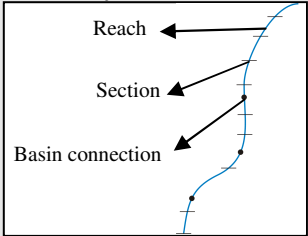

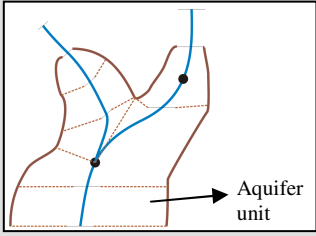

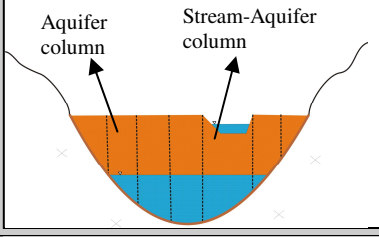

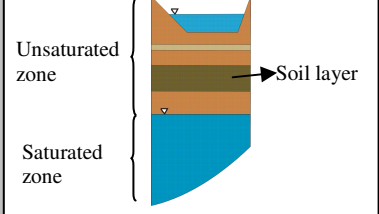

Component	Spatial evolution/ Process	Sub-model
<p><b>1 Basin system:</b></p> 	<p>Distribution of streamflow generated from sub-basins into the main river</p>	<p>In-basin streamflow distribution</p>
<p><b>2 River system:</b></p> 	 <p>Streamflow in natural rivers</p>	<p>Flood wave routing</p>
<p><b>3 Aquifer system:</b></p> 	 <p>Groundwater flow, parallel to the river course, in unconfined aquifers, which takes place beyond the basins' limits</p>	<p>Groundwater flow model</p>
<p><b>4 Aquifer unit:</b></p> 	 <p>Lateral (stream-)aquifer interaction, including the development of a groundwater mound</p>	<p>Lateral (stream-)aquifer dynamics model</p>
<p><b>5 Stream-aquifer column:</b></p> 	 <p>Unsaturated seepage under in-channel variable ponding depth through a stratified alluvium and vertical subsurface water redistribution beneath the stream</p>	<p>Unsaturated stream infiltration and vertical soil water redistribution models</p>

Figure 1. Spatial components of the model structure, which link the sub-models of the governing processes involved in channel transmission losses.

The whole channel transmission losses model includes six interacting sub-models for the aforementioned governing processes, which are presented in detail in sections 2.1 to 2.5. and schematicised in Fig. 2.

The calculation begins with the flood wave routing without stream-aquifer interaction, i.e. we predict firstly streamflow and stream water stage excluding stream-aquifer interaction fluxes. Then, we use these predicted “intermediate” values of streamflow and water stage to run the other sub-models (2, 3, 4 and 5), which estimate a) the stream-aquifer interaction flux and b) the moisture in the underlying aquifer. Afterwards, we apply the streamflow routing again, but now with the estimated stream-aquifer interaction flux, to predict finally the streamflow and water stage at the end of the time step. This kind of solution of streamflow and water stage is a two-step procedure, which was discussed

e.g. by Mudd (2006) and Bronstert et al. (2005).

As long as the stream-aquifer column is not saturated, the stream and groundwater flows are hydraulically disconnected, while channel transmission losses are dominated by the unsaturated zone beneath the stream. Once the stream-aquifer column has been saturated, the stream and groundwater turn into a hydraulically connected system, wherein channel transmission losses are driven by the saturated zone, which either can discharge to or recharge from the stream.

The following sub-sections 2.1 to 2.5 describe the physical assumptions and the main mathematical formulations for the sub-models of our channel transmission losses model. We detail the stream-aquifer interaction calculation in the Sect. 2.6. Finally, we summarize the information required to run the model (both input data and model parameters) in Sect. 2.7.

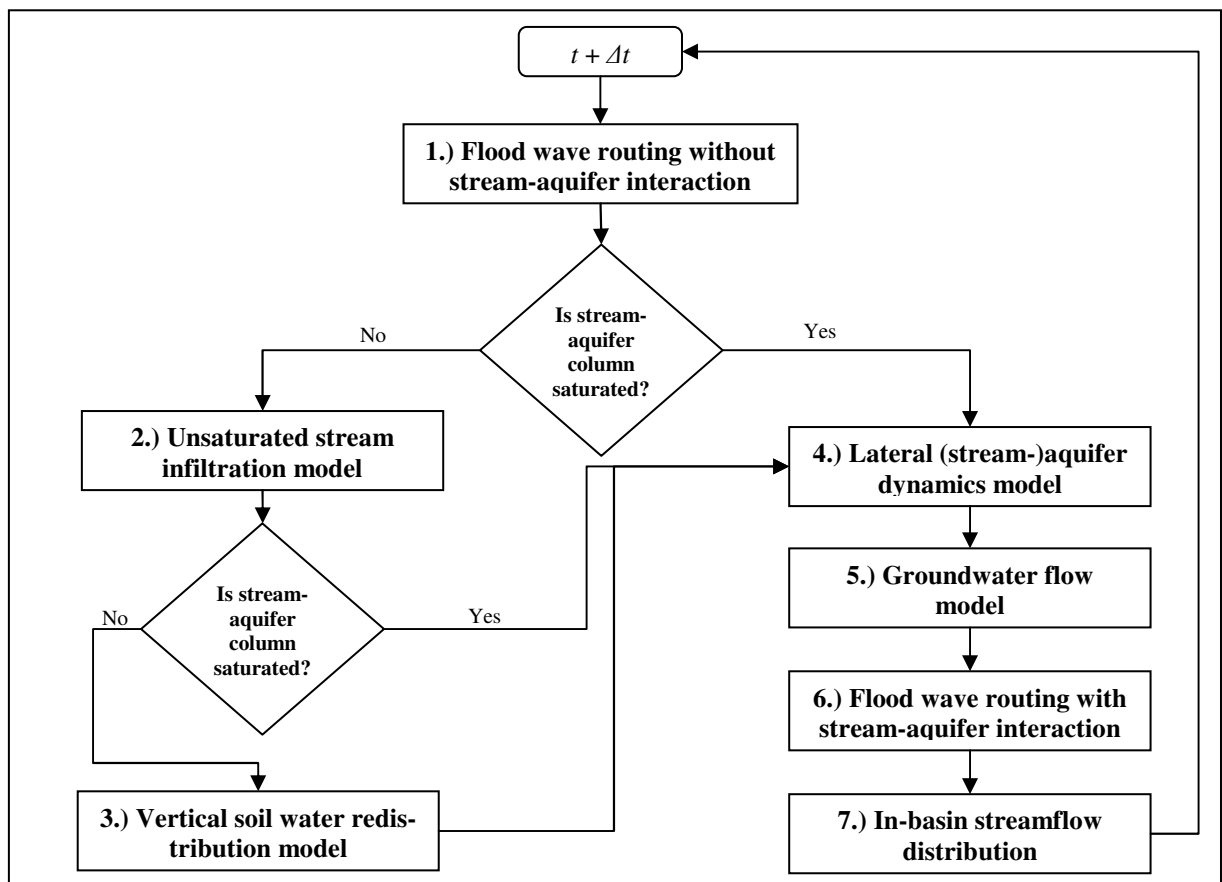


Figure 2. Interplay and temporal sequence of model approaches, where  $t$  is time.

### 2.1. Flood wave routing

Normally the full Saint-Venant equations and its simplified diffusion analogy form are applied to simulate streamflow in a natural drainage network, when the up- and downstream boundary conditions are available. However, most dryland streams have no “fixed” downstream boundary conditions because many hydrographs end somewhere between initial streamflow and an assumed outlet, which is normally ungauged. Moreover, sparse monitoring can mean that entire drainage network from the initial streamflow is completely ungauged. Furthermore, simple routing approaches such as the Muskingum-method and the Manning-formula may yield poor approximation of the river dynamics when both inertial and pressure forces are important, such as in mild-sloped rivers, and backwater effects from downstream disturbances are not negligible (see Chow et al., 1988). Therefore, we propose here an alternative flood wave routing.

First, we use a form of conservation of mass equation:

$$\frac{\partial Q}{\partial x} + s \frac{\partial A}{\partial t} = q + I_{RA} \quad (1)$$

where  $t$  is the time (T),  $x$  is the length along the channel axis (L),  $Q$  is the stream discharge ( $L^3.T^{-1}$ ),  $A$  is the wetted cross-sectional area ( $L^2$ ),  $s$  is the sinuosity coefficient (dimensionless),  $q$  is the lateral inflow per unit of length of channel ( $L^3.T^{-1}.L^{-1}$ ) and  $I_{RA}$  is the stream-aquifer interaction term per unit of length of channel ( $L^3.T^{-1}.L^{-1}$ ), which can be stream infiltration (negative) or groundwater discharge (positive).

Applying the four-implicit numerical scheme (see Fread, 1993) to (1), yields

$$Q_{i+1}^{j+1} = Q_i^{j+1} - \frac{(1-\theta)}{\theta} (Q_{i+1}^j - Q_i^j) + \frac{\Delta x_i}{\theta} \left[ \bar{q} + I_{RA} - s \frac{(A_{i+1}^{j+1} + A_i^{j+1} - A_{i+1}^j - A_i^j)}{2.\Delta t_j} \right] \quad (2)$$

where  $j$  and  $i$  are indexes of time and stream section, respectively, and  $\theta$  is a weighting factor for the spatial derivative.

Equation (2) has two unknown variables: the stream discharge and the wetted cross-sectional area (related to the stream water stage) at the future time and at the next stream section:  $Q(j+1, i+1)$  and  $A(j+1, i+1)$ , respectively.

Since, in natural streams, the channel morphology is a function of both the short and the long term stream hydrology, the channel cross-section is a function of the past and upstream flood events. It means that all the information (e.g. change in the velocity, in the water depth and in the bed slope) for the future and further stream discharge  $Q(j+1, i+1)$  is already “imprinted on” the wetted cross-sectional area  $A(j+1, i+1)$ . Taking this hypothesis into account, we get all the states for  $A(j+1, i+1)$  and substitute into (2) to find possible states for  $Q(j+1, i+1)$  according to the conservation of mass equation. Then, we average over the possible states of  $Q(j+1, i+1)$  and  $A(j+1, i+1)$ , which obey the following simple physical rules

$$\begin{cases} Q_{i+1}^{j+1} \geq 0 \\ \text{if } Q_i^{j+1} < Q_{i+1}^{j+1}, \text{ then } A_i^{j+1} < A_{i+1}^{j+1} \\ \text{if } Q_i^{j+1} > Q_{i+1}^{j+1}, \text{ then } A_i^{j+1} > A_{i+1}^{j+1} \\ \text{if } Q_{i+1}^{j+1} \neq 0, \text{ then } A_{i+1}^{j+1} \neq 0 \\ \text{if } Q_{i+1}^{j+1} = 0, \text{ then } A_{i+1}^{j+1} = 0 \end{cases} \quad (3)$$

Equation (3) can be seen as a physical filter of the states for  $Q(j+1, i+1)$  and  $A(j+1, i+1)$ . It can be applied for both stream stretches in sub-basins and for the main river stretch, see Fig. 1. If the next stream section is the last section in a sub-basin, the calculated stream discharge at this section, i.e. the catchment runoff from the sub-basin, is added as lateral inflow into the reach of the main river stretch.

The *Courant-Friedrichs-Lewy* (CFL) condition may be used as a condition for numerical stability

$$\Delta t_{sim} \leq \frac{\Delta x_{min}}{v_{max}} \quad (4)$$

where  $v_{max}$  is the maximum expected stream velocity ( $L.T^{-1}$ ),  $\Delta x_{min}$  is the minimum stream reach and  $\Delta t_{sim}$  is the time step (T) for simulation.

This simplified formulation for flood-wave dynamics in dryland rivers is, however, able to mimic loop rating curves and backwater effects, which have been observed during the unsteady, non-uniform flow propagation along natural streams. We expect that hydrograph uncertainties (e.g. timing of the hydrograph) will inevitably arise because of the very high dependence of flow velocity on the actual channel cross-sections and roughnesses, whose data may be highly variable with time (affected by the seasonality of riverine vegetation or by previous flood events) and such data may be rarely available and whose seasonal and long-term changes between different simulation periods might not be measured.

## 2.2. Unsaturated stream infiltration model

We adapt here the modified Green-and-Ampt model proposed by Chu and Mariño (2005), because we consider it a suitable compromise between computation time, data requirement and simplifying assumptions (e.g. constant infiltration rates). The alluvium beneath the stream (Fig. 1) consists of  $N$  layers with hydraulic conductivities  $K_N$  ( $L.T^{-1}$ ), wetting-front suctions  $\psi_N$  (L), porosities  $\eta_N$  ( $L^3.L^{-3}$ ), initial soil moisture  $\theta_N$  ( $L^3.L^{-3}$ ) and depths of cumulative infiltration  $z_N$  (L). When the wetting front is in a layer  $y$  at location  $z$  ( $Z_{y-1} < z \leq Z_y$ ), the governing equations are

$$f_z = \frac{H_0 + z + \psi_y}{\sum_{k=1}^{y-1} \frac{Z_k - Z_{k-1}}{K_k} + \frac{z - Z_{y-1}}{K_y}} \quad (5)$$

$$F_z = F_{z_{y-1}} + (z - Z_{y-1})(\eta_y - \theta_y) = \sum_{k=1}^{y-1} (Z_k - Z_{k-1})(\eta_k - \theta_k) + (z - Z_{y-1})(\eta_y - \theta_y) \quad (6)$$

$$f_z = \frac{dF_z}{dt} = (\eta_y - \theta_y) \frac{dz}{dt} \quad (7)$$

where  $f$  is the infiltration rate ( $L.T^{-1}$ ),  $F$  is the cumulative infiltration (L),  $t$  is the time for the wetting front to arrive at location  $z$  and  $H_0$  is the hydraulic head at surface (L),

which was admittedly negligible in Chu and Mariño's formulation because their focus was on hillslope hydrology. Substituting Eq. (5) into (7) yields

$$\frac{H_0 + z + \psi_y}{\sum_{k=1}^{y-1} \frac{Z_k - Z_{k-1}}{K_k} + \frac{z - Z_{y-1}}{K_y}} = (\eta_y - \theta_y) \frac{dz}{dt} \quad (8)$$

Separating (8), since the hydraulic head at the surface is constant at a certain time step, we have

$$\int_{t_{z_{y-1}}}^{t_z} dt' = (\eta_y - \theta_y) \times \int_{z_{y-1}}^z \frac{\left( \sum_{k=1}^{y-1} \frac{Z_k - Z_{k-1}}{K_k} + \frac{z' - Z_{y-1}}{K_y} \right)}{H_0 + z' + \psi_y} dz' \quad (9)$$

Solving (9):

$$t_z = t_{z_{y-1}} + \frac{(\eta_y - \theta_y)(z - Z_{y-1})}{K_y} + (\eta_y - \theta_y) \times \left[ \sum_{k=1}^{y-1} Z_k \left( \frac{1}{K_k} - \frac{1}{K_{k+1}} \right) - \frac{\psi_y + H_0}{K_y} \right] \times \ln \left( \frac{z + \psi_y + H_0}{Z_{y-1} + \psi_y + H_0} \right) \quad (10)$$

which is similar to the equation of the travel time of the wetting front from Chu and Mariño (2005), but with the hydraulic head at surface  $H_0$ . We use (5) and (10) to estimate the actual infiltration and the location of the wetting front  $z$ .

Before applying the above procedure to the next time step, when we have a new hydraulic head at the surface, the initial soil moisture has to be updated according to the location  $z$  ( $Z_{y-1} < z \leq Z_y$ ) of the wetting front using

$$\theta_y^{j+1} = \begin{cases} \eta_y, & \text{for } z \leq Z_{y-1} \\ \frac{\eta_y \cdot (z - Z_{y-1}) + \theta_y^j \cdot (Z_y - z)}{Z_y - Z_{y-1}}, & \\ \text{for } Z_{y-1} < z \leq Z_y \\ \theta_y^j, & \text{for } z > Z_y \end{cases} \quad (11)$$

In this model, the hydraulic head at the surface (the upper boundary condition) is the average "intermediate" predicted values of stream water stage obtained from the solution of the flood wave routing (Sect. 2.1). The lower boundary condition

is a layer, which can either represent fractured bedrocks (time independent) or be the soil layer immediately above the groundwater level (time dependent).

Once the wetting-front achieves the lowest layer, a hydraulically connected *stream-lowest layer* should now be considered and a groundwater mound is to be developed (Sect. 2.4). In contrast, the wetting-front flows vertically downward to the lowest layer (Sect. 2.3). For the first case, the infiltration rate tends to be constant and the capillary head zero as in Chu and Mariño (2005). Equation (5) can be rewritten as

$$f_{z_N} = \frac{H_0 + Z_N}{\sum_{k=1}^N \frac{Z_k - Z_{k-1}}{K_k}} \quad (12)$$

where  $Z_N$  is the depth of the considered alluvium profile above the groundwater level and  $f_{z_N}$  is the infiltration rate for a hydraulically connected surface-boundary condition system. The infiltration rate from unsaturated to saturated regime can be formulated as

$$f_{unsat-sat} = \frac{t_z \cdot f_z}{\Delta t} + \frac{(\Delta t - t_z) \cdot f_{z_N}}{\Delta t} \quad (13)$$

where  $\Delta t$  is the time step. Note that the second element of the right term of Eq. (13) represents the first recharge to groundwater, if it exists, before the development of a groundwater mound.

### 2.3. Vertical soil water redistribution model

In most unsaturated zone studies, the fluid motion is assumed to obey the classical Richards' equation (Hillel, 1980) and its 1-D soil moisture-based form is shown in the first two terms of Eq. (14), which is applicable in homogeneous media only and requires soil head-conductivity-moisture curves. We use here a simplification of the classical equation, which allows application in unsaturated heterogeneous media and needs less fitting parameters than the original form. First, we neglect the pressure head term  $\psi(\theta)$  in (14), but we assume that percolation from one soil layer to the

next layer below occurs if and only if the actual soil moisture exceeds soil moisture at field capacity  $\theta_{fc}$ . This assumption was also used in other hydrological models (e.g. Arnold and Williams, 1995; Güntner and Bronstert, 2004), leading to

$$\frac{\partial \theta}{\partial t} = \frac{\partial}{\partial z} K(\theta) \frac{\partial [\psi(\theta) + z]}{\partial z} \approx \frac{\partial}{\partial z} K(\theta) \quad (14)$$

We include in (14) the actual soil evaporation  $Eva$  for the upper soil layers and the actual evapotranspiration  $Eta$  for the soil layers in the root zone, in the case of existence of in-channel associated or riparian vegetation, which may be important for eco-hydrological studies and may allow insights into the relationship between channel transmission losses, in-alluvium temporal water storage and ecological water demand. Furthermore we apply an explicit finite difference scheme to it:

$$\frac{\theta_k^{j+1} - \theta_k^j}{\Delta t} = \frac{K_{k-(1/2)}^j - K_{k+(1/2)}^j}{\underbrace{\Delta z}_{Percolation}} - \frac{\underbrace{Eta_k^{j+1,j} + Eva_k^{j+1,j}}_{Transpiration}}{\Delta z} \quad (15)$$

where  $k$  and  $j$  are indexes of depth and time, respectively. The percolation terms of (15) are solved as follows

$$K_{k+(1/2)}^j = \begin{cases} \min \left\{ \frac{\overbrace{\Delta z \cdot (\theta_k^j - \theta_{fc,k})}^{in-layer drainable water}}{\Delta t}; \sqrt{K_k(\theta_k^j) \cdot K_{k+1}(\theta_{k+1}^j)} \right\}, \\ \text{for } \theta_k^j > \theta_{fc,k} \\ 0, \text{ for } \theta_k^j \leq \theta_{fc,k} \end{cases} \quad (16)$$

$$K_{k-(1/2)}^j = K_{(k-1)+(1/2)}^j \quad (17)$$

where  $K(\theta)$  is the unsaturated hydraulic conductivity, which is approached by the Brooks-and-Corey equation (see Rawls et al., 1993):

$$K(\theta) = K_{sat} \left( \frac{\theta - \theta_r}{\eta - \theta_r} \right)^{3 + \frac{2}{\lambda}} \quad (18)$$

where  $K_{sat}$  is the saturated hydraulic conductivity ( $L.T^{-1}$ ),  $\theta_r$  is the residual water

content ( $L^3.L^{-3}$ ) and  $\lambda$  is the pore size distribution index (-).

Note that if the lower layer ( $k+1$ ) is groundwater, there is a recharge to groundwater before the development of a groundwater mound because of the vertical movement of the soil water.

A separate hydrological catchment model can provide the potential soil evaporation and the potential evapotranspiration. Then, we assumed that evapotranspiration and soil evaporation occur if and only if the actual soil moisture exceeds soil moisture at permanent wilting point  $\theta_{pwp}$  and at hygroscopic water  $\theta_{ha}$ , respectively. The computation begins with percolation, followed by an updating of  $\theta_k^j$  and then the transpiration calculation.

#### 2.4. Lateral (stream-)aquifer dynamics model

We consider that each aquifer unit is formed by  $M$  columns, which may consist of saturated and unsaturated zones (Fig. 1). All these columns can be stratified such as that below the stream (Sects. 2.2 and 2.3). The lateral flow between the columns is considered saturated; consequently, we do not account for lateral unsaturated flow. Our aim is to predict in-column groundwater level (stream and groundwater levels for stream-aquifer columns), comparing the hydraulic heads between two column neighbours. During a time step, the calculation begins from the centre of the stream-aquifer column to the right (or the left) lateral boundary conditions (Fig. 1).

First, we calculate the hydraulic head of two column neighbours at the equilibrium ( $h_e$ ), i.e.

$$h_e(A, A+1) = \frac{Cw_A h_A + Cw_{A+1} h_{A+1}}{Cw_A + Cw_{A+1}} \quad (19)$$

where  $A$  is the column index (-),  $h$  is the in-column hydraulic head (L) and  $Cw$  is the column width (L). Then, assuming a subsurface water flow velocity similar to the order of magnitude of the lateral saturated hydraulic conductivity, we estimate the necessary time ( $dt_e$ ) to reach that equilibrium head using

$$dt_e = \frac{|h_e(A, A+1) - h_{A+1}|}{\bar{K}_{A+1}} \quad (20)$$

where  $\bar{K}_{A+1}$  is an average lateral saturated hydraulic conductivity from the actual head to the equilibrium ones ( $L.T^{-1}$ ). If  $dt_e$  is equal to or smaller than the simulation time step  $\Delta t_{sim}$ , then the heads of the column neighbours reach the equilibrium head, otherwise

$$h_{A+1}^* = h_{A+1} + \frac{\Delta t_{sim}}{dt_e} [h_e(A, A+1) - h_{A+1}] \quad (21)$$

where  $h_{A+1}^*$  is the new hydraulic head of column  $A+1$  due to the exchanges with the column  $A$ . Afterwards, the column  $A+1$  with the new hydraulic head  $h_{A+1}^*$  will interact with its next neighbour  $A+2$ .

#### 2.5. Groundwater flow parallel to the river

We use a simple water balance-based approach (similar to Niu et al., 2007) in order to simulate groundwater flow between aquifer units parallel to the river course (see Fig. 1)

$$\frac{\partial S_{GW}}{\partial t} = \underbrace{(Q_{Up,GW} + Q_{V,Inf} + Q_{La,GW})}_{Inflow} - \underbrace{(Q_{Do,GW} + Q_S + Q_{V,DP})}_{Outflow} \quad (22)$$

where  $S$  is the groundwater storage in the aquifer unit ( $L^3$ ),  $Q_{Up,GW}$  and  $Q_{La,GW}$  are the upstream and the lateral groundwater flow from other aquifer units ( $L^3.T^{-1}$ ), respectively, which are known from a previous time,  $Q_{V,Inf}$  is the vertical channel transmission losses ( $L^3.T^{-1}$ ), which come from unsaturated seepage (Sect. 2.2) or unsaturated soil water redistribution (Sect. 2.3),  $Q_{Do,GW}$  is the downstream groundwater flow ( $L^3.T^{-1}$ ),  $Q_S$  is a sink term ( $L^3.T^{-1}$ ), which can be groundwater pumping and/or transpiration, and  $Q_{V,DP}$  is the vertical deep percolation ( $L^3.T^{-1}$ ), which is considered a constant (in)outflow. The downstream groundwater flow between aquifer units is estimated as follows

$$Q_{Do,GW} = \frac{\overbrace{\min\left(\bar{h}_{u+1} - \bar{h}_u / \bar{K}_u; \Delta t_{sim}\right)}^{\text{Time Factor}}}{\Delta t_{sim}} \quad (23)$$

$$\times \bar{K}_u \frac{\bar{h}_{u+1} - \bar{h}_u}{dx_u/2} \cdot \bar{h}_u \cdot W_u$$

where  $u$  is an index of aquifer unit,  $\bar{h}$  is the average groundwater head of the aquifer unit (L),  $W$  is the aquifer unit width (L),  $dx_u$  is the aquifer unit length (L),  $\bar{K}$  is the average aquifer unit saturated hydraulic conductivity ( $L.T^{-1}$ ). Note that the downstream groundwater flow is compensated by a time factor, which is adopted similarly as was done in the previous section. The upstream boundary conditions are a constant flux. The user can define the downstream boundary conditions a) as no-flow or b) assuming that the gradient of the most downstream aquifer unit is equal to its closest upstream one.

After the estimation of aquifer water balance components, the difference between aquifer inflow and outflow is distributed for each column of the aquifer unit as follows

$$Q_{In(Out),A} = \frac{\partial S_{GW}}{\partial t} \cdot C_{W_A}}{W_U} \quad (24)$$

where  $Q_{in(out),A}$  is the in-column inflow or outflow from the aquifer water balance ( $L^3.T^{-1}$ ). If  $Q_{in(out),A}$  is inflow, than the updating of in-column groundwater level due to the aquifer water balance is modelled by

$$Q_{In(Out),A} = \frac{\sum_{c < k \leq b-1} (Z_{k+1} - Z_k) (\eta_{k+1} - \theta_{k+1})}{\Delta t_{sim}} \quad (25a)$$

where  $Z$  is depth (L),  $\eta$  is the porosity ( $L^3.L^{-3}$ ) and  $\theta$  is the soil moisture ( $L^3.L^{-3}$ ),  $c$  is the actual groundwater level and  $b$  is the new groundwater level. On the other hand, if  $Q_{in(out),A}$  is outflow, than

$$|Q_{In(Out),A}| = \frac{\sum_{b < k \leq c-1} (Z_{k+1} - Z_k) (\eta_{k+1} - \theta_{fc_{k+1}})}{\Delta t_{sim}} \quad (25b)$$

where  $\theta_{fc}$  is the soil moisture at field capacity ( $L^3.L^{-3}$ ).

Moreover, we assume that if the soil in the floodplains adjacent to the river reaches will be completely saturated, i.e.

“groundwater head” in the floodplains will rise above the terrain surface, the excess water does not flow into the river course, because it will be temporarily stored on the floodplain surface and then evaporate. We consider this assumption being appropriate because the floodplains are usually very wide and the depth of possible surface excess water is very shallow (a few centimetres at most). Therefore, we do not model in detail flow processes on the floodplain, instead assume that this excess water will evaporate soon.

## 2.6. Stream-aquifer interaction calculation

The stream-aquifer interaction term per unit of length of channel  $I_{RA}$  ( $L^3.T^{-1}.L^{-1}$ ) (Sect. 2.1) can be estimated by

$$I_{RA} = \begin{cases} -\min[\bar{h}_s / \Delta t_{sim}; |f^*|] \cdot \bar{P}_s, \\ \text{for } f^* < 0 \\ f^* \cdot \bar{P}_s, \text{ for } f^* \geq 0 \end{cases} \quad (26)$$

where  $\bar{h}_s$  and  $\bar{P}_s$  are the average stream water stage and wetted perimeter, respectively, and  $f^*$  is the potential infiltration determined in Sect. 2.2 as long as the stream-aquifer column is not saturated. Once the stream-aquifer layer is saturated, then  $f^*$  is calculated as follows

$$f^* = \frac{\Delta h^*}{\Delta t_{sim}} \quad (27)$$

where  $\Delta h^*$  is the increase or decrease difference of the hydraulic head in the stream-aquifer column determined using Eq. (21) in Sect. 2.4.

If all the available stream water is to be infiltrated, then we apply no flood wave routing and set the predicted stream discharge and wetted cross-sectional area (related to stream water stage) equal to zero, in order to avoid numerical fluctuations when we use the stream-aquifer interaction term in the flood wave routing.

## 2.7. Required input data, boundary conditions and model parameters

In this section, we summarize the initial conditions, the boundary conditions and

the model parameters of the approach presented in the previous sub-sections. The initial conditions for the flood wave routing of the river system are the initial stream discharge, wetted area, wetted perimeter and water level. The soil moisture in the unsaturated zone and the groundwater level in the aquifer columns (see Fig. 1) are also required initially to run the model.

The streamflow series of the uppermost river sections (see Fig. 1, river system) are the external boundary conditions for the flood wave routing in the river system (Sect. 2.1), while the lowest boundary conditions are not necessary to run it (Sect. 2.1). The groundwater flow model of the aquifer system (Fig. 1) can have the groundwater (in)outflows as the uppermost boundary condition (Sect. 2.5). In contrast, its downmost boundary condition is defined as no-flow or assuming that the gradient of the downmost aquifer unit is equal to its closest upstream one (see Sect. 2.5). The internal boundary conditions of the

groundwater flow model are the groundwater pumping and the transpiration in the aquifer units (Sect. 2.5).

In the case of simulation at the basin-scale, one can include the surface flow from the small tributaries or from the hillslopes between the river cross-sections for the flood wave routing (Sect. 2.1) and the in-channel potential soil evaporation and evapotranspiration for the vertical soil water redistribution model (Sect. 2.3) as internal boundary conditions.

The parameters required to run the channel transmission losses model using all its model components are shown in Table I. The simulation domain, where the model parameters are distributed, are provided after a spatial discretization of the case study (basin or river reach) into the model components (see Fig. 1), e.g. main river with reaches and cross-sections, aquifer units with (stream-)aquifer columns and soil layers per aquifer column.

**Table I. Required parameters for the channel transmission losses model (when using all sub-models).**

Component	Parameter
River system	Area ( $L^2$ ), Perimeter (L), and Elevation (L) of Cross Sections
	Channel Length (L)
	Sinuosity Coefficient (-)
Aquifer Unit	Number of Aquifer Columns (-)
	Location of Stream-Aquifer Column (-)
	Aquifer Column Width (L)
	Number of Soil Layers per Aquifer Column (-)
Soil Layer	Vertical/ Lateral/ Parallel Saturated Hydraulic Conductivity ( $L.T^{-1}$ )
	Wetting Front Suction (L)
	Porosity ( $L^3.L^{-3}$ )
	Field Capacity ( $L^3.L^{-3}$ )
	Permanent Wilting Point ( $L^3.L^{-3}$ )
	Residual Water Content ( $L^3.L^{-3}$ )
	Poro-size-distribution Index (-)

Considering the variability of processes covered by this model we think that the model has a relatively small, but necessary, number of parameters. The parameters of the river systems may be derived from

digital elevation models and topographical surveys, and those of the aquifer units and soil layers from hydrogeological and soil maps, stratigraphic data and by using pedo-transfer functions and literature data. Con-



sequently, we expect to be able to apply our model for data-scarce areas in drylands (see next section).

### 3. Case Studies of the Channel Transmission Losses Model

We evaluated our channel transmission losses model for two stream reaches with different scales and dominant processes: a large reach of the Middle Jaguaribe River (MJR), Ceará, Brazil and a much smaller one in the Walnut Gulch Experimental Watershed (WGEW), Arizona, USA. The data description of these sites and their parametrization are provided in the following sub-sections. The reason why we chose these two particular river case studies was to demonstrate the general applicability of the model for water planning and management in different types of data-scarce dryland rivers, i.e. to predict the streamflow volume and peak in the MJR (flow events in the rainy season) and in the WGEW (in case of convective storm rainfall / flash flood events). This prediction was based on the specific perceptual hydrological models of the study sites, without performing any parameter calibration procedure. Therefore, we emphasise that it is not intended to reach a ‘best fit’ with measured hydrographs, rather to achieve a profound hydrological system understanding, to enable the simulation of the overall system’s response without calibration. This means that the model is not suited for, for example, flood forecasting, where the timing of the flood peak is highly relevant.

#### 3.1. Middle Jaguaribe River, Ceará, Brazil

##### 3.1.1. Data and parametrization

We simulated a losing/gaining, hydraulically connected 30 km reach of the Middle Jaguaribe River, Ceará, NE-Brazil, which drains a catchment area of 20 000 km<sup>2</sup>. The Jaguaribe river basin’s (total area 74 000 km<sup>2</sup>) hydrology is determined by an annual

cycle of rainy and dry seasons, which are driven mainly by the position of the Inter-tropical Convergence Zone and secondarily by cold fronts from the South Atlantic (Xavier, 2001; Werner and Gerstengarbe, 2003). The basin upstream the MJR receives annual precipitation between 400 mm (in the SW) to 800 mm (in the NE), most of which falls in the months between December and May (van Oel et al, 2008). The areal potential evaporation (class A pan) amounts to 2200 mm yr<sup>-1</sup>. Temporal rainfall variability is highly significant on a suite of scales: inter-annual variability, seasonal variability and variability at the time scale of a week.

The simulated reach is dominated by unconfined aquifers (Fig. 3) belonging to an alluvium with a 20 m average depth and composed of layers of fine and coarse sand, gravel and clay (IBGE, 2003). According to Costa et al. (2012), on the one hand, during the dry and at the beginning of the rainy seasons, no pre-event river flow is expected and streamflow events will create predominantly vertical infiltration into the alluvium. On the other hand, at the middle and end of the rainy seasons, river flow sustained by base flow occurs before and after streamflow events and lateral infiltration into the alluvium plays a major role during events. Moreover, most channel transmission losses are certainly infiltrated only through the cross section of the main channel and not through the floodplains (Costa et al., 2012).

We assumed that the inflow from the drainage area between the stream gauges can be neglected for medium and large floods in the Jaguaribe river reach, because a) the drainage area between the gauges is about 20 times less than the upstream catchment area and b) it has about 130 surface reservoirs in its drainage network (based on Costa et al., 2012), which retains almost all of generated runoff.

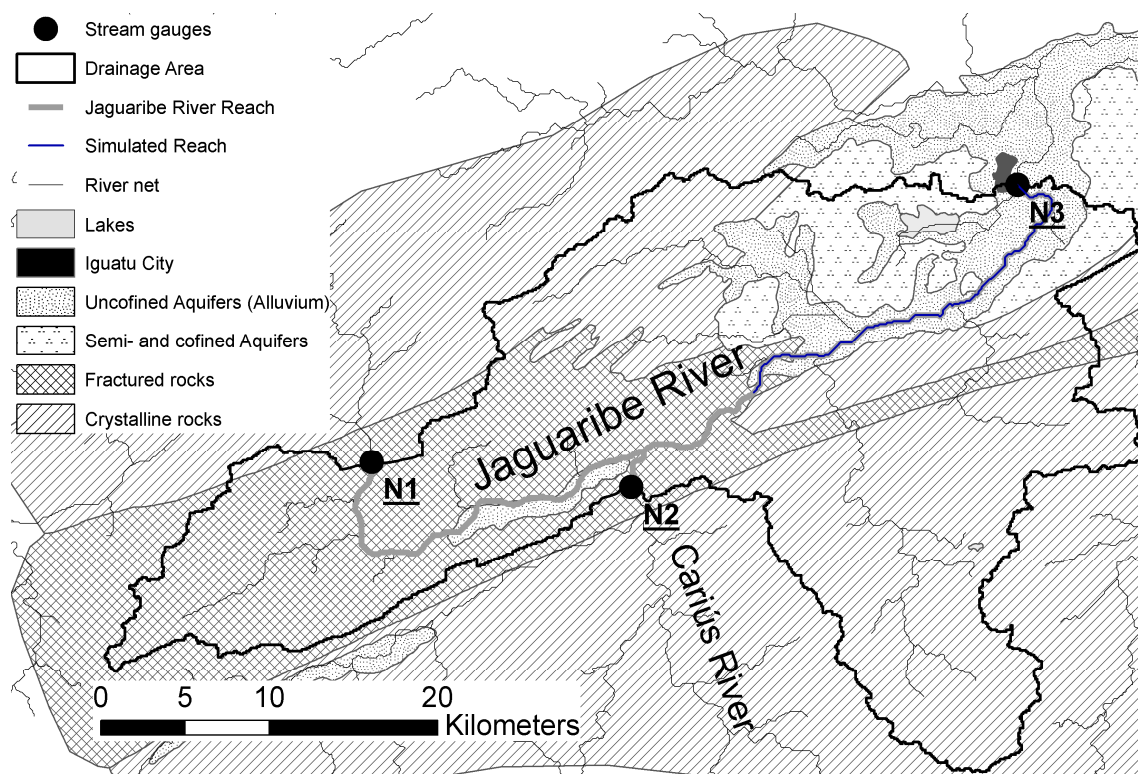


Figure 3. Jaguaribe river reach studied by Costa et al. (2012). The hydrogeological map was adapted from IBGE (2003).

Measurements on the initial moisture of the aquifer-system were not available. However, since at the middle of the rainy seasons river flow is expected to be sustained by base flow, we may assume the riverine groundwater level to be close to the river bed at the middle of the rainy seasons, for which we applied the model. We assumed from Costa et al. (2012) that the actual inflow into the simulated reach is a sum of the actual streamflow measured at the N2 stream gauge, close to the confluence of the Cariús river into the Jaguaribe river, and the one-day-before streamflow measured at the N1 stream gauge in the Jaguaribe river (see Fig. 3). The simulated output streamflow was compared to the streamflow measured at the N3 stream gauge in the Jaguaribe river.

We used alluvial stratigraphy data, 15 boreholes and one electrical resistivity survey (Carneiro, 1993), and alluvium extension information from a hydrogeological map (Fig. 3) to derive the aquifer units (see Fig. 1). We used remote sensing-based data available from Costa et al. (2012) to delineate the channel length and the maximum channel width, whereas field obser-

vation provided the maximum channel depth. Then, we derived stream cross-sectional areas by assuming a triangular channel cross-sectional area. We did not account for infiltration into floodplains; since for our example it is not considered relevant for channel transmission losses, as discussed above in this section.

The simulated MJR was spatially modelled (see Fig. 1) as one basin system, which has one river with 4 reaches and 5 sections. Its aquifer system was formed by 4 units containing respectively 7, 17, 13 and 21 (stream-)aquifer columns from up-to downstream. The typical up-to-down stratigraphy of an aquifer column was: sandy loam (topsoil), fine to coarse sand (1<sup>st</sup> alluvial layer), coarse gravel and very coarse sand (2<sup>nd</sup> alluvial layer) and silty clay (boundary condition), being the last three for the stream-aquifer columns. Moreover, the soil layer interval was set at 0.2 m for all (stream-)aquifer columns. The texture of the aquifer was used to derive its soil physical properties, such as saturated hydraulic conductivity and porosity, obtained from experimental tables published

in Rawls et al. (1993) and Dingman (2002).

The time step of the calculation, which gave the best numerical stability of flood wave routing and, consequently, used for this simulation, was 12 hours. Since the original input time series were not sampled every 12 hours, but only daily, we had to disaggregate them.

### 3.1.2. Model application

We selected three rainy seasons from 2005 until 2010, namely 2005, 2009 and 2010, which met the conditions described in the previous sub-section. Figure 4a-c shows the input and observed output streamflow series of those rainy seasons.

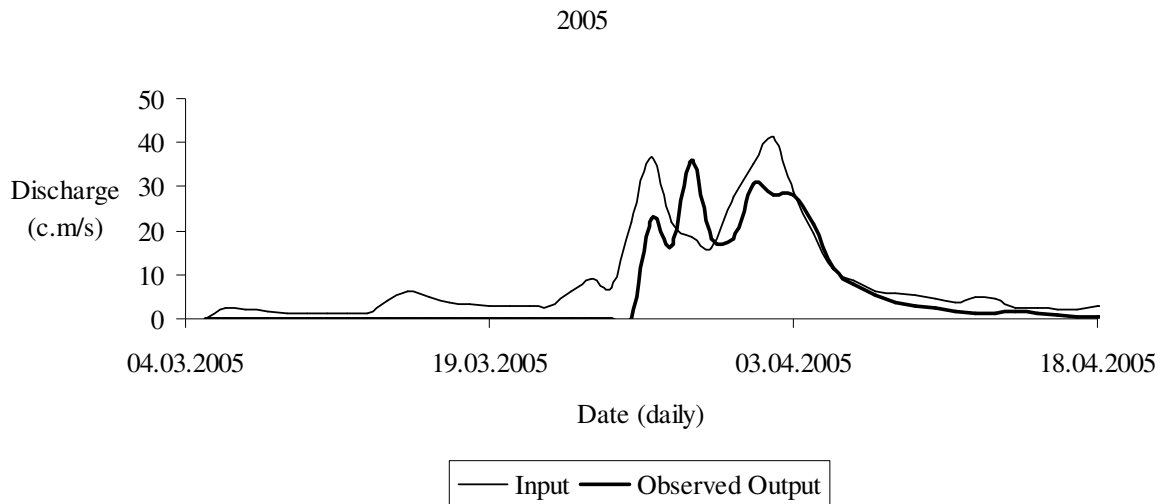


Figure 4a. Input and observed output streamflow series of the studied reach of the Jaguaribe River reach in 2005.

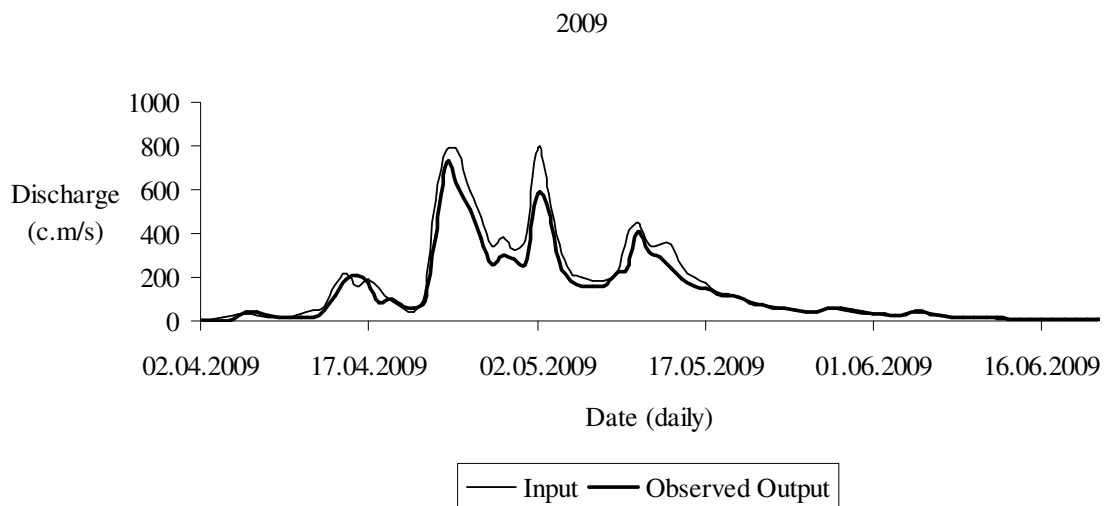


Figure 4b. Input and observed output streamflow series of the studied reach of the Jaguaribe River reach in 2009.

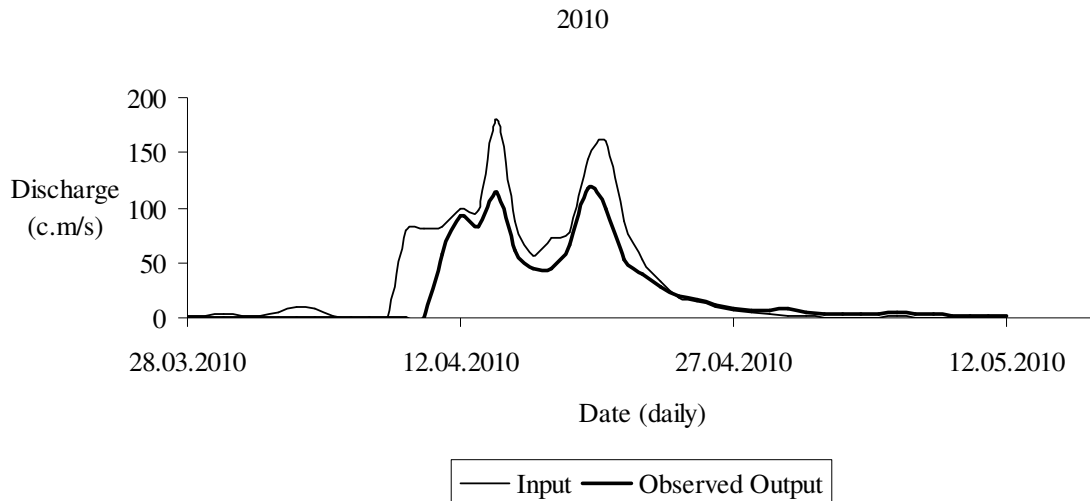


Figure 4c. Input and observed output streamflow series of the studied reach of the Jaguaribe River reach in 2010.

Using those rainy seasons, we evaluated which model structure would provide the best simulation, i.e. the minimum of both root mean square error (RMSE) and mean absolute error (MAE) of peak and event volume time series. Using the same parameter set and the spatial discretization, which were derived without calibration as shown in the previous sub-section, we defined three possible model structures: a) flood wave routing only, i.e. no aquifer

system, and no transmission losses, respectively (FW); b) flood wave routing with lateral (stream-)aquifer dynamics, but without groundwater flow parallel to the river course, (FW+LD); and c) the same as (b) but now including parallel groundwater flow (FW+LD+GW). Figure 5a-c shows the simulated and observed output streamflow series.

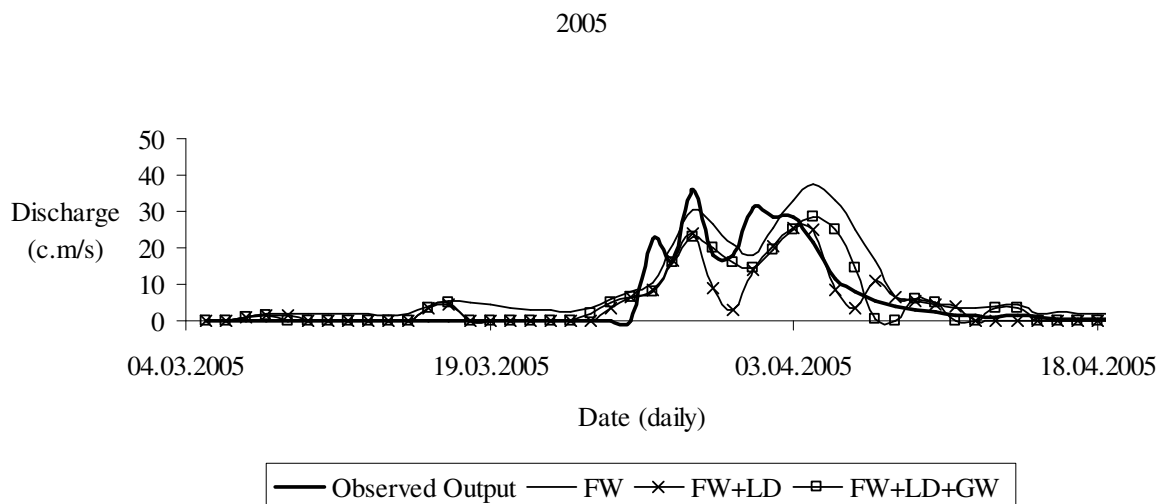
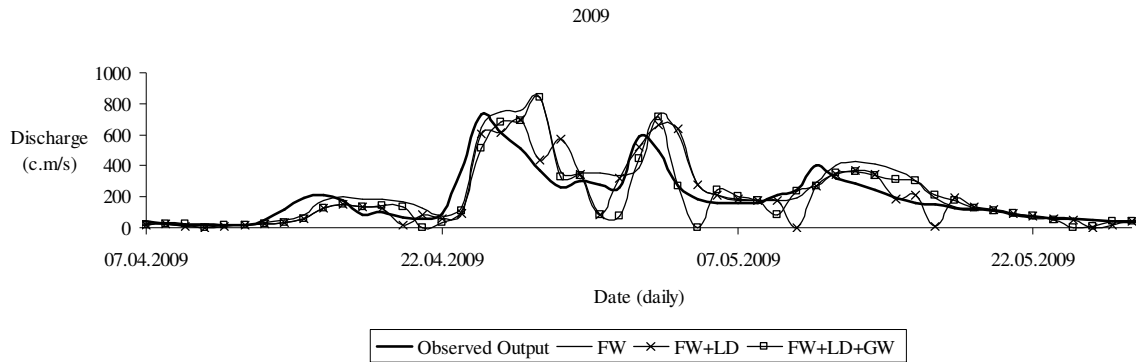
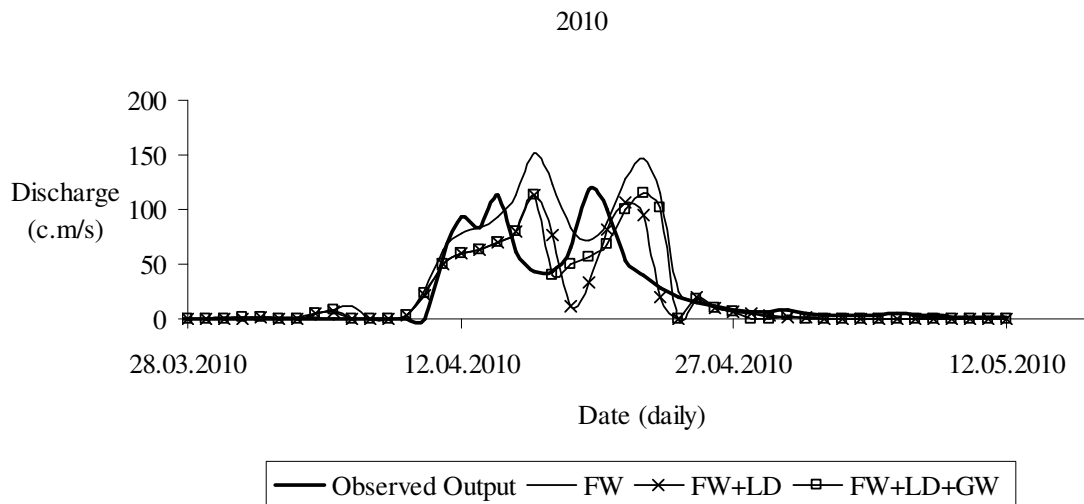


Figure 5a. Simulated and observed output streamflow series of the studied reach of the Jaguaribe River reach in 2005. The three model structures tested were: 1) only flood wave routing, i.e. no aquifer system, (FW); 2) flood wave routing with lateral (stream-)aquifer dynamics, but without groundwater flow parallel to the river course, (FW+LD); and 3) equal to the last one, but now with parallel groundwater flow (FW+LD+GW).



**Figure 5b.** Simulated and observed output streamflow series of the studied reach of the Jaguaribe River reach in 2009. The three model structures tested were: 1) only flood wave routing, i.e. no aquifer system, (FW); 2) flood wave routing with lateral (stream-)aquifer dynamics, but without groundwater flow parallel to the river course, (FW+LD); and 3) equal to the last one, but now with parallel groundwater flow (FW+LD+GW).



**Figure 5c.** Simulated and observed output streamflow series of the studied reach of the Jaguaribe River reach in 2010. The three model structures tested were: 1) only flood wave routing, i.e. no aquifer system, (FW); 2) flood wave routing with lateral (stream-)aquifer dynamics, but without groundwater flow parallel to the river course, (FW+LD); and 3) equal to the last one, but now with parallel groundwater flow (FW+LD+GW).

The FW-based model overestimated both the streamflow peak and the volume. The (FW+LD)- and (FW+LD+GW)-based models predicted similar peaks, but the (FW+LD)-based simulated hydrograph

decreased more sharply during the recession flow than the (FW+LD+GW)-based one. The models' performance is shown in Table II.

**Table II.** Mean absolute error (MAE) and root mean square error (RMSE) of the three model structures tested: 1) only flood wave routing, i.e. no aquifer system, (FW); 2) flood wave routing with lateral (stream-)aquifer dynamics, but without groundwater flow parallel to the river course, (FW+LD); and 3) equal to the last one, but now with parallel groundwater flow (FW+LD+GW).

Model Structure	Volume		Peak	
	MAE (%)	RMSE ( $10^6 \text{ m}^3$ )	MAE (%)	RMSE ( $\text{m}^3 \text{ s}^{-1}$ )
FW	41	96	20	74
FW+LD	10	31	12	36
FW+LD+GW	4	41	13	67

The (FW+LD)- and (FW+LD+GW)-based models had comparable performance and both were better than the FW-based. Because the (FW+LD+GW)-based model had the most similar behaviour to the observed hydrographs than the (FW+LD)-based one, we consider the (FW+LD+GW)-based model structure as the best suited for this study site.

### 3.2. Walnut Gulch Experimental Watershed, Arizona, USA

#### 3.2.1. Data and parametrization

We simulated here a losing, hydraulically disconnected 1.5 km channel reach in the Walnut Gulch Experimental Watershed (WGEW), Arizona, USA, from the flume

FL008 (input flow) to the FL006 (output flow) (Fig. 6). Based on previous publications (e.g. Renard, 1970; Goodrich et al., 2004; Renard et al., 2008; Stone et al., 2008; Emmerich, 2008; Osterkamp, 2008), we assumed that streamflow infiltrates into a sandy alluvium with enough depth such that it never becomes completely saturated during a streamflow event, because depth to groundwater within the WGEW ranges from ~50 m at the lower end to ~145 m in the central portion of the watershed (Goodrich et al., 2004; also see Spangler, 1969). Hydrological data and geo-information were made available at <http://www.tucson.ars.ag.gov/dap/>.

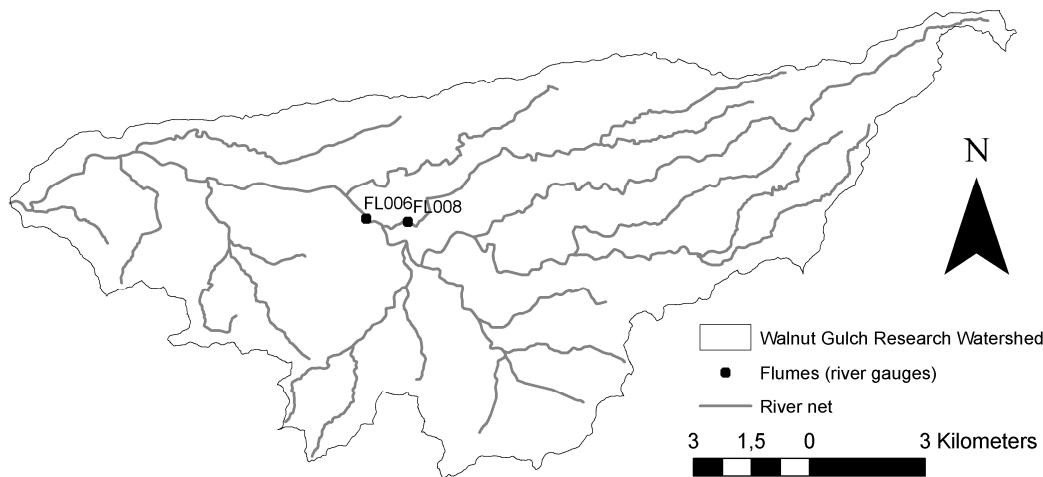


Figure 6. Walnut Gulch Research Watershed (PCS: NAD83 and GCS: North American 1983) based on data made available at <http://www.tucson.ars.ag.gov/dap/>.

We selected hydrographs from streamflow events in which:

- (i) the input flow was only registered by the selected upstream flume (FL008);
- (ii) the event volume, duration and peak flow at the selected upstream flume (FL008) were greater than at the downstream flume (FL006);
- (iii) the soil moisture content of the underlying alluvium could be assumed close to the residual moisture content, i.e. at the beginning of the rainy season or after a long time between runoff events during the rainy season, since no soil moisture data of the underlying alluvium were made available.

Maximum channel cross-sectional area and channel width were derived by stream channel morphology relationships provided by Miller et al. (2003). The stream cross-sectional areas were then derived assuming a triangular channel cross-sectional area. We did not account for floodplains, because no data about them were available and also because we considered them to be of minor importance for transmission losses in that stream reach. Consequently, the floods had to be assumed as sub-bank flows.

The simulated reach in the WGEW was spatially modelled (see Fig. 1) as one basin system, which has one stream with 3 reaches and 4 sections. Its aquifer system

was formed by 3 units, each containing only one stream-aquifer column. The aquifer system was assumed to be uniformly sandy. Moreover, its soil layer interval was set 0.1 m for all stream-aquifer columns. The texture of the aquifer was used to derive its soil physical properties, such as saturated hydraulic conductivity and porosity, obtained from experimental tables published in Rawls et al. (1993) and Dingman (2002).

The time step of calculation, which gave the best numerical stability of flood wave routing and which was consequently used for this simulation, was 2 minutes. Since the original input time series were

not sampled for every 2 minutes, we had to resample them.

### 3.2.2. Model application

We selected 6 streamflow events which met the conditions described in the previous sub-section, in order to simulate the channel transmission losses from flume FL008 to flume FL006 (Fig. 6) using the parameters set and the spatial discretization derived without calibration, as already explained in the previous sub-section. Table III compares the observed and simulated flow volume and peak of those events and shows the differences between the observed and simulated peak times.

*Table III. Comparison between the observed and simulated volume and peak flow and the differences between observed and simulated peak times of the selected events from the studied 1.5 km reach in the Walnut Gulch Experimental Watershed, Flume FL006.*

Event	Volume ( $10^3 \text{ m}^3$ )		Peak ( $\text{m}^3 \text{ s}^{-1}$ )		Peak time error (min.km $^{-1}$ )
	Observed	Simulated	Observed	Simulated	
2 Aug 1968	2.0	1.0	1.3	0.7	-6.7
28 Aug 1969	0.0	0.1	0.0	0.1	na*
24 Jul 1970	1.2	0.7	0.8	0.5	-2.7
28 Jul 1972	0.5	0.2	0.3	0.3	-3.3
29 Aug 1972	1.2	0.6	0.8	0.8	6.0
7 Aug 1983	0.0	0.0	0.0	0.1	na

\*not applicable.

The volume of the events was clearly always underestimated, its MAE being equal to  $0.4 \cdot 10^3 \text{ m}^3$  and its RMSE equal to  $0.5 \cdot 10^3 \text{ m}^3$ . The peak flow of the events was better predicted than its volume, where its error did not show a clear trend, its MAE being equal to  $0.2 \text{ m}^3 \text{ s}^{-1}$  and its RMSE equal to  $0.3 \text{ m}^3 \text{ s}^{-1}$ . We show the best and the worst predicted output hydrographs, which occurred on 29 August 1972 (Fig. 7) and on 2 August 1968 (Fig. 8), respectively.

The simulation results made clear some distinct problems with the hydrograph shape (see e.g. Fig. 7, but also Fig 5c for the MJR) and some pronounced errors be-

tween the observed and predicted peak time of the events simulated in the WGEW (Table III). This is explained because the flow velocity in our simplified flood wave routing (Sect. 2.1) is controlled by the channel cross-sections, which were approximated through simple relationships. This only vague approximation of the channel cross-sections can be considered as a typical problem of dryland regions. Therefore, the inherent data scarcity of the channel morphology will inevitably lead to uncertainties in the timing of the hydrograph.

08.29.1972

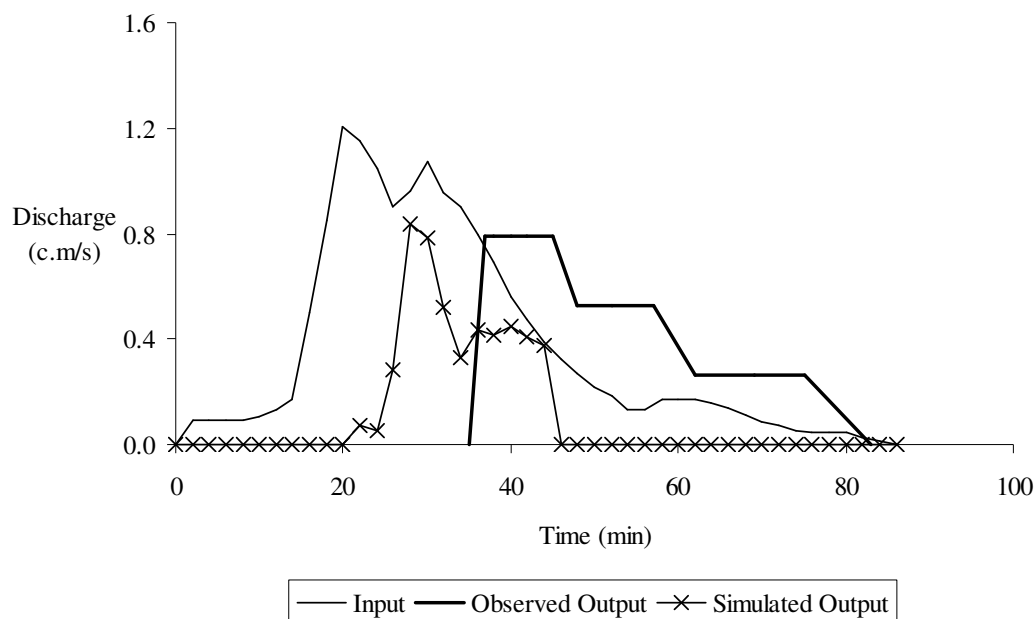


Figure 7. The best predicted output hydrograph for the studied reach in the Walnut Gulch Research Watershed (at Flume FL006).

08.02.1968

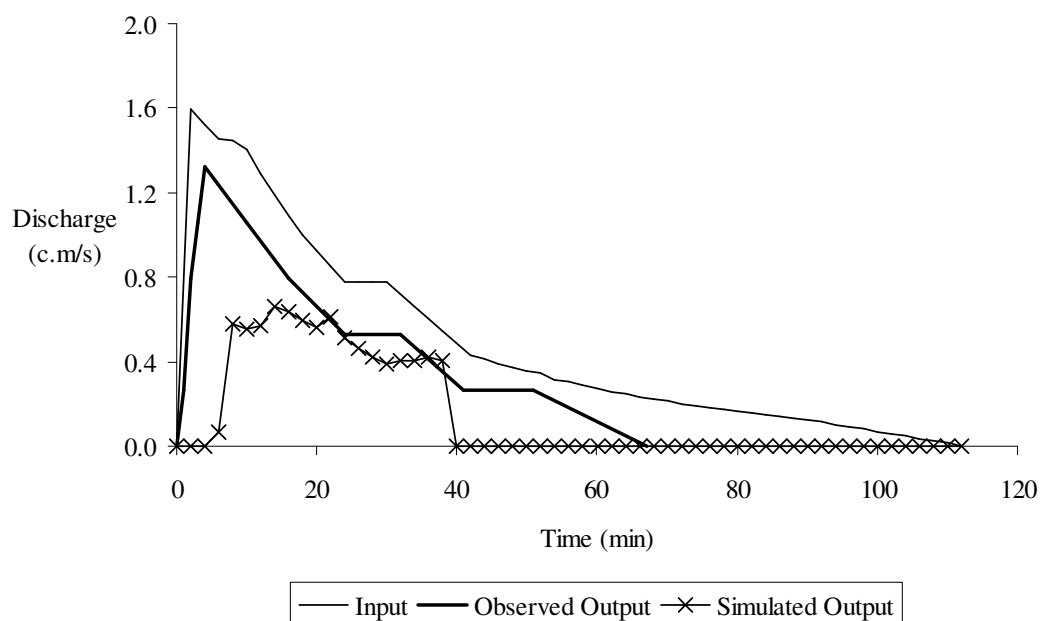


Figure 8. The worst predicted output hydrograph for the studied reach in the Walnut Gulch Research Watershed (at Flume FL006).

#### 4. Model Reliability

Important model uncertainties in hydrological modelling may be classified in three fields: numerical or mathematical uncertainty (dealing with numerical stability and accuracy of the adopted solvers for

the process equations), parameter uncertainty (including individual and combined sensitivity of model parameters, multiple-valid parameter sets, sub-scale parameter variability) and structural uncertainty (comprising the selection of model processes and their interactions, effects of un-



certain initial and boundary conditions and/or the model-representation of the simulation domain).

The model structure uncertainty was analyzed previously for the Jaguaribe river reach and was negligible for the WGEW's stream.

In this section, we evaluate the numerical and the model parameter uncertainty by a) analysis of numerical stability and accuracy of the subsurface simulations, and b) individual sensitivity analysis of the model parameters; and an overall (combined) model parameter uncertainty analysis. The structural uncertainty has been approached to a limited extent in the previous section, where we discussed the influence of different process representations of the subsurface (i.e. with / without considering interactions of the groundwater with channel water and with / without considering parallel groundwater flow and by prescribing initial and boundary conditions according to the available field data and the perceptual hydrological models of the river reaches). We think that a more comprehensive elaboration of the structural uncertainty (e.g. by choosing a variety of different possible interpretations of hydrogeological structures or by applying different hydrological process formulations) would clearly go beyond the scope of this paper.

#### **4.1. Numerical issues**

Here we present simulation results, which enable us to evaluate whether the spatial and temporal discretization (Sect. 3.1.1 and 3.2.1) and the numerical approximations (Sect. 2) are such that the model is numerically stable and accurately represents the governing equations. Therefore, we selected some simulations of the subsurface systems, i.e. the unsaturated zone in the WGEW and the saturated zone in the MJR, to be presented here. We do not show all results of the subsurface systems because this would not add more information.

##### **4.1.1. Unsaturated zone in the Walnut Gulch Experimental Watershed**

We present here the soil moisture simulation of the unsaturated zone of the uppermost stream reach (see Sect. 3.2.1 for the discretization) during the streamflow event on 28 July 1972 in the WGEW. We used a time step of 2 minutes, which gave the best numerical stability for flood wave routing. Then, we assumed the soil layer intervals 0.1 m, which was adopted for the previous application, 0.2 m, 0.4 m and 0.8 m, respectively. Figures 9a-d show the first 8 minutes of the soil moisture simulation, i.e. the propagation of the downward soil wetting.

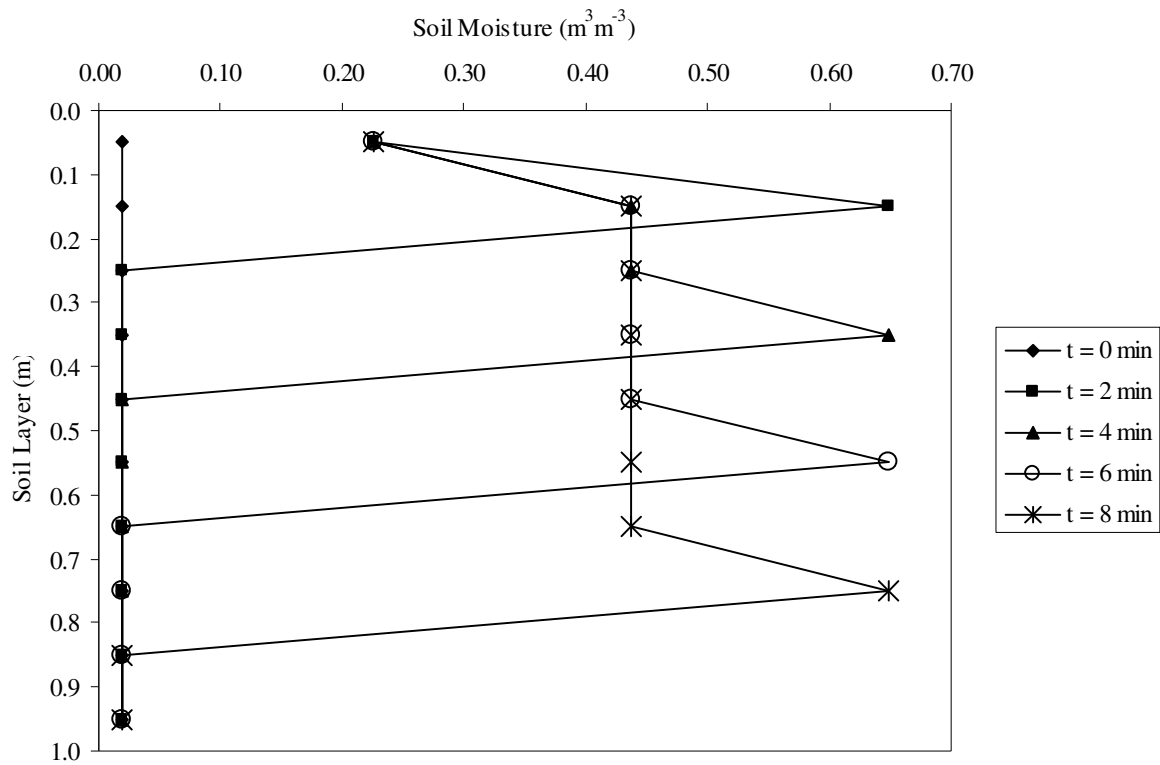


Figure 9a. The soil moisture simulation of the unsaturated zone of the first reach during the event on 28 July 1972 in the Walnut Gulch Research Watershed (time step equal to 2 min and soil layer interval 0.1 m).

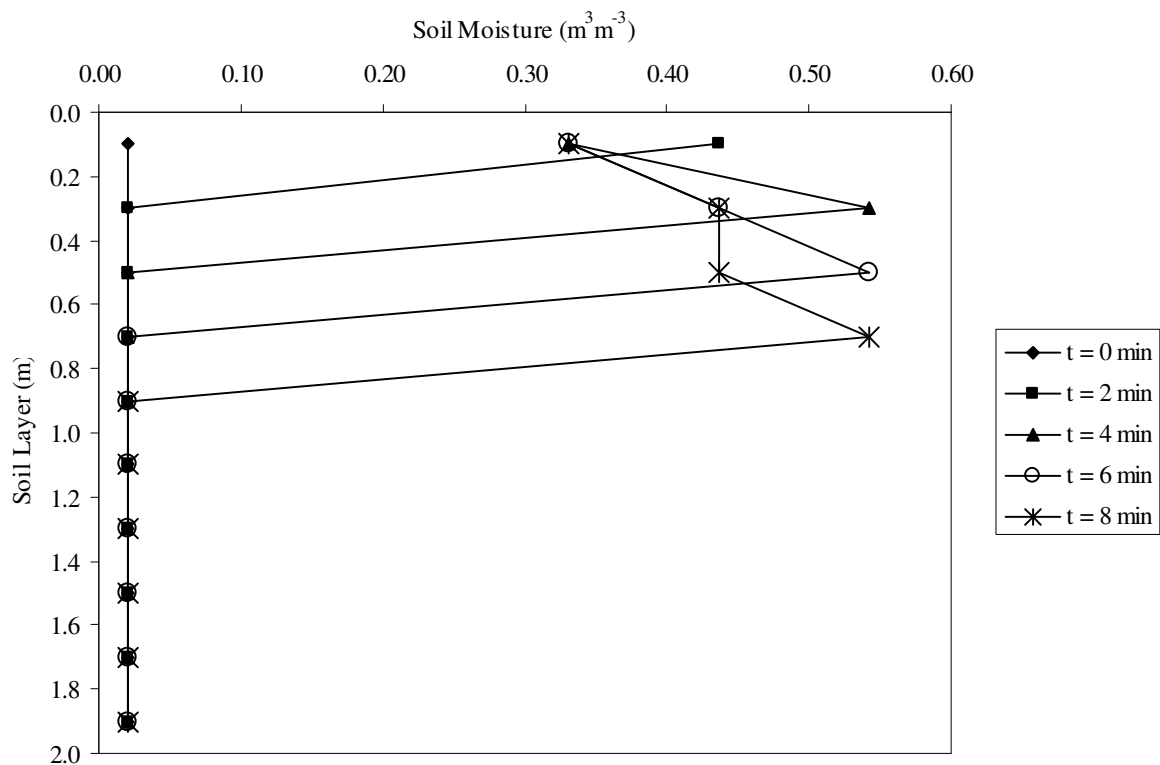


Figure 9b. The soil moisture simulation of the unsaturated zone of the first reach during the event on 28 July 1972 in the Walnut Gulch Research Watershed (time step equal to 2 min and soil layer interval 0.2 m).

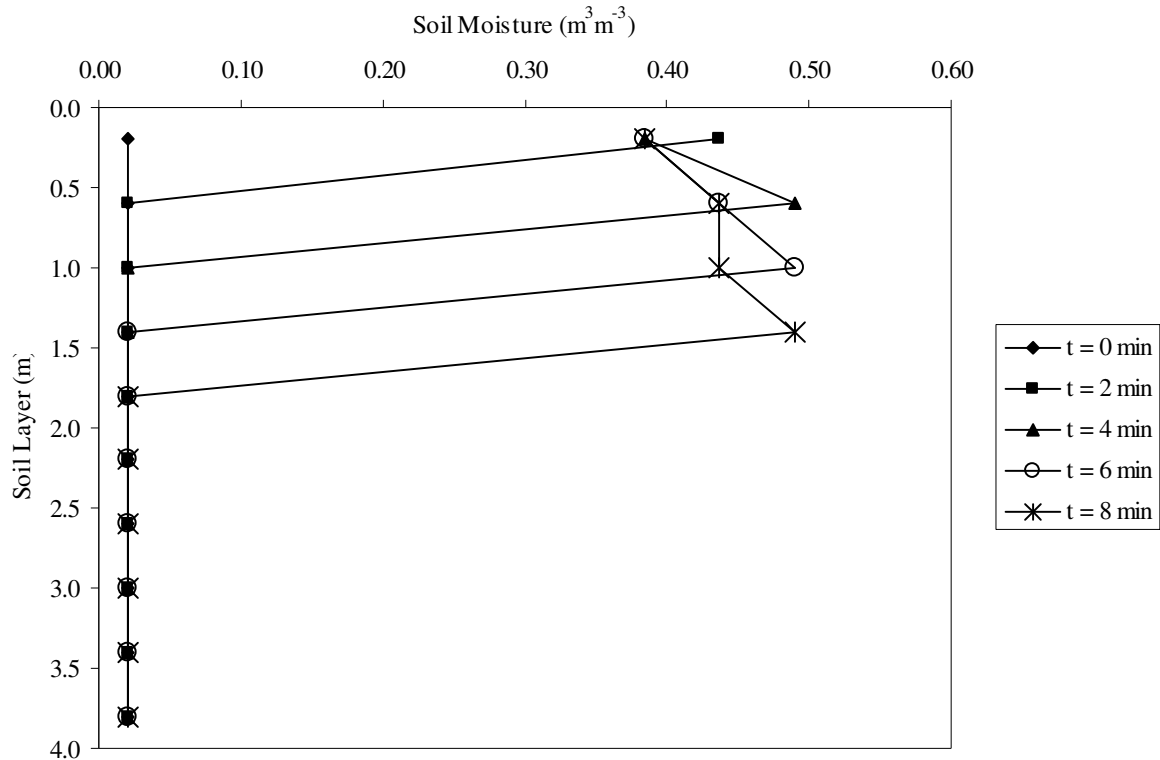


Figure 9c. The soil moisture simulation of the unsaturated zone of the first reach during the event on 28 July 1972 in the Walnut Gulch Research Watershed (time step equal to 2 min and soil layer interval 0.4 m).

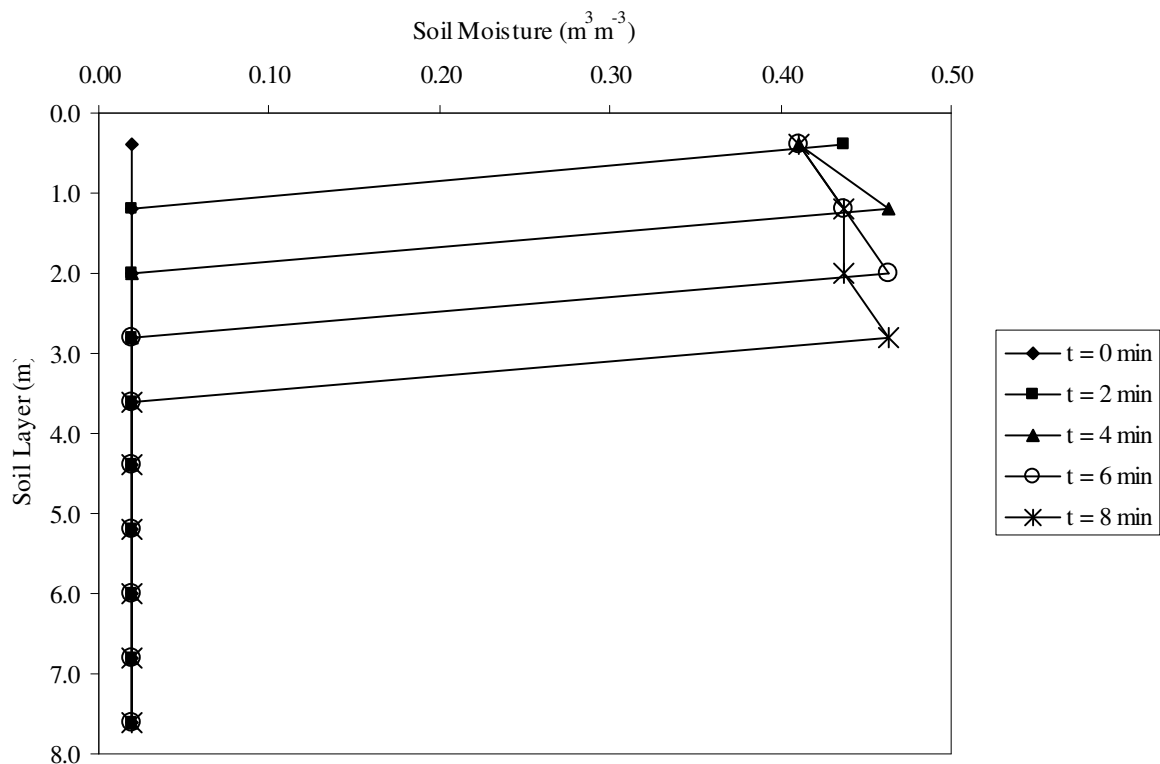


Figure 9d. The soil moisture simulation of the unsaturated zone of the first reach during the event on 28 July 1972 in the Walnut Gulch Research Watershed (time step equal to 2 min and soil layer interval 0.8 m)

The soil moisture simulation is governed by both the unsaturated stream infiltration model (Sect. 2.2) and the vertical

soil water redistribution model (Sect. 2.3). While the stream water infiltrated through the soil column, the uppermost soil layer

was never completely saturated and the lowest wetted soil layer had always the greatest moisture (peak). The former can be explained by the hydraulic conductivity term  $K^j_{k-(1/2)}$ , which approaches zero in Eq. (16) for the uppermost soil layer. The latter seems to be inevitable if the moisture or the hydraulic conductivity between two soil layers is rather different. These numerical “artefacts” were smoother when the interval of the soil layer increased but, consequently, the infiltrated water into the soil column also reached a higher depth.

Instead of using the harmonic mean between the hydraulic conductivity of the soil layers (see Eq. (16)), one can adopt the

arithmetic mean (see e.g. van Dam and Feddes, 2000). Considering now the arithmetic mean and a soil layer interval equal to 0.2 m, we found that those numerical artefacts were even smoother (Fig. 10). Moreover, there were no significant changes in the simulated streamflow volume and peak (smaller than 5%) between 0.1 and 0.2 m soil layer interval and using harmonic or arithmetic mean. However, we found +30% and +16% difference in simulated volume and peak, respectively, between 0.1 and 0.4 m intervals and +42% and +26% between 0.1 and 0.8 m.

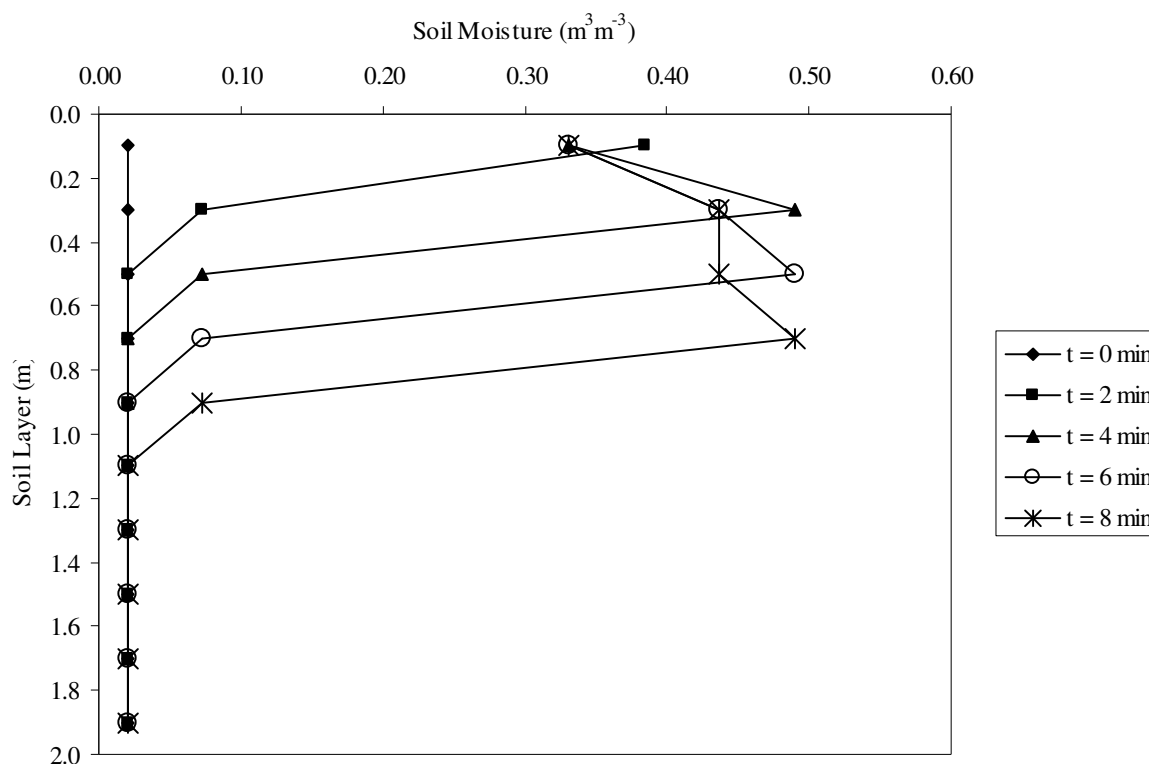


Figure 10. The soil moisture simulation of the unsaturated zone of the first reach during the event on 28 July 1972 in the Walnut Gulch Research Watershed (time step equal to 2 min and soil layer interval 0.2 m), but using the arithmetic mean in Eq. 16, instead of the harmonic mean.

#### 4.1.2. Saturated zone in the Middle Jaguaribe River

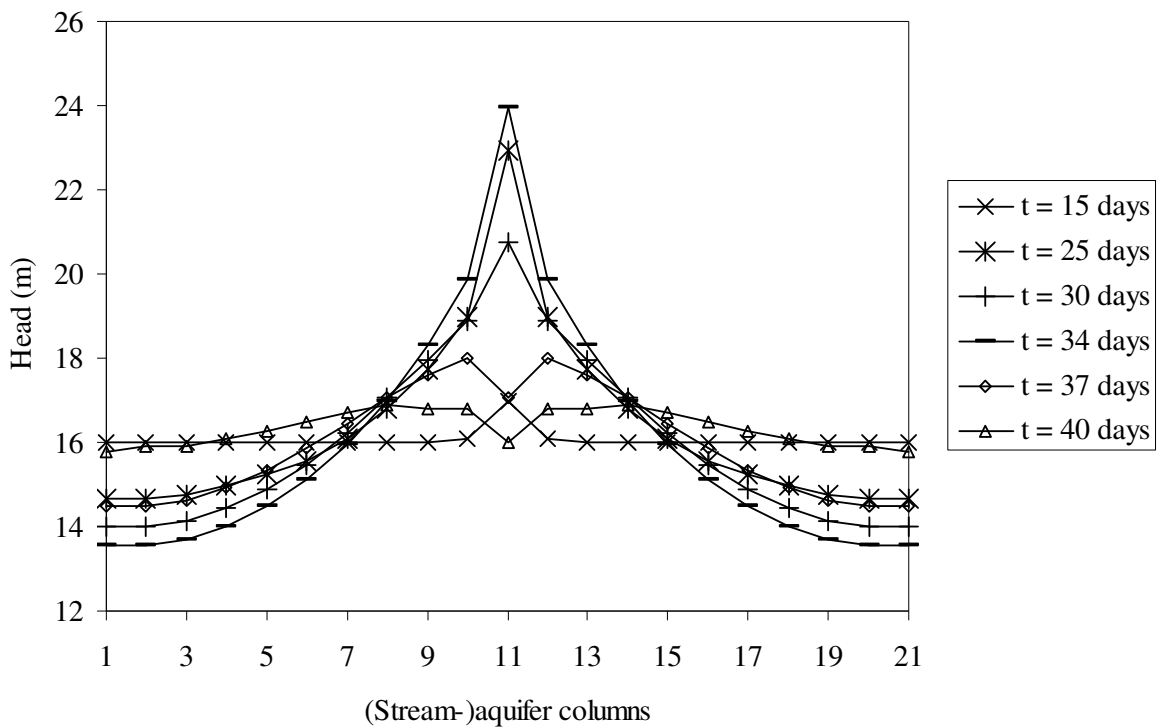
We present the groundwater and stream levels’ simulation of the farthest downstream stream reach of the MJR (see Sect. 3.1.1 for the temporal and spatial discretization) during the rainy season in 2010 in the Jaguaribe River. The width of the aquifer columns was defined as half the width

of the stream-aquifer columns for all the stream reaches.

Fig. 11a shows the groundwater and stream levels’ simulation using the best model structure found previously for the streamflow series, i.e. the combination of the flood wave routing, the lateral river-aquifer dynamics and the groundwater flow parallel to the river course (Sect. 3.1.2). These simulation results showed the

flow from the river (stream-aquifer column 11 in Fig. 11a) into the surrounding groundwater in the times equal to 15, 25, 30 and 34 days and the flow from the groundwater into the river during the rest of the times, as we expected. However, during the infiltration from the river into the groundwater, the groundwater levels in the most distant aquifer columns (seen from the stream-aquifer column) decreased approximately from 16 m to 14 m (see Fig. 11a), which is probably too much for a period of 20 days in this environment. A large groundwater outflow from the aquifer unit in the lowest reach can explain this

decrease in groundwater level. In order to check this hypothesis, we plotted the simulation of the model structure without considering the groundwater flow parallel to the river course (Fig. 11b). The groundwater level of all the aquifer columns then works as expected. Thus, assuming the gradient of the unit of the aquifer furthest downstream to be equal to the unit closest to it upstream (see Sect. 2.5), we may overestimate its outflow. Nevertheless, the groundwater flow model needs to be taken into account to achieve the best fit for the streamflow series (Sect. 3.1.5).



**Figure 11a.** The simulation of groundwater and river levels in the farthest downstream stream reach during the rainy season in 2010 in the Jaguaribe River. The streambed level is 16 m and the surface level 30 m. The stream-aquifer column is volume No 11 in the x-axis. The model structure was that which provided the best fit for the streamflow series (Sect. 3.1.2), i.e. including the simulation of flood wave routing, lateral river-aquifer dynamics and groundwater flow parallel to the river course.

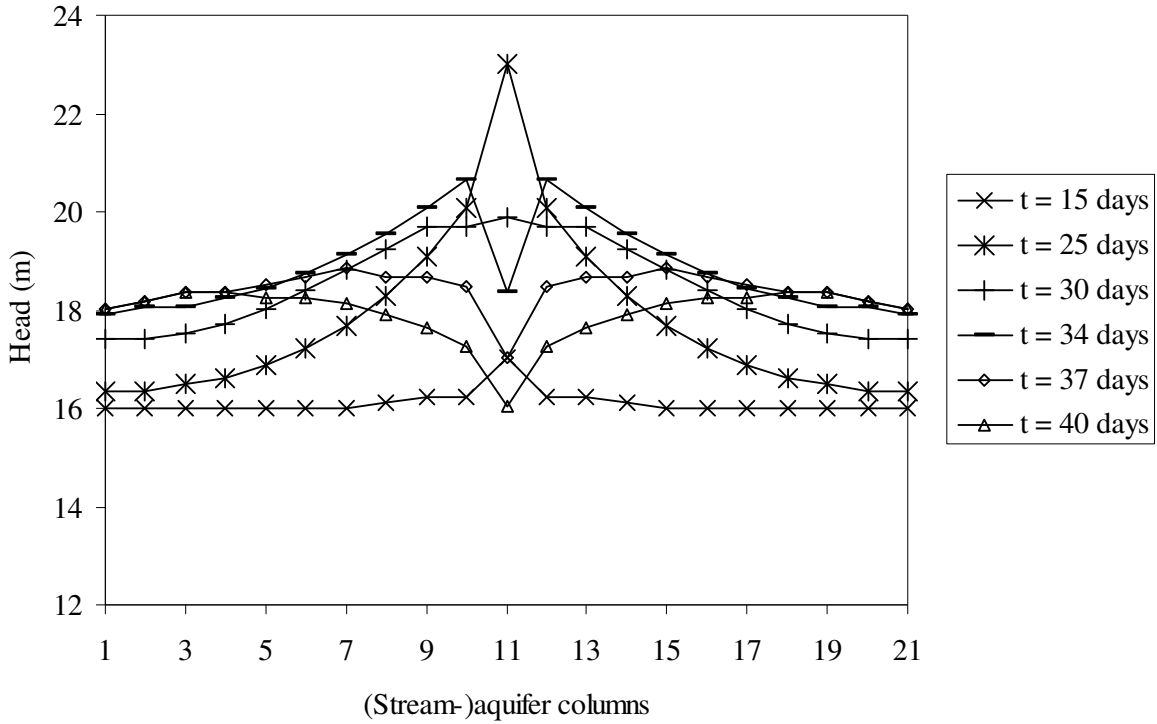


Figure 11b. The simulation of groundwater and river levels in the farthest downstream stream reach during the rainy season in 2010 in the Jaguaribe River. The streambed level is 16 m and the surface level 30 m. The stream-aquifer column is volume No 11 in the x-axis. The model structure did not consider the groundwater flow parallel to the river course.

#### 4.2. Individual parameter sensitivity analysis

We carried out a classical parameter sensitivity analysis in order to guide the efforts on data acquisition and parameter calibration in future applications. We used for the parameter sensitivity analysis the following standard formulation

$$\phi_i = \frac{y(P_i) - y_{reference}}{y_{reference}} \quad (28)$$

where  $\phi$  is the sensitivity coefficient,  $y$  is here a simulated variable, streamflow peak or event volume, and  $P$  is a model parameter. To carry out the sensitivity analysis, we selected the driest and the wettest streamflow events, whose upstream flow reached the lowest stream section.

##### 4.2.1. Middle Jaguaribe River

Once the (FW+LD+GW)-based model structure had presented the best simulation performance for streamflow volume and maximum peak, we chose the following set

of parameters for sensitivity analysis: a) porosity  $\eta$  and b) soil moisture at field capacity  $\theta_{fc}$ , which are related to groundwater level computation (Eq. 25); c) lateral saturated hydraulic conductivity  $K_A$  of column A, which is related to lateral (stream-)aquifer dynamics (Eq. 20); and d) “parallel” saturated hydraulic conductivity  $K_u$  of aquifer unit u, which is related to groundwater flow parallel to the river course (Eq. 23).

Streamflow volume and maximum peak simulated by the (FW+LD+GW)-based model for the years 2005 and 2009 were used as reference variables (see Eq. 28) because those years were the driest and the wettest. Then, we multiplied a variable factor with the original values of the parameters a), b), c) and d) and ran the (FW+LD+GW)-based model again, in order to estimate the sensitivity coefficients (Eq. 28) for streamflow volumes and maximum peaks.

The sensitivity was very small, i.e. the results did not vary with changes of poros-

ity (range between  $\theta_{fc}$  and  $1.5 \times \eta$ ) neither with changes of soil moisture at field capacity (range between  $0.5 \times \theta_{fc}$  and  $\eta$ ). In contrast, the sensitivity was high due to changes on lateral and parallel saturated

hydraulic conductivities. Figures 12a-b show the results of sensitivity analysis of those conductivity parameters for 2005 and Figs. 13a-b for 2009.

2005

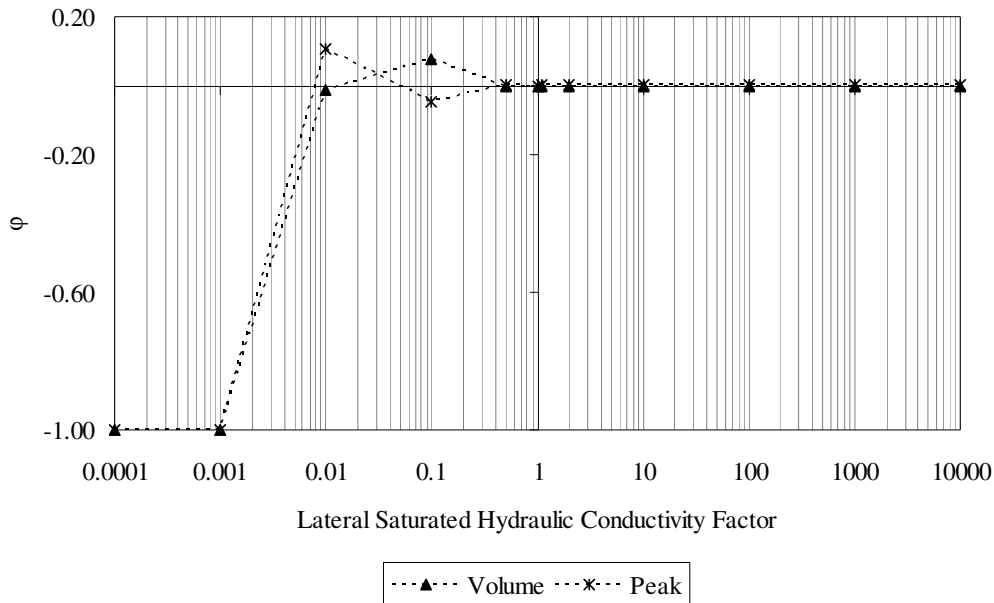


Figure 12a. Sensitivity analysis of lateral saturated hydraulic conductivity, where  $\phi$  is the sensitivity coefficient (Eq. 28) and x-axis is the factor which was multiplied with the original values of the parameter (MLR, March to April 2005).

2005

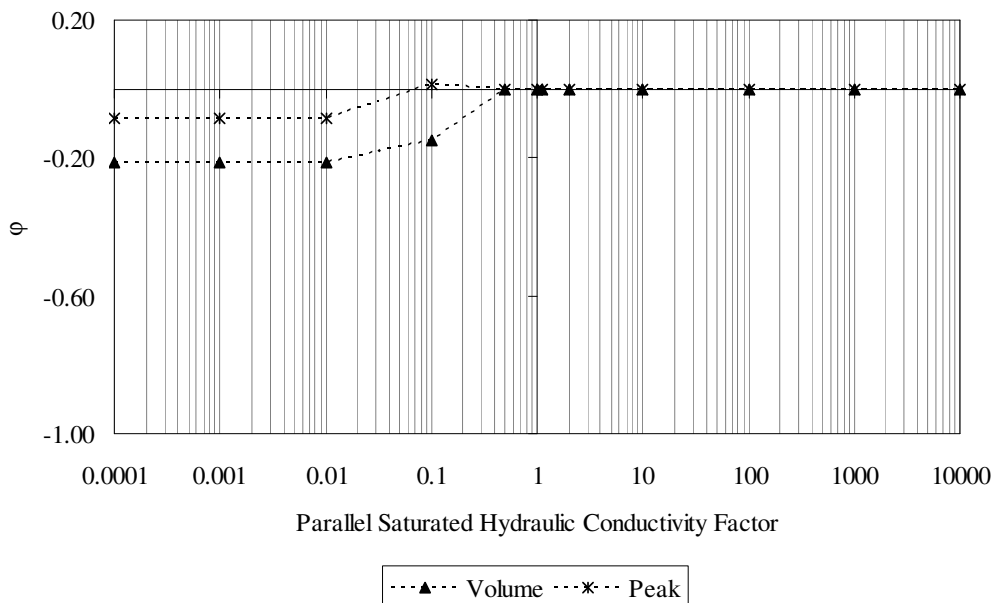


Figure 12b. Sensitivity analysis of parallel saturated hydraulic conductivity, where  $\phi$  is the sensitivity coefficient (Eq. 28) and x-axis is the factor which was multiplied with the original values of the parameter (MLR, March to April 2005).

2009

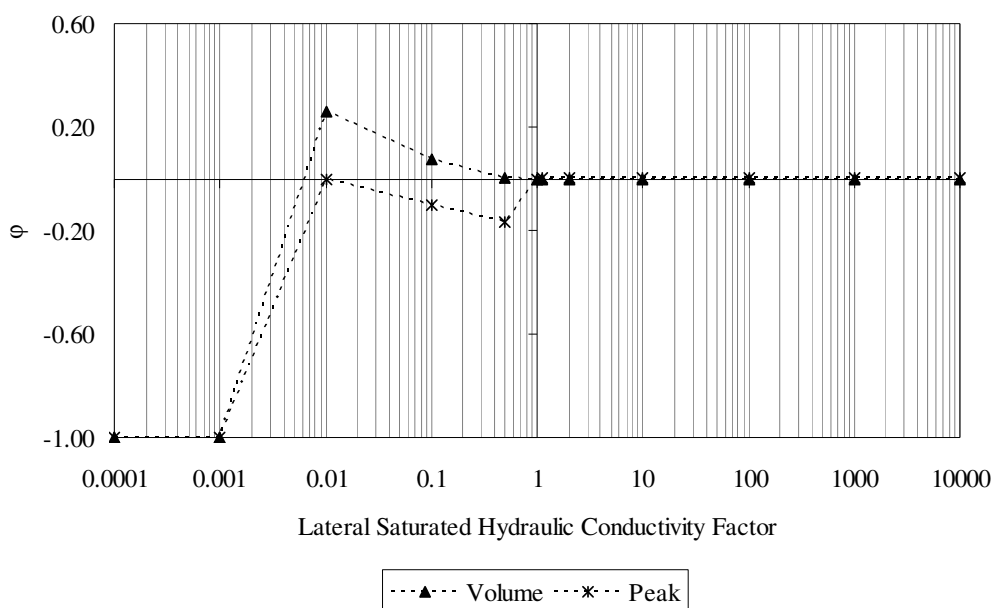


Figure 13a. Sensitivity analysis of lateral saturated hydraulic conductivity, where  $\phi$  is the sensitivity coefficient (Eq. 28) and  $x$ -axis is the factor which was multiplied with the original values of the parameter (MLR, April to June 2009).

2009

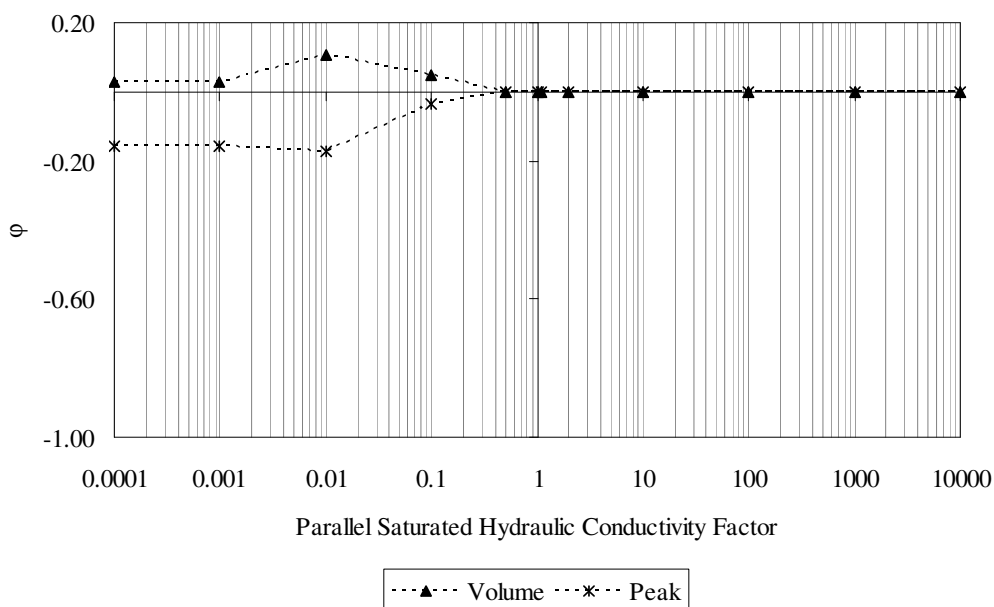


Figure 13b. Sensitivity analysis of parallel saturated hydraulic conductivity, where  $\phi$  is the sensitivity coefficient (Eq. 28) and  $x$ -axis is the factor which was multiplied with the original values of the parameter (MLR, April to June 2009).

In general, high values of both saturated hydraulic conductivities showed little sensitivity to the reference simulation, because large fluxes between model units are restricted by their hydraulic gradient (see Eq.

20 and 23) and the reference simulation was already driven by the hydraulic gradient between the model units.

The sensitivity coefficients of lateral and parallel saturated hydraulic conductivi-



ties can still be considered negligible for both streamflow volume and peak for parameter values greater than 50% of their original values. On the other hand, less than 50% of the original values of lateral and parallel saturated hydraulic conductivities, their sensitivity coefficients could no longer be considered negligible. However, from 50% to 10% of the original values, their sensitivity coefficient was between the range [-0.20; 0.20].

Even when parallel saturated hydraulic conductivity decreased to values less than 10% of its original values (Figs. 12b and 13b), its sensitivity coefficients converged to a value between the aforementioned range. On the other hand, after lateral saturated hydraulic conductivity reached 1% of its original values (Figs. 12a and 13a), its sensitivity coefficient decayed rapidly to its lowest value of -1.00. This agreed with the results of the case studies presented previously that the lateral (stream-)aquifer dynamics model is more relevant than the model of the groundwater flow parallel to the river course for simulating streamflow in the Jaguaribe river.

Therefore, the sensitivity showed the largest values with changes in lateral saturated hydraulic conductivity followed by parallel saturated hydraulic conductivity.

#### 4.2.2. Walnut Gulch Experimental Watershed

We selected the following set of parameters to carry out the sensitivity analysis: soil moisture at field capacity  $\theta_{fc}$ , pore size distribution index  $\lambda$ , porosity  $\eta$ , wetting front suction  $\psi$  and saturated hydraulic conductivity  $K_{sat}$ . Streamflow volume and maximum peak simulated for the events on 28 July 1972 and 2 August 1968 were used as reference variables (see Eq. 28), because those were the driest and the wettest events. Then, we multiplied a variable factor with the original values of those parameters and ran the channel transmission losses model again, in order to estimate the sensitivity coefficients (Eq. 28) for streamflow volumes and maximum peaks.

The sensitivity did not vary with changes in soil moisture at field capacity and pore size distribution index. In contrast, the sensitivity varied significantly with changes in porosity, wetting front suction and saturated hydraulic conductivity. Figures 14a-c show the results of sensitivity analysis of those parameters for 28 July 1972 and Figs. 15a-c for 2 August 1968.

07.28.1972

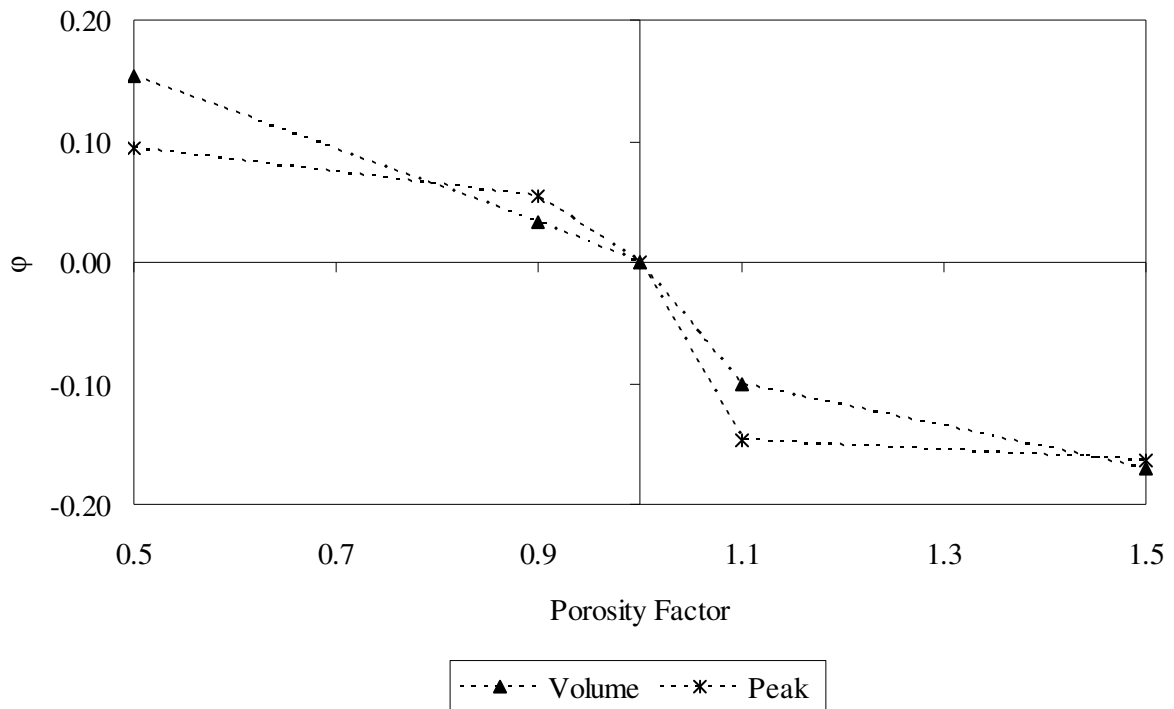


Figure 14a. Sensitivity analysis of porosity, where  $\phi$  is the sensitivity coefficient (Eq. 28) and x-axis is the factor which was multiplied with the original values of the parameter (WGEW, 28 July 1972).

07.28.1972

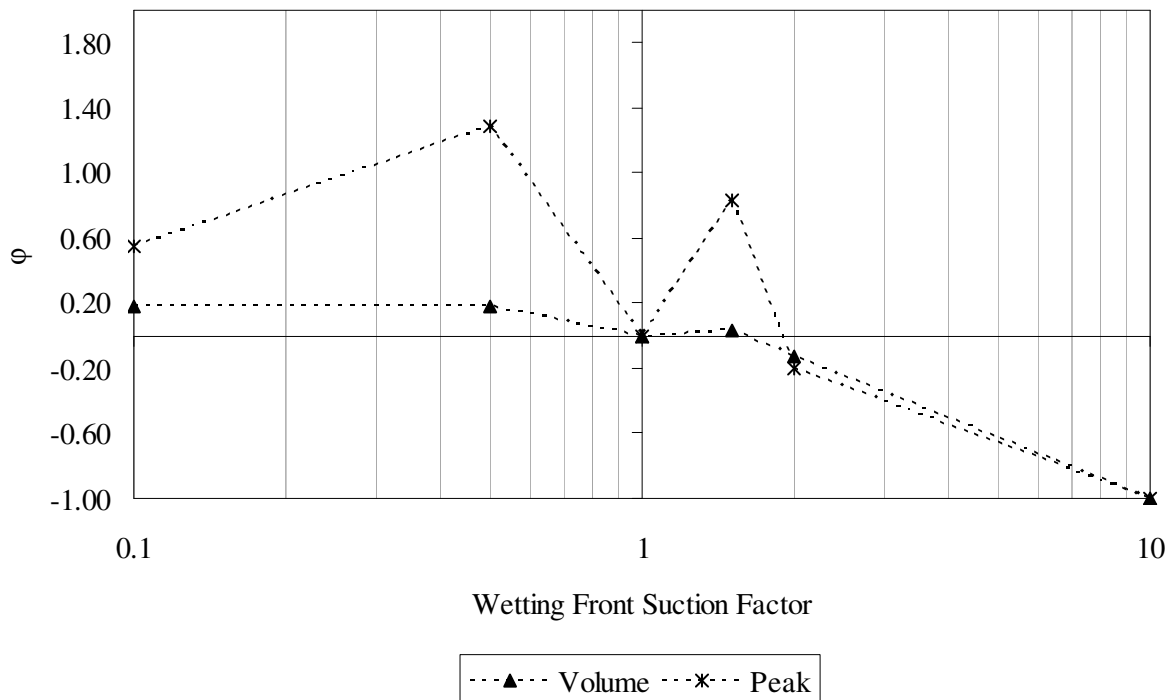


Figure 14b. Sensitivity analysis of wetting front suction, where  $\phi$  is the sensitivity coefficient (Eq. 28) and x-axis is the factor which was multiplied with the original values of the parameter (WGEW, 28 July 1972).

07.28.1972

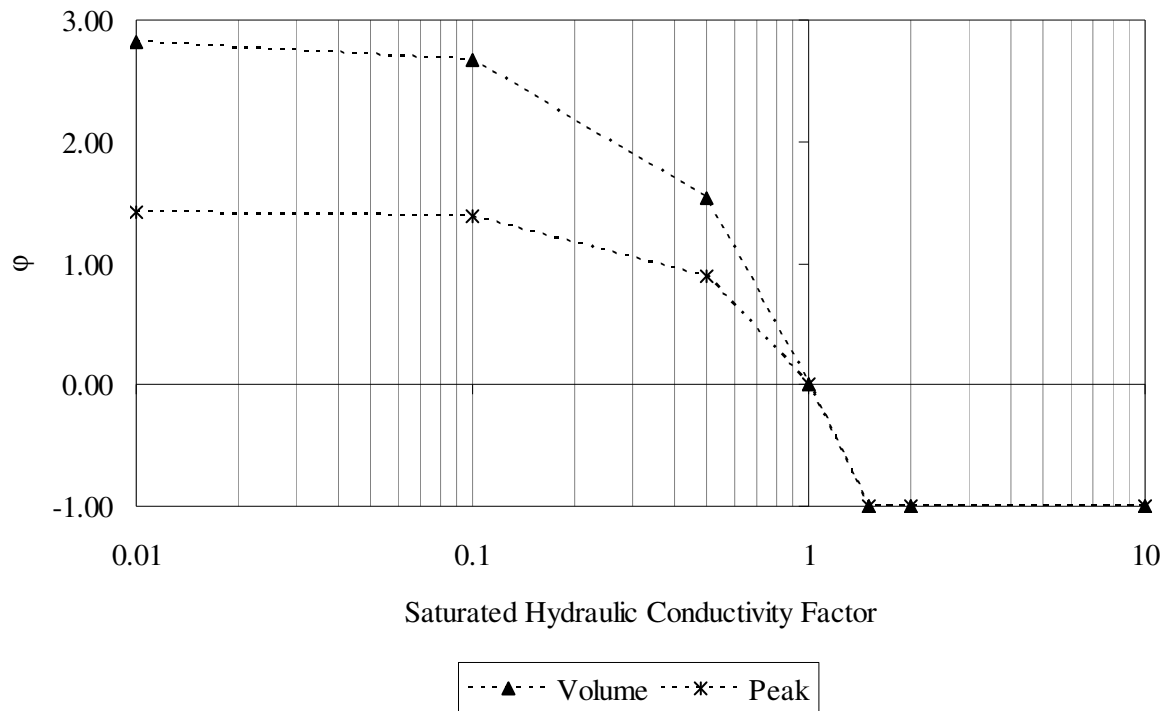


Figure 14c. Sensitivity analysis of saturated hydraulic conductivity, where  $\phi$  is the sensitivity coefficient (Eq. 28) and x-axis is the factor which was multiplied with the original values of the parameter (WGEW, 28 July 1972).

08.02.1968

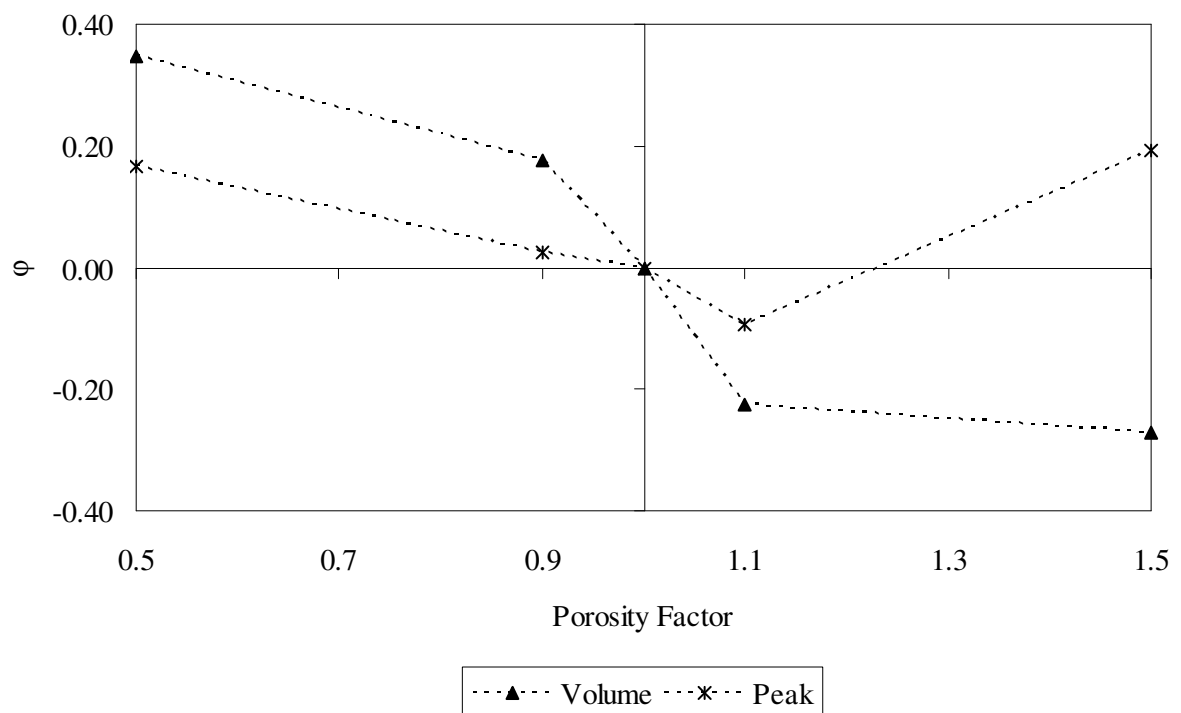


Figure 15a. Sensitivity analysis of porosity, where  $\phi$  is the sensitivity coefficient (Eq. 28) and x-axis is the factor which was multiplied with the original values of the parameter (WGEW, 2 August 1968).

08.02.1968

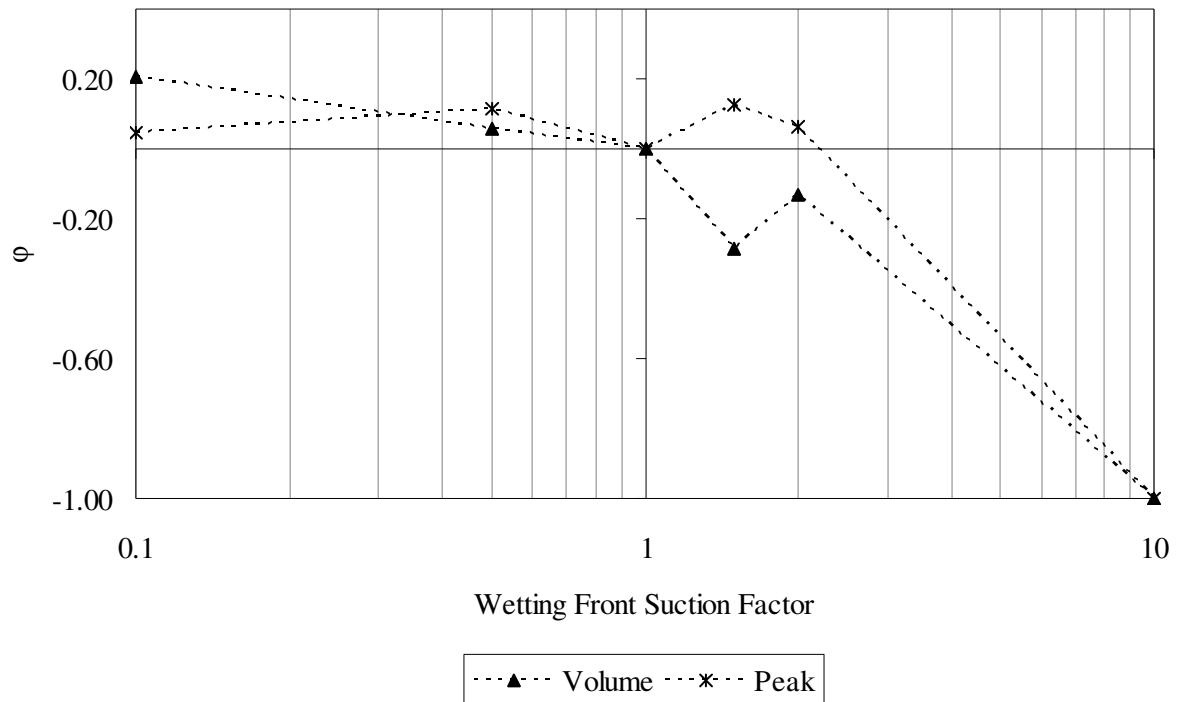


Figure 15b. Sensitivity analysis of wetting front suction, where  $\phi$  is the sensitivity coefficient (Eq. 28) and x-axis is the factor which was multiplied with the original values of the parameter (WGEW, 2 August 1968).

08.02.1968

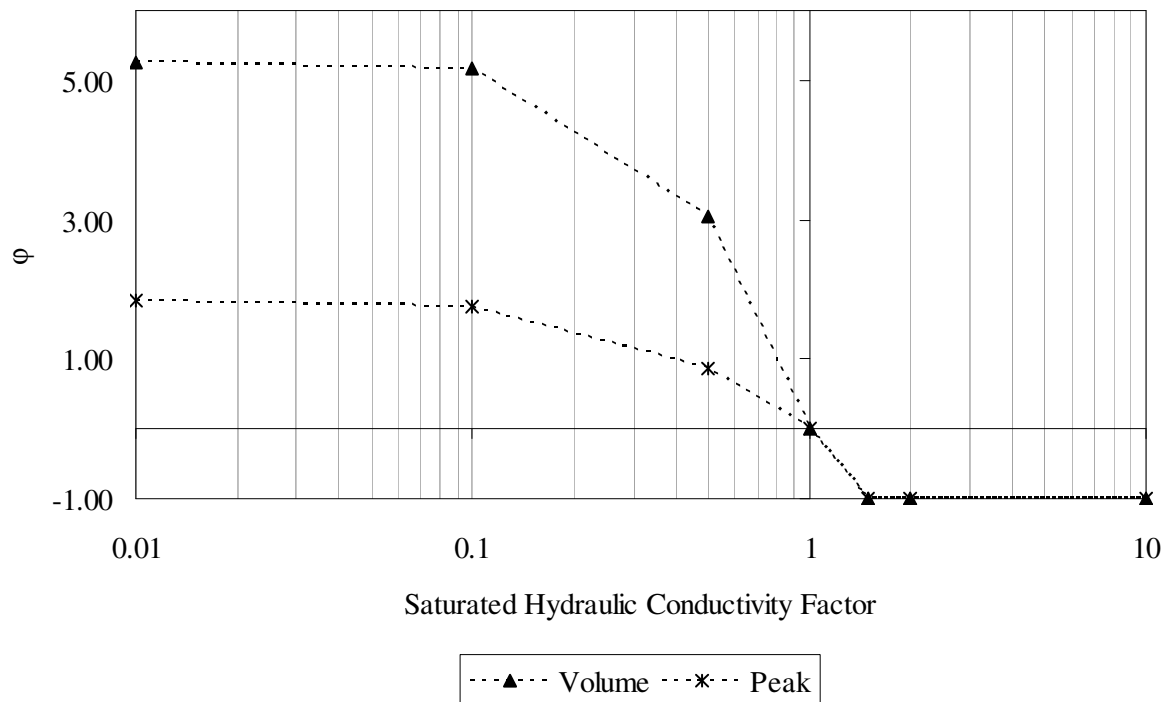


Figure 15c. Sensitivity analysis of saturated hydraulic conductivity, where  $\phi$  is the sensitivity coefficient (Eq. 28) and x-axis is the factor which was multiplied with the original values of the parameter (WGEW, 2 August 1968).

The sensitivity showed the largest values with changes in saturated hydraulic conductivity followed by wetting front suction and porosity. The higher those parameters are, the smaller is their sensitivity, i.e. the higher the infiltration from the stream into the alluvium. However, fluctuations in that behaviour could be found for peak flow in relation to wetting front suction, which might be related to numerical instabilities.

The sensitivity coefficient reached its lowest value of -1.00 with a change of +50% in the saturated hydraulic conductivity for both the streamflow volume and peak (Figs. 14c and 15c), whereas the sensitivity coefficient of the porosity remained between the range [-0.30; 0.20] for the same change (Figs. 14a and 15a). The sensitivity coefficient of the wetting front suction remained mostly between the aforementioned range (Figs. 14b and 15b).

Small values of the saturated hydraulic conductivity increased significantly the sensitivity coefficients of the streamflow volume and peak (Figs. 14c and 15c), whereas small values of the wetting front suction and the porosity did not imply an increase in the sensitivity coefficient greater than 0.40 for the streamflow volume and peak, excluding a sensitivity coef-

ficient value of the wetting front suction for the streamflow peak (Fig. 14b).

The sensitivity coefficient of the streamflow volume varied more than that of the streamflow peak for the saturated hydraulic conductivity and porosity.

### ***4.3. Overall parameter sensitivity analysis***

We selected the best simulated rainy season for the Middle Jaguaribe River (2005) and streamflow event for the Walnut Gulch Experimental Watershed (29 August 1972) and chose the most sensible parameters found previously (Sect. 4.2) for both case studies, in order to carry out a combined (“overall”) parameter uncertainty analysis based on the Monte Carlo approach. In this way, we ran the model 1000 times for the Jaguaribe river varying randomly the lateral and parallel saturated hydraulic conductivities from 1% to 199%, and for the WGEW the saturated hydraulic conductivity and the wetting front suction from 1% to 199% and the porosity from 70% to 130%. Then, we calculated the relative errors of the simulated streamflow volume and peak for the MJR and the WGEW. The relative errors are presented as box-plots in Figs. 16a-b:

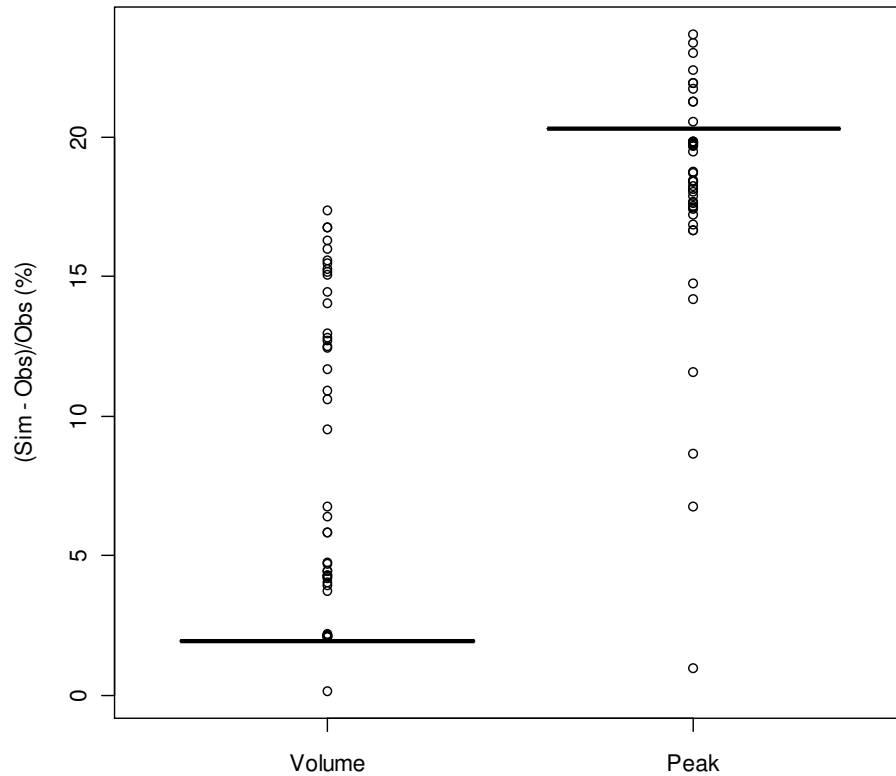


Figure 16a. Relative errors of the simulated streamflow volume and peak in 2005 for the Jaguaribe river after 1000 simulations varying randomly the lateral and parallel saturated hydraulic conductivity from 1% to 199%.

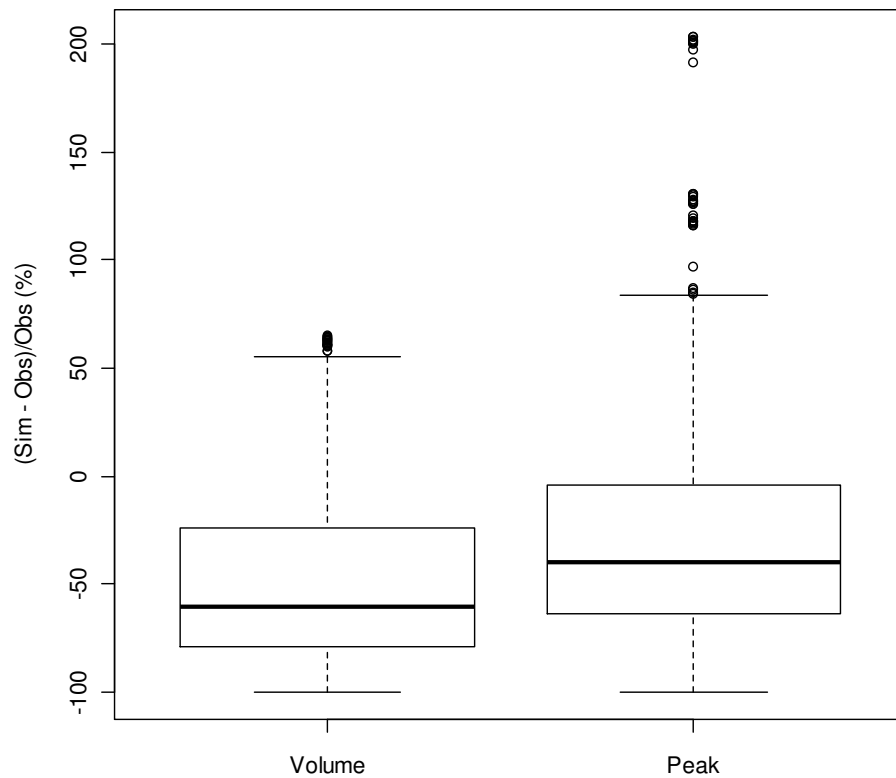


Figure 16b. Relative errors of the simulated streamflow volume and peak on 29 August 1972 for the Walnut Gulch Experimental Watershed after 1000 simulations varying randomly the saturated hydraulic conductivity and the wetting front suction from 1% to 199% and the porosity from 70% to 130%.

The relative errors of the simulations carried out for the WGEW (Fig. 16b) were much more variable than those for the MJR (Fig. 16a). The relative errors for the MJR were mostly in a very narrow range, where their inner quartile range (IQR) was practically zero, for both volume and peak. This rather stable behaviour (little overall parameter uncertainty) can be explained by the compensating effects of fluxes between/beneath the river and adjacent aquifer and the associated levelling of hydraulic gradients. The fluxes are represented in the model by mathematically simple water budgeting in aquifer columns and the levelling effects are considered by the coupled processes, including backwater effects, see Sects. 2.4 and 2.5. Therefore, for the MJR rainy season 2005, the relative error of the streamflow volume and peak was low, approximately 2% and 20%, respectively, with 90% of certainty related to the model parameters.

The relative errors for the WGEW fell within much larger ranges, where their IQR was approximately 54% for the volume and 59% for the peak. This was a result of the non-linearity involved in the unsaturated flow processes that prevail in disconnected dryland river systems. Such a non-linear behaviour is represented, e.g., by the Green-and-Ampt equation (Sects. 2.2 and 2.3). In addition, a damping through feedback effects such as for the saturated fluxes does not exist. Thus, for such conditions, the uncertainty is high, as demonstrated for the event on 29 August 1972, with a relative error (%) of the streamflow volume and peak between [-91; 26] and [-75; 46], respectively, with 80% of certainty related to the model parameters.

## 5. Discussion

The channel transmission losses model presented here has been developed for applications to different climate and hydrogeologic controls and scales of dryland rivers, covering a variety of hydrological processes relevant for in-channel transmission losses. In two case studies, it has pre-

dicted well the streamflow volume and peak for both a large losing/gaining, hydraulically connected river and a small losing, hydraulically disconnected stream. The model structure was chosen according to the hydrological perceptual models of the case studies, but no further parameter calibration procedure has been applied. That is why we consider the model to be well suited to the typical data scarce conditions in dryland areas. However, large uncertainties occur with reference to the timing of hydrographs, which is due to the simplified flood wave routing implemented, which is based only on the conservation of mass and the channel morphology. Therefore, the model can be used for water resources topics with a relatively long time scale, such as water resources planning and management purposes. However, it should not be applied to issues with short time scales, such as forecasting of flood wave timing as is necessary for flood warning.

The evaluation of the different model structures, which was conducted for the MJR case study, has shown that this procedure is promising for reducing structural model uncertainties and thus improving the capability for streamflow prediction in ungauged areas. This evaluation showed that adequate process representation improves the model reliability, e.g. in our case that both lateral (stream-)aquifer water fluxes and groundwater flow in the underlying alluvium parallel to the river course are necessary for physically-based prediction of streamflow and channel transmission losses, the former process being more relevant than the latter. The combination of the hydrological perceptual model of the MJR, which has been derived from field observations and data with the modelling-based hypothesis-testing on the dominant processes complement each other and may provide a guide for further field campaigns and model expansions.

The analysis of the subsurface system simulations has shown that the reliable predictions of the surface flow volume and peak discharge are not necessarily suffi-

cient to ensure a stable numerical solution of the subsurface processes in the unsaturated and saturated zones. Even if the influence of simulation time step and spatial discretization (e.g. the soil layer interval on the unsaturated flow) or of the boundary conditions (e.g. the groundwater flow of the downmost aquifer unit) is analysed, a comprehensive evaluation of the model performance, comprising all processes of the model, is severely constrained by the particular data scarcity in dryland environments.

The sensitivity analysis showed that the model results were relatively little sensitive to the parameters related to the saturated fluxes (lateral stream-aquifer dynamics and groundwater flow parallel to the river course). This rather stable behaviour can be explained by the compensating effects of fluxes between the river and adjacent groundwater and the associated levelling of hydraulic gradients. In other words, even if highly saturated hydraulic conductivities could “potentially” produce large fluxes between saturated model units, large fluxes did not happen because they were restricted by the actual hydraulic gradient between the model units, which are generally low, or may level out rather quickly.

These parameters, which are related to the saturated part of the model, produced much smaller variation in the sensitivity coefficient than those which drive the unsaturated part of the channel transmission losses model (unsaturated stream infiltration and vertical soil water redistribution). This is explained by the aforementioned restriction of the subsurface hydraulic gradient, and on the other hand by a rather strong non-linear behaviour of the equations, which govern the unsaturated flow.

The overall parameter analysis (1000 simulation runs with different combinations of lateral and parallel saturated hydraulic conductivities) of the conditions in the Middle Jaguaribe River reach, where the saturated processes are dominant, yielded at most rather small relative errors (2% for streamflow volume and 20% for peak). In contrast, the mean absolute error

of the streamflow volume of the selected events was 41%, 10% and 4% for different model structure settings (Table II). Therefore, at least for this case study, the uncertainties related to the model structure are considered to be larger than those related to the model parameters.

Rather large ranges for the simulated streamflow volume and peak based on 1000 simulations with different combinations of saturated hydraulic conductivity, wetting soil suction and soil porosity were found for the WGEW’s stream, where unsaturated processes are dominant for runoff generation. Thus, applications of this model to real-world problems in data-scarce streams dominated by unsaturated processes may compromise inevitably high parameter uncertainties. Nevertheless, one has to acknowledge that this uncertainty is not a purely model uncertainty (or model artefact), rather that it is typical behaviour resulting from unstructured (or random) process dynamics for this kind of disconnected dryland rivers.

## 6. Conclusions and Outlook

We developed a new process-oriented channel transmission losses model, which was designed to account for the surface-subsurface water fluxes in data-scarce dryland environments. Channel transmission losses modelling is indispensable for simulation of arid and semi-arid watershed hydrology, as long as the underlying aquifer system has not been fully saturated, as is expected to occur in ephemeral streams and in intermittent rivers in the dry seasons and at the beginning and in the middle of the rainy seasons (Renard, 1970; Costa et al., 2012). Moreover, in (sub-)humid rivers vertical and lateral groundwater recharge can occur from winter to spring, when the surface water stages are higher than the groundwater table (see e.g. Krause and Bronstert, 2007). This recharge after drought periods or during extensive groundwater pumping may be intensified and resemble channel transmission losses of dryland rivers.



The main findings of our work can be described as follows:

1. A mathematically flexible and hydrologically complex modelling of the channel transmission losses can represent well the most relevant hydrological processes for streamflow prediction in dryland rivers throughout different scales and controls.

2. A test of different model structures enables the comparative application of the channel transmission losses model to a poorly gauged river and yields information on the relevance of different sub-systems and processes.

3. High nonlinear approaches, which were used for the unsaturated zone processes, are much more sensible to parameter variability than those of mathematically simple, but hydrologically two-way-coupled, approaches, which were used for the saturated zone.

4. Uncertainties arising from the model structure were more relevant than those related to the parameter variability of the saturated part of the model in the Middle Jaguaribe River application.

5. The scarcity of data in dryland environments and the process complexity involved in the unsaturated flow lead to the view that disconnected systems (e.g. the WEGW's) controlled by the unsaturated zone generally compromise model uncertainties much more than do connected systems (e.g. the MJR) that are driven by the saturated flow. Therefore, the degree of aridity of a dryland river may be an indicator of its model uncertainty/predictability.

The model might be further tested and possibly improved – particularly its subsurface part – based on comparison with additional groundwater observational data. This may improve the reliability of its internal processes representation (e.g. unsaturated flow and groundwater flow) and subsequently its applicability for ungauged situations (based on Andréassian et al.,

2007, 2009, 2010; Bronstert, 2004). In this respect, we have been monitoring groundwater level close to the outlet of the studied reach of the Middle Jaguaribe River, whose first results were presented in Costa et al. (2012). Moreover, an obvious aim is the integration of this model with a dryland hydrological catchment model for semi-arid hydrology (see, e.g. Güntner and Bronstert, 2004; Güntner et al., 2004).

The increase in data availability, in particular from the subsurface structures, may allow a finer spatial discretization of model units, i.e. moving from the actual semi-distributed to a distributed hydrological concept and/or introducing additional processes. Such a strategy, for example, was followed over the past decades for the hydrological modelling of the Okavango Delta System in Botswana, where surface-subsurface fluxes were simulated initially by conceptual models and then later on by fully-distributed ones (e.g. Bauer et al., 2006; Milzow et al., 2009).

## 7. Acknowledgements

The first author thanks the Brazilian National Council for Scientific and Technological Development (CNPq) for the PhD-scholarship. We thank David Goodrich for his comments on the literature review section and the section applicable to Walnut Gulch Research Watershed. We thank the Brazilian Geological Service (CPRM), the Brazilian Water Agency (ANA) and the Meteorological and Water Resources Foundation of the State of Ceará (FUNCEME). Datasets were also provided by the USDA-ARS Southwest Watershed Research Center. Funding for these datasets was provided by the United States Department of Agriculture, Agricultural Research Service. We are also grateful to the two reviewers for their comments and suggestions, which improved this paper significantly.

## Chapter IV:

# Probabilistic flood forecasting for a mountainous headwater catchment using a nonparametric stochastic dynamic approach

### Abstract

Hydrological models are commonly used to perform real-time runoff forecasting for flood warning. Their application requires catchment characteristics and precipitation series that are not always available. An alternative approach is nonparametric modelling based only on runoff series. However, the following questions arise: Can nonparametric models show reliable forecasting? Can they perform as reliably as hydrological models? We performed probabilistic forecasting one-, two- and three-hours ahead for a runoff series, with the aim of ascribing a probability density function to predicted discharge using time series analysis based on stochastic dynamics theory. The derived dynamic terms were compared to a hydrological model, LARSIM. Our procedure was able to forecast with 95% confidence interval one-, two- and three-hour ahead discharge probability functions with about 1.40 m<sup>3</sup>/s of range and relative errors (%) in the range [-30; 30]. The LARSIM model and the best nonparametric approaches gave similar results, but the range of relative errors was larger for the nonparametric approaches.

*Keywords: streamflow probabilistic forecasting; time series analysis; stochastic dynamical systems; parametric and nonparametric comparison*

Published as

Costa, A.C., Bronstert, A., and Kneis, D.: Probabilistic flood forecasting for a mountainous headwater catchment using a nonparametric stochastic dynamic approach, *Hydrological Sciences Journal*, 57(1), 10-25, 2012.

## 1. Introduction

Hydrologists commonly use distributed hydrological models to perform real-time streamflow forecasting for flood warning purposes. These models require large data sets of catchment physical characteristics and precipitation series that are not always available. Furthermore, the results from these models can be rather uncertain due to large errors in precipitation input, initial catchment moisture conditions and/or modelling parameters/processes. An alternative approach is to use nonparametric models based on streamflow series only, to overcome the requirement for data on catchment physical characteristics and precipitation series. However, it is not known whether nonparametric models for meso-scale catchments can show reliable streamflow forecasting for flood warning, or whether they can perform as reliably as, or even outperform, distributed hydrological models.

Since the beginning of the 1990s, runoff series have been assumed as responses of dynamical systems with a low-dimensional chaotic attractor resulting from the nonlinear coupling of precipitation and catchment state that depends on climatic condition and geo-patterns, such as land cover, soils, river network and geology (Liu et al., 1998; Porporato and Ridolfi, 1997; Sivakumar et al., 2001). A fundamental characteristic of a dynamical system is that it returns or recurs to former states (recurrence) (see discussion in Marwan et al., 2007).

This assumption means that the “catchment-runoff-system” should obey a deterministic operator, a set of coupling ordinary differential equations of the involved variables (e.g. runoff, precipitation and soil moisture). This operator projects a trajectory in the state space (or phase space), which establishes all states of the involved variables. The catchment runoff system states return or recur to former states during their trajectory in the state space. However, recently, the hypothesis that hydrological processes are governed by dynam-

ics with low-dimensional attractors has been disputed e.g. in Koutsoyiannis (2006).

In this context, chaotic systems theory has been applied to hourly, daily and monthly runoff series employing nonparametric models by the phase space reconstruction technique (Jayawardena and Lai, 1994; Liu et al., 1998; Jayawardena and Gurung, 2000; Sivakumar et al., 2001; Porporato and Ridolfi, 1997, 2001; Sivakumar et al., 2002; Laio et al., 2003). Moreover, even without low-dimensional chaotic attractor, this nonlinear dynamics approach can also give good predictions (Koutsoyiannis et al., 2008).

This nonlinear approach can provide accurate *one-discharge-value-per-time-step* forecasting, but it does not always offer insight into the probabilistic structure of the data resulting from the shortness of series, and the inevitable presence of dynamical noise in open physical systems, such as catchment runoff (Porporato and Ridolfi, 2001; Kantz and Schreiber, 2004). Moreover, the ability of the nonlinear approach to give information on uncertainties associated with forecasts is limited (Korník et al., 2006), and this is central to the implementation of effective flood warning or flood protection measures (see Todini, 2004). To address the last issue, Tamea et al. (2005) proposed: (a) an ensemble-based nonlinear prediction with parametric deterministic range similar to the GLUE method (Beven and Binley, 1992; Beven, 1993); and (b) a probabilistic prediction using global errors of a training set to “dress” the deterministic forecasts, which was also done by Chen and Yu (2007) using support vector machine background.

In this paper, we deal with real-time probabilistic forecasting of river discharge. For this task, we apply stochastic dynamics theory related to time series analysis in hydrology to deal with both deterministic evolution and inherent fluctuations in river discharge data. In this way, we consider a dynamical system (autonomous set of deterministic equations), such as the Lorenz

equations, contaminated by external noise (van Kampen, 1992; Anishenko et al., 2003; Kantz and Schreiber, 2004), as the driving physical assumption for catchment runoff.

A stochastic dynamical system can be expressed mathematically by time series models, where the dynamic or deterministic part is approached by a regression model and the stochastic part by noise, which does not depend on the states of the dynamic part.

The objectives of this work are to perform one-, two- and three-hour ahead probabilistic forecasting for runoff series, i.e. to ascribe a probability density function (pdf) to predicted discharge, in a mountainous headwater catchment (49 km<sup>2</sup>) using time series models. Furthermore, the deterministic evolution of the time series models will be compared to a comprehensive hydrological model called LARSIM, which has been used for operational forecasts of floods, low flow and water temperature in Germany (Ludwig and Bremler, 2006).

In this way, we intend to identify an underlying dynamical system for a noisy runoff series and approach it by a proposed nonparametric stochastic dynamic model.

Identifying a dynamical system for catchment runoff means that a similar flood magnitude will be expected for an actual set of catchment runoff states similar to a previous one (determinism). This deterministic paradigm is quite different, if we assume a random nature of the data and then apply time series models, which has been done using nonparametric stochastic forecasting approaches only.

## 2. Nonparametric Modelling

### 2.1. Dynamical systems

A dynamical system may be thought as a set of variables  $\mathbf{x}$  ( $x^1, x^2, \dots, x^n$ ), whose states are observed in time  $t$  as simply a result of the action of a deterministic evolution operator that does not depend on  $t$ , in some state space  $R^n$ . Once a state is

known, the states of all surroundings are determined as well by:

$$\mathbf{x}_{t+\Delta t} = F(\mathbf{x}_t), t \in R \quad (1)$$

The value of a variable specifies a point in state space, and *vice versa*. Hence, one can approach the deterministic evolution operator by the dynamics of values of a unique variable, which is called phase space or delay reconstruction (see Anishchenko et al., 2003; Kantz and Schreiber, 2004).

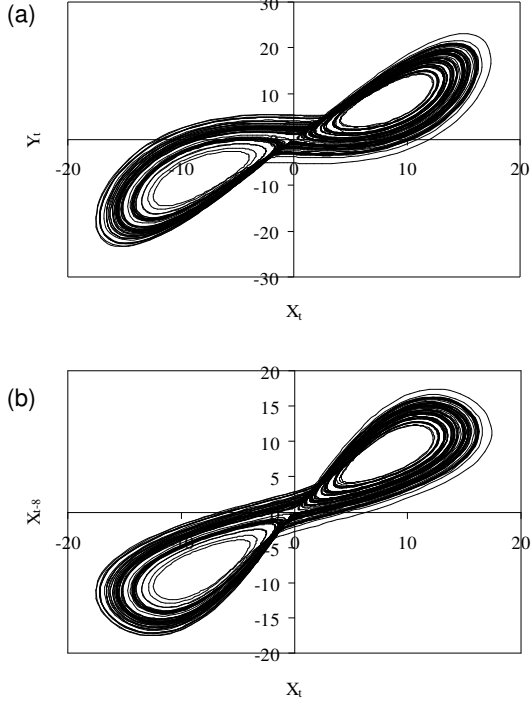
Considering  $\mathbf{x}_t$  in  $R^n$ , the delay reconstruction of  $\mathbf{x}_t$  can be written based on Takens (1980) as:

$$\mathbf{x}_t = (x_t, x_{t-\Delta t}, \dots, x_{t-\Delta t \cdot (n-1)}) \quad (2)$$

As an example we consider the Lorenz equations (Lorenz, 1963)

$$\begin{cases} \dot{x} = 10 \cdot (y - x) \\ \dot{y} = 28x - y - xz \\ \dot{z} = -\frac{8}{3}z + xy \end{cases} \quad (3)$$

We integrated equation (3) using a Runge-Kutta routine with small step size. Then, we plotted their 2D-evolution ( $x_t$  vs  $y_t$  variables in Fig. 1a and their reconstructed 2D-evolution ( $x_t$  vs  $x_{t-8}$  variables in Fig. 1b).



**Figure 1.** (a) 2D-evolution ( $x_t$  vs  $y_t$  variables); and (b) reconstructed 2D-evolution ( $x_t$  vs  $x_{t-8}$  variables) of Lorenz equations.

Thus, the evolution of a dynamical system is “printed” on the past observations of a unique variable of it. Now, suppose a time series of a variable of the dynamical system  $x_t$ ; it is validated from equations (1) and (2) that:

$$x_{t+\Delta t} \approx F(x_t, \dots, x_{t-\Delta t \cdot (n-1)}) \quad (4)$$

If one aims to predict  $x_t$  using the map (4), it can be modelled by a regression model, where a forecast state is estimated by the values of the variable at  $n$  past steps. This needs a short-range dependence of the time series, that is, its autocorrelation function (acf)  $c_{j,\Delta t}$  in relation to a step  $\Delta t$  has to reach approximately zero at a *short* shift  $K$  (based on Koutsoyiannis et al., 2008):

$$c_{j,\Delta t} = \frac{\langle (x_\eta - \langle x \rangle)(x_{\eta-j\Delta t} - \langle x \rangle) \rangle}{\sigma^2} \rightarrow 0, \quad \text{when} \\ j \rightarrow K \ll l \quad (5)$$

where  $l$  is the total number of events,  $j$  and  $K$  are non-zero natural numbers. However, as pointed out by Fisher (1928), the variance  $s_{c,l}^2$  of the empirical coefficient of correlation  $c_{K,\Delta t}$  follows:

$$s_{c,l}^2 = \frac{1}{\sqrt{l-3}} \quad (6)$$

Then, for a finite sample, the Fisher’s interval  $[-s_{c,l}; s_{c,l}]$  limits the region around the acf’s zero, where the uncorrelated behaviour of its acf cannot be rejected.

Furthermore, the  $n$  past steps can be approximated by the  $(K-1)$  neighbours with coefficient of correlation greater than  $s_{c,l}$  (see also Fig. 2) as:

$$\hat{x}_\eta = F(x_{\eta-j\Delta t}, \dots, x_{\eta-(K\Delta t-1)}) \quad (7)$$

## 2.2. Probabilistic approach

Our main point in this paper is that the determinism is broken up due to the presence of fluctuations in open physical systems like catchment runoff. Therefore, we add a global stochastic term on the map (7), modifying it to:

$$\hat{x}_\eta = F(x_{\eta-j\Delta t}, \dots, x_{\eta-(K\Delta t-1)}) + \zeta \quad (8)$$

where  $\zeta$  could be white or coloured noise. Adopting an *a priori* regression model to  $F$ , we can afterwards estimate the distribution of  $\zeta$  from a training set, diminishing the training set measurement  $X_{ts}$  and prediction of the dynamic term  $F$ . Then, we can define different confidence intervals, e.g. 90 and 95%, for the distribution of  $\zeta$  as a histogram with zero mean. Note that  $x_t$  has to be normalized to a pdf with zero mean and standard deviation equal to one.

Using the relationship (8), the expected value of  $\hat{x}_\eta$  is predicted by  $F$  (dynamic term) and its uncertainty by the distribution of  $\zeta$  (stochastic term) with a confidence interval, ascribing in this manner a pdf for  $\hat{x}_\eta$ .

When measurements in a validation set occur outside the limits of the confidence intervals of the pdf given by equation (8),  $[F + \zeta^-; F + \zeta^+]$ , we achieve the validation set error  $\varepsilon$ , defined as:

$$\varepsilon = \begin{cases} 0, & \text{if } F + \zeta^- \leq x_v \leq F + \zeta^+ \\ F + \zeta^- - x_v, & \text{if } x_v < F + \zeta^- \\ F + \zeta^+ - x_v, & \text{if } x_v > F + \zeta^+ \end{cases} \quad (9)$$

where  $x_v$  is measurement in a validation set. Note that the distribution of  $\zeta$  includes the uncertainty not only from the inherent fluctuations of the runoff data, but also from the fitting of the underlying dynamic term by an assumed regression model.

The probabilistic approach presented in this section is quite similar to the probabilistic forecast method found in Tamea et al. (2005). However, our approach simplifies the Tamea et al. (2005) method, which needs many realizations of the forecast error and calibration of a correction term for the distribution of the residuals.

### 2.3. Regression models

Several authors (Jayawardena and Lai, 1994; Liu et al., 1998; Jayawardena and Gurung, 2000; Sivakumar et al., 2001; Porporato and Ridolfi, 1997, 2001; Sivakumar et al., 2002; Laio et al., 2003) have presented cases in which local approaches, i.e. locally fitted models, have outperformed nonlinear and linear global ones, although Koutsoyiannis et al. (2008) presented a case in which a global stochastic model outperformed a locally fitted and a global nonlinear approaches.

In this method, we adopt regression models that are: (a) locally averaged, whose only unknown parameter is the number of neighbourhoods ( $n$  past steps), and (b) locally constant, in that the predicted value is assumed to be equal to the last measurement.

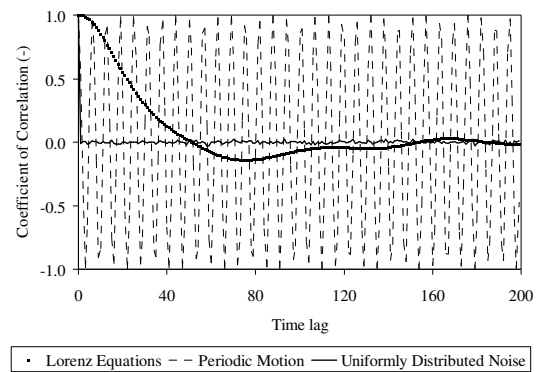
We also use the autoregressive model (AR), whose unknown parameters are the number of neighbourhoods and its coefficients from an acf, for the dynamic term  $F$  as reference to test the hypothesis of linear random data. Note that we do not apply an ARMA, because the noise inputs of the moving average model (MA) are not known before the application of equation (8) and must be averaged over. This was also done by Kantz and Schreiber (2004) applying nonlinear methods only.

### 2.4. Identifying dynamical systems from noisy time series

Before the application of equation (8), we must identify experimentally whether a dynamical system can be assumed from a given noisy runoff series.

The identification of dynamical systems by nonlinear methods (e.g. correlation or

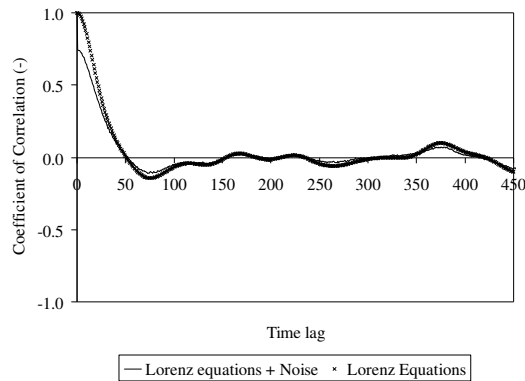
entropy dimensions) requires a large amount of noise-free data (Kantz and Schreiber, 2004). Therefore, we use autocorrelation functions (acfs) to identify qualitatively dynamical systems from very noisy time series. In this section, we compare the acfs of: (a) uniformly-distributed noise, (b) a sine function (periodic motion), and (c) the  $x$  variable of the Lorenz equations. The acfs of these three systems are plotted in Fig. 2.



**Figure 2.** Autocorrelation functions (acfs) of: (a) uniformly-distributed noise, (b) a sine function (periodic motion), and (c) the  $x$  variable of the Lorenz equations.

Figure 2 shows that the acf of a dynamical system decays exponentially to zero and then oscillates quasi-periodically around zero, whereas that of uniformly-distributed noise has small fluctuations around zero. The acf of the periodic motion only reflects its “periodicity”.

Now, if we include external uniformly-distributed noise into the time series of the  $x$  variable of the Lorenz equations (Fig. 3), the acf of the new noisy system decays rapidly at the initial time lags and then exponentially to zero. After the time lag equal to 50, it oscillates quasi-periodically around zero with lower correlation compared to the noise-free acf.



**Figure 3.** Autocorrelation functions of the  $x$  variable of the Lorenz equations with and without uniformly-distributed noise.

### 3. Parametric Modelling

In this study, we compare the presented nonparametric modelling to a comprehensive hydrological model called LARSIM, which has been used for operational forecasts of floods, low flow and water temperature in Germany (Ludwig and Bremicker, 2006). LARSIM is a distributed hydrological model, which distinguishes most relevant hydrological processes such as interception, evapotranspiration, snow accumulation, snow compaction and snowmelt, soil water storage and water flow and storage in streams and lakes (Ludwig and Bremicker, 2006). It can apply a raster-based spatial discretization for easy usage of routinely available physical catchment data (e.g. slope, land use and field capacity) and hydro-meteorological time series (Ludwig and Bremicker, 2006).

## 4. An Example for Probabilistic Flood Prediction

### 4.1. Data overview

The time series analysis was carried out for Ammeldorf stream gauge, which limits a catchment of about  $49 \text{ km}^2$  located in the eastern Ore Mountains, Germany, close to the Czech–German border (Fig. 4). About 2 km downstream of this gauge is the artificial reservoir Lehmühle, which dampens or adjusts the river discharge, particularly during flood events. According to Reusser et al. (2009) and Bronstert et al.

(2011), the catchment has an elevation of 530 to about 900 m a.s.l and slopes are gentle, with an average of  $7^\circ$ . The climate is moderate with mean temperatures of  $11^\circ\text{C}$  and  $1^\circ\text{C}$  for the periods April–September and October–March, respectively, and annual precipitation is about 1100 mm/year. High flows can be induced by either convective rainfall during the summer or snowmelt in the spring. Land use is characterized by forests (58.3%), natural grassland (20.1%), agriculture (9.6%), pasture (6.1%), peat bog (3.7%) and urban areas (2.2%).

Discharge data were obtained from the Saxony state office for environment and geology. Discharge data for the Ammeldorf stream gauge was made available hourly and the series runs from January 2000 to October 2009. The average discharge was  $1.01 \text{ m}^3/\text{s}$  and the coefficient of variation was 1.5, with 0.04 and  $35.44 \text{ m}^3/\text{s}$  being the minimum and maximum measured discharge, respectively. The discharge series for 2007–2009 is shown as an example in Fig. 5.

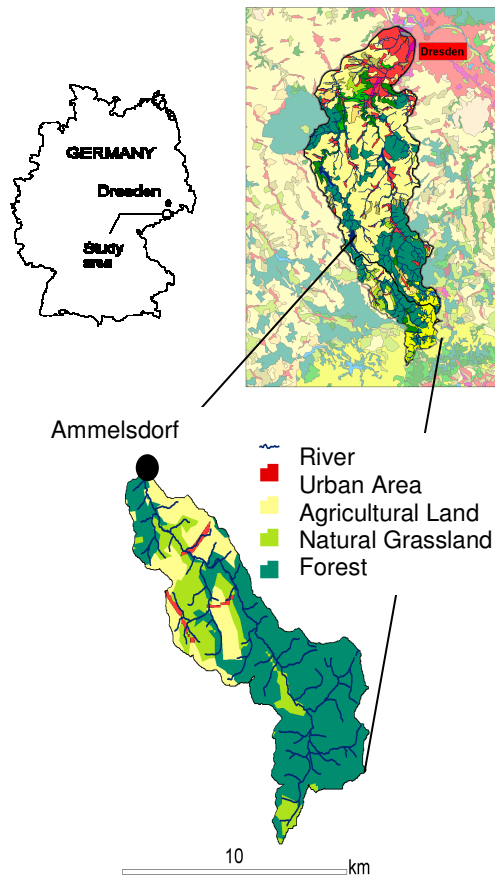


Figure 4. Location of the Weisseritz headwater catchment, upstream of the Ammelsdorf stream gauge.

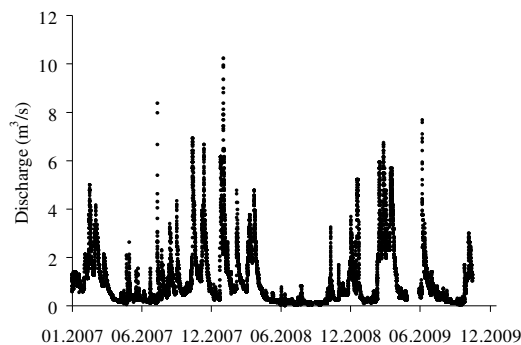


Figure 5. Hourly discharge series for the Ammelsdorf stream gauge for 2007–2009.

## 4.2. Runoff nonparametric modelling

### 4.2.1. Identifying an underlying dynamical system

Previous works on nonparametric discharge forecasting (Jayawardena and Lai, 1994; Liu et al., 1998; Jayawardena and Gurung, 2000; Sivakumar et al., 2001; Porporato and Ridolfi, 1997, 2001; Sivakumar et al., 2002; Laio et al., 2003; Tamea et al., 2005) have used the dis-

charge time series as the independent variable, but if its autocorrelation function does not reach the uncorrelated behaviour (short-range dependence), even if the time series are driven by a dynamical system, we should not fit a regression model to the dynamic term  $F$  in equation (8).

We calculated here the autocorrelation function (acf) for the discharge time series ( $Q$ ) and also for its first ( $Q'$ ) and second ( $Q''$ ) time derivatives (Fig. 6) to find out whether a dynamical system can be assumed in a qualitative way from our original time series.

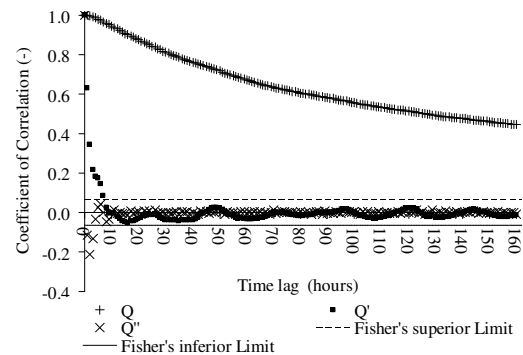


Figure 6. Autocorrelation function of the hourly discharge series ( $Q$ ) and of its first ( $Q'$ ) and second ( $Q''$ ) time derivatives for the Ammelsdorf stream gauge (2000–2009 with gaps), Fisher's interval limits indicating the region, where the uncorrelated behaviour that cannot be rejected.

Figure 6 shows that the discharge time series did not exhibit a short-range dependence, rather it exhibited a long-range dependence (i.e. power-type decay of autocorrelation also known as the Hurst phenomenon (e.g. Koutsoyiannis, 2002)), and, consequently, we should not use these time series for regression model-based approaches. The second derivative of discharge series for a time lag equal to four hours reached the uncorrelated behaviour, but its acf is similar to that of noise systems, showing its very low predictability. However, the first derivative of discharge series exhibited a short-range dependence and its acf presented a structure similar to that of dynamical systems contaminated with noise, i.e. a rapid decay in the initial time lags and then exponential decay to zero. After a time lag of about seven hours,



it oscillates quasi-periodically around zero. Consequently, we used the first derivative of discharge time series to forecast the original discharge time series.

#### 4.2.2. One-, two- and three-hour ahead probabilistic prediction

The hourly first time derivative of discharge time series was re-sampled to also create two- and three-hour series by applying:

$$Q'_{i,\Delta t} = \frac{Q_{t+\Delta t} - Q_t}{\Delta t} \quad (10)$$

where  $Q_t$  is the original discharge time series and  $i$  is  $t + \Delta t/2$ . The time interval  $\Delta t$  was set as one-, two- and three-hours.

We then multiplied the first time derivative of runoff, equation (10), by its time interval for all the one-, two- and three-hour time series, defining in this way the difference between two runoff measurements—the runoff difference—as the independent variable in this study.

Applying equation (8), probabilistic predictions of runoff differences  $\Delta \hat{Q}_{i,\Delta t}$  in  $\text{m}^3/\text{s}$  for one time interval  $\Delta t$  ahead were carried out for one-, two- and three-hour time series using:

$$\Delta \hat{Q}_{i,\Delta t} = F(\Delta Q_{i-\Delta t,\Delta t}, \dots, \Delta Q_{i-\Delta t \cdot m,\Delta t}) + \xi; \quad i > \Delta t \cdot m \quad (11)$$

We considered three approaches for the dynamic term  $F$ : (a) an autoregressive model, (b) a locally averaged model, and (c) a locally constant model. The term  $\xi$  was defined previously. Afterwards, the prediction of runoff differences for one-, two- and three-hour time series was used in equation (12) below to achieve the probabilistic prediction of stream discharges for one-, two- and three-hour ahead:

$$\hat{Q}_{t+\Delta t} = Q_t + \Delta \hat{Q}_{i,\Delta t} = Q_t + F(\Delta Q_{i-\Delta t,\Delta t}, \dots, \Delta Q_{i-\Delta t \cdot m,\Delta t}) + \xi; \quad i > \Delta t \cdot m \quad (12)$$

where  $Q_t$  is the measured stream discharge and  $\hat{Q}_{t+\Delta t}$  is the predicted probability function of stream discharge. Note that stream discharge assimilation is taken into account by equation (12).

#### 4.2.3. Runoff event filter

The procedure described in the last section was only applied for what we called runoff events of the time series. Given a series of runoff differences

$\{\Delta Q_{i,\Delta t}, \Delta Q_{i+1,\Delta t}, \dots, \Delta Q_{i+k,\Delta t}\}$ , we defined a runoff event within it when continuous measurements obey: (a)  $\Delta Q_{i,\Delta t} \neq 0$  or (b)  $\Delta Q_{i,\Delta t} = 0$ , if  $\Delta Q_{i-1,\Delta t} \neq 0$  and  $\Delta Q_{i+1,\Delta t} \neq 0$ .

In addition, only the runoff events with duration greater than 6 h were taken into account to avoid trends in fitting of the autoregressive model and the locally averaged model due to a large quantity of small runoff events in the time series.

#### 4.2.4. Performance criterion

As an error measure we used relative error, RE (in %; equation (13)), to assess the differences between runoff measurements ( $\text{m}^3/\text{s}$ ) and the confidence interval limits of the predicted pdfs of equation (11):

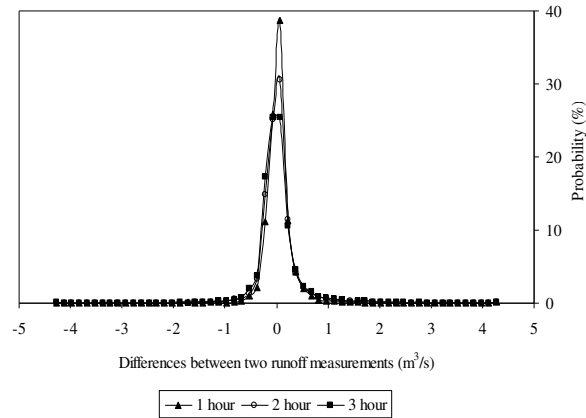
$$RE = \frac{\hat{Q}_{t+\Delta t} - Q_{t+\Delta t}}{Q_{t+\Delta t}} = \frac{Q_t + \Delta \hat{Q}_{i,\Delta t} - Q_{t+\Delta t}}{Q_{t+\Delta t}} = \frac{\Delta \hat{Q}_{i,\Delta t} - \Delta Q_{i,\Delta t}}{Q_{t+\Delta t}} = \frac{\varepsilon}{Q_{t+\Delta t}} \quad (13)$$

where  $\varepsilon$  was defined as in equation (9). To ease the derivation of equation (13), the range-based formulation of  $\varepsilon$  was not taken into account here. As this work is intended to forecast probabilistic streamflow for flood warning purposes, the best approach for a given confidence interval of the probability distribution of  $\xi$  in equation (12) minimizes the range of (a)  $\xi$  and (b) relative error (RE).

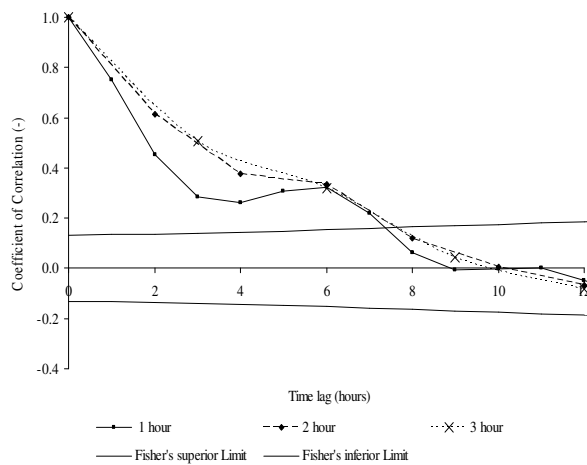
### 4.3. Results

#### 4.3.1. Nonparametric forecasting

Adopting the first 75% of the runoff series as a training set, we calculated the pdfs (Fig. 7) and the partial autocorrelation functions (acfs) (Fig. 8) for one-, two- and three-hour time series.



**Figure 7.** Probability density function of the hourly differences between two runoff measurements, runoff differences, using the first 75% of the runoff differences as the training set.



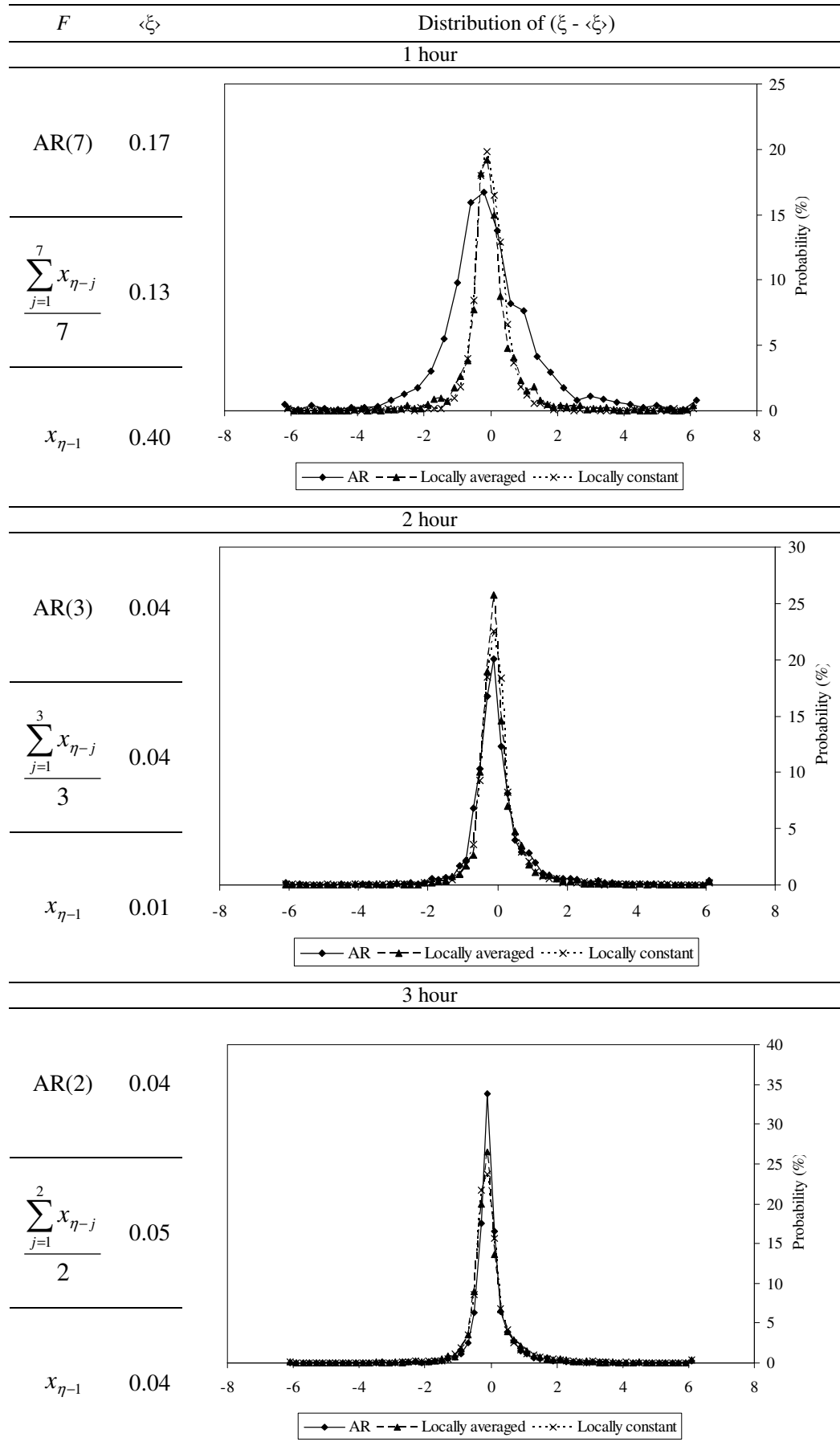
**Figure 8.** Partial autocorrelation function of the hourly differences between two runoff measurements, runoff differences, using the first 75% of the runoff differences as the training set, Fisher's interval limits indicating the region where the uncorrelated behaviour cannot be rejected.

Because of the runoff events filter, the following statistics and the coefficients of partial acfs changed for one-, two- and three-hour time series (Fig. 8). The pdfs of in-training set runoff differences for one-, two- and three-hour time series were approximately similar to a Gaussian distribution. The most runoff differences were in narrow ranges. Runoff differences larger than  $2.1 \text{ m}^3/\text{s}$  showed 0.2, 0.4 and 0.8% probability for one-, two- and three-hour time series, respectively. The mean and the standard deviation are 0.04 and 0.33, 0.03 and 0.48, 0.03 and  $0.58 \text{ m}^3/\text{s}$  for one-, two- and three-hour time series, respectively.

Comparing the mean and standard deviation of training and validation sets for one-, two- and three hour time series, we found that the means of both sets were practically the same, but the standard deviation of the validation set is about 33% smaller than that of the training set. This means that the data variability of the validation set is not a source of uncertainty for forecasting results.

The runoff differences whose coefficient of correlations of the partial acfs were greater than Fisher's superior limit were adopted as neighbourhoods in time for both autoregressive and locally averaged model-based approaches, and their coefficients of correlation for autoregressive models. After a normalization of stream discharge data, we applied autoregressive, locally averaged and locally constant model-based approaches to the training set. We had the following dimensionless time series models for one-, two- and three-hour time series (Table I). Note that we had to diminish the mean  $\langle \zeta \rangle$  of the distribution  $\zeta$  to achieve a histogram with zero-mean as stochastic term.

Table I. Dynamic and stochastic terms of time series models (dimensionless), adopting autoregressive (AR), locally averaged and locally constant models as approaches for the dynamic term F.



It can be seen from Table I that the distributions of  $(\xi - \langle \xi \rangle)$  (the stochastic part of equation (8)) were in narrow ranges, approximately similar to a Gaussian distribution, for one-, two- and three-hour time series, excluding only the AR(7)-based distribution. The sharpest distribution for one- and two-hour time series was the locally averaged model-based one; in contrast, the sharpest distribution for three-hour time series was the autoregressive model-based one.

After the derivation of these approaches, we applied them and computed the range of relative errors considering 97.5, 95 and 90% confidence intervals of the distribution of  $(\xi - \langle \xi \rangle)$  for one-, two- and three-hour time series. For this calculation, we used not only the last 25% of the runoff differences, but also the training set as well, because it presented high runoff differences with low probability (see above in this section), which can generate, for instance, high relative errors.

We adopted absolute relative errors (see equation (13)) about smaller than 30% with 90% confidence interval as the criterion of reliability for stream discharge forecasting. In this manner, we found from previous investigation that reliable forecasting was produced only when measured stream discharges,  $Q_t$  were: (a) higher than  $5.5 \text{ m}^3/\text{s}$  for one-hour time series, and (b) higher than  $8.8 \text{ m}^3/\text{s}$  for two- and three-hour time series. Note that reliability is subjective and these discharge thresholds can vary between applications.

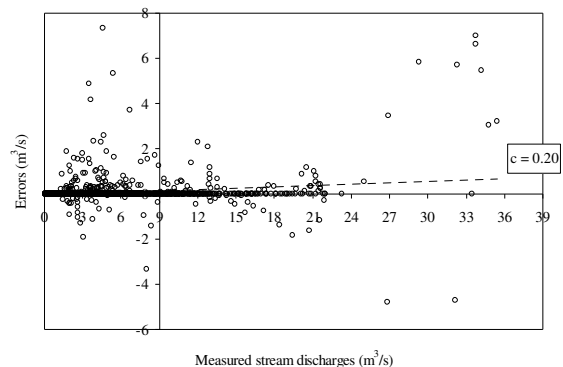
The above discharge thresholds can be explained by equation (13), whereby the higher the measured stream discharges, the smaller the relative errors. Nevertheless, although one could argue that from a certain discharge threshold the errors could be smaller, no statistical evidence of this trend was found in the time series (e.g. Fig. 9 shows measured stream discharges vs errors from the application of the autoregressive approach to two-hour time series with 95% confidence interval).

We carried out further performance analysis of the nonparametric models, con-

sidering discharge threshold levels for one-, two- and three-hour time series (see Table II). Hence, the number of predicted stream discharges for one-, two- and three-hour time series, respectively, was 516, 300 and 347.

As the best approach minimizes the range of: (a)  $(\xi - \langle \xi \rangle)$  and (b) relative error, RE, we tried to find an optimum among these criteria to choose the best approach for each confidence interval in each time series. In this way we found from Table II that the locally averaged model-based approach was the best for one- and two-hour time series and the autoregressive approach for three-hour time series.

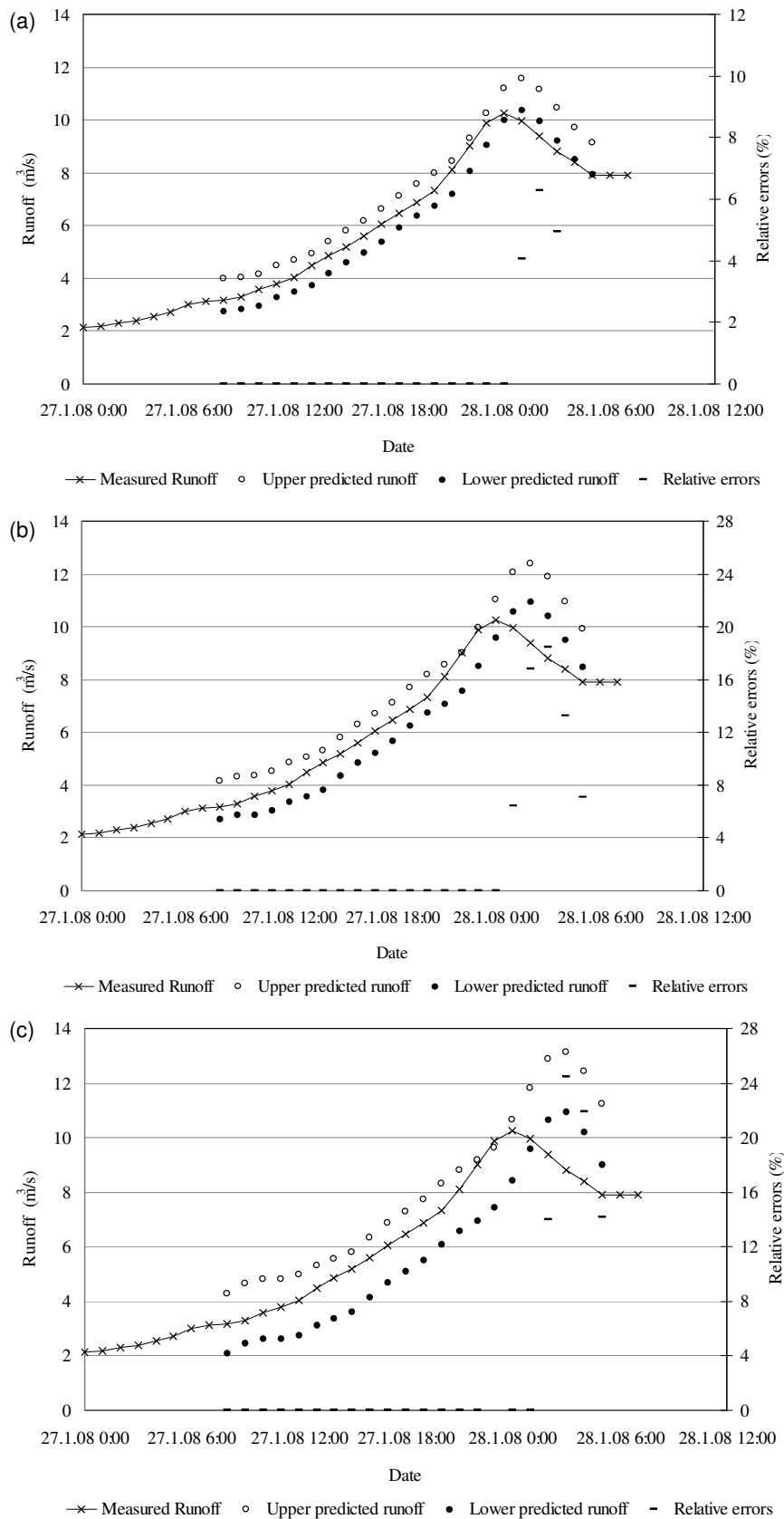
Now, taking a look at the largest runoff events, we chose the largest runoff events in both validation and training sets. The analysis of the training set event was carried out because it was the largest event in the discharge time series, showing  $35.44 \text{ m}^3/\text{s}$  of peak runoff and high runoff differences with low probability. We used the best chosen approaches with 95% confidence interval for 1-, 2- and 3-h ahead probabilistic runoff forecasting of these events. Figures 10a–c show the results of validation set prediction and Fig. 11a–c that for the training set.



**Figure 9.** Measured stream discharges versus errors from the application of autoregressive approach to two-hour time series with 95% confidence interval, where  $c$  is the coefficient of correlation.

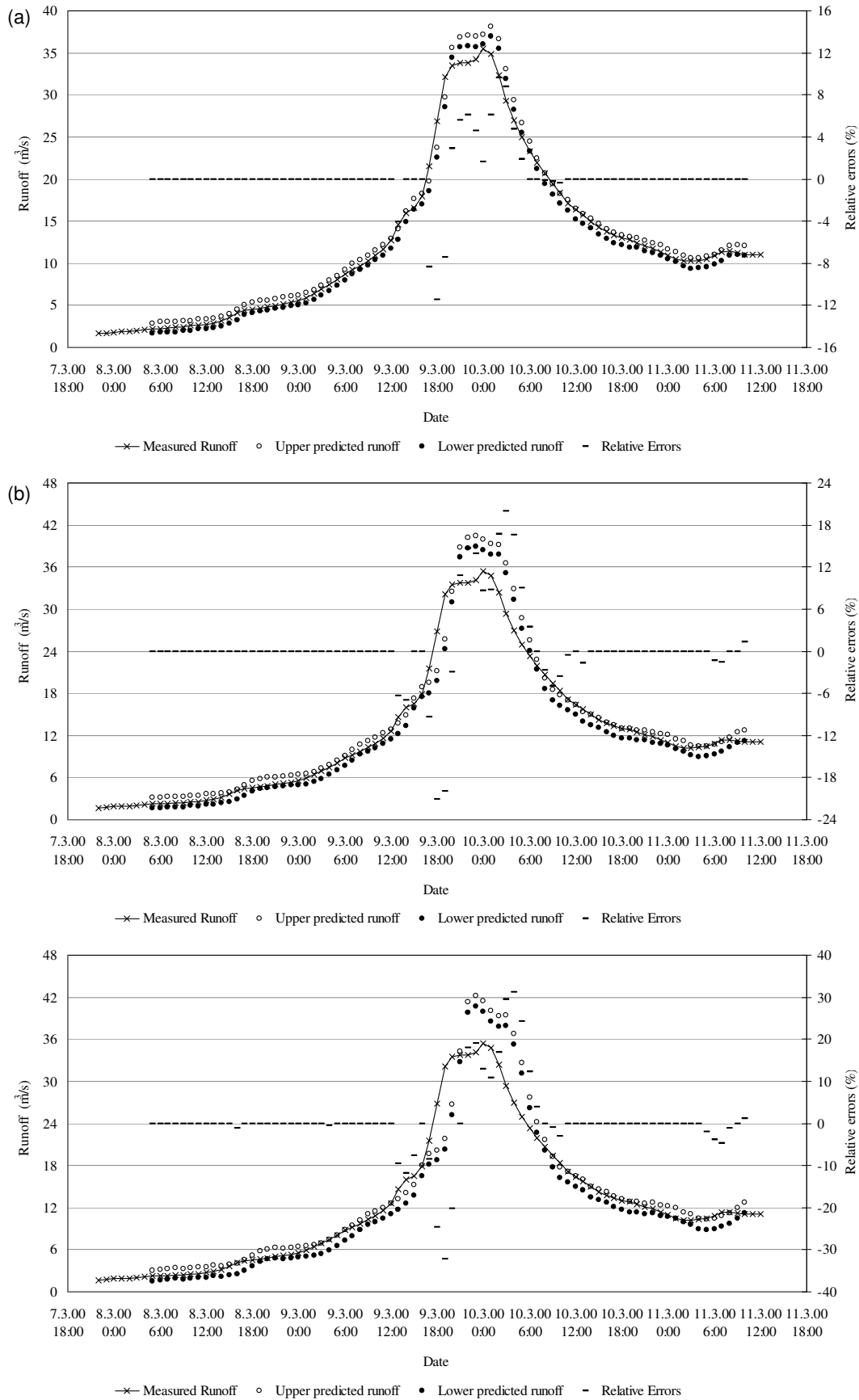
**Table II.** Performance of autoregressive (AR), locally averaged and locally constant model-based approaches for 97.5, 95 and 90% confidence intervals of the distributions of  $(\xi - \langle \xi \rangle)$  ( $m^3/s$ ) in one-, two- and three-hour time series, where relative error, RE (in %) is related to the differences between runoff measurements ( $m^3/s$ ) and confidence interval limits of the predicted probability density functions (equation (13)). These results are only valid for certain discharge threshold levels ( $5.5 m^3/s$  for one-hour time series, and  $8.8 m^3/s$  for two- and three-hour time series).

Approach	Stochastic terms	1 h, p = 7			2 h, p = 3			3 h, p = 2		
		97.5%	95%	90%	97.5%	95%	90%	97.5%	95%	90%
AR [p]	Range length of $(\xi - \langle \xi \rangle)$	2.94	2.14	1.60	2.52	1.84	1.21	2.20	1.50	0.98
	Range interval of RE	[-11; 38]	[-12; 46]	[-13; 50]	[-16; 20]	[-18; 21]	[-19; 23]	[-31; 30]	[-32; 31]	[-33; 33]
Locally averaged [p]	Range length of $(\xi - \langle \xi \rangle)$	1.74	1.20	0.74	1.89	1.45	0.92	2.66	1.85	1.16
	Range interval of RE	[-10; 27]	[-12; 30]	[-13; 32]	[-20; 19]	[-21; 20]	[-22; 22]	[-28; 32]	[-30; 36]	[-31; 40]
Locally constant	Range length of $(\xi - \langle \xi \rangle)$	1.00	0.74	0.53	2.04	1.36	0.92	2.83	1.85	1.16
	Range interval of RE	[-8; 34]	[-8; 35]	[-9; 36]	[-21; 24]	[-23; 25]	[-24; 25]	[-28; 35]	[-30; 40]	[-32; 43]



**Figure 10. Probabilistic runoff forecasting of the largest runoff event in the validation set for: (a) 1 h ahead, (b) 2 h ahead and (c) 3 h ahead, with 95% confidence interval, corresponding to differences (between upper and lower predicted runoff) of 1.20, 1.45 and 1.50 m<sup>3</sup>/s, respectively.**

## 4 An Example for Probabilistic Flood Prediction



**Figure 11. Probabilistic runoff forecasting of the largest runoff event in the training set for: (a) 1 h ahead, (b) 2 h ahead, and (c) 3 h ahead, with 95% confidence interval, corresponding to differences (between upper and lower predicted runoff) of 1.20, 1.45 and 1.50  $\text{m}^3/\text{s}$ , respectively.**

Figures 10 and 11 show that the measured rising limb and falling limb of the largest runoff events in the validation and training sets were almost within the predicted runoff ranges for the three time series. However, overestimation of peak flow was not negligible for two- and three-hour events (Figs 10b–c and 11b–c), and one high runoff underestimation (about –30%) in the rising limb was observed in the three-hour ahead, largest event of the training set (Fig. 11c).

It is also important to evaluate whether measurements of runoff differences  $\Delta Q_{i,\Delta t}$  and validation set residuals  $F(\Delta Q_{i-\Delta t,\Delta t}, \dots, \Delta Q_{i-\Delta t-m,\Delta t}) + \langle \xi \rangle - \Delta Q_{i,\Delta t}$  were systematic, because, if they were, it means that part of the determinism was not identified by modelling (Kantz and Schreiber, 2004). Considering the best approaches for one-, two- and three-hour time series, we plotted validation set residuals vs measurements of runoff differences in Figs. 12a–c and computed their coefficients of correlation and Fisher’s limits.

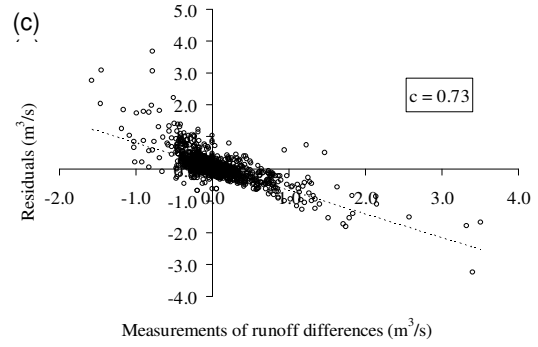
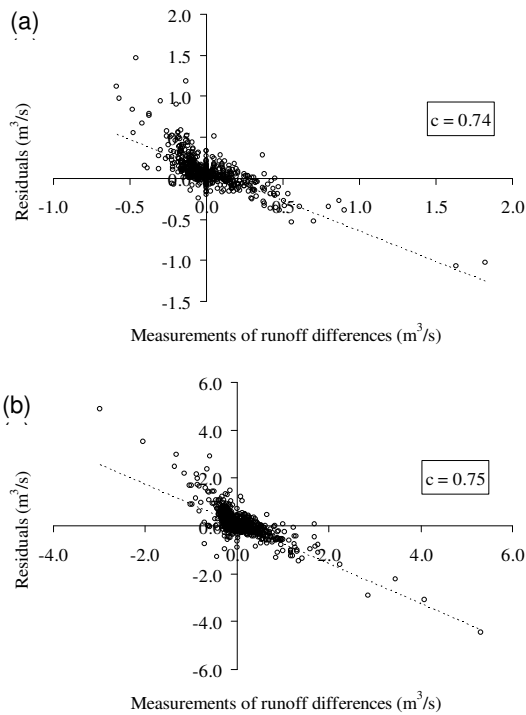


Figure 12. Measurements of runoff differences vs validation set residuals, considering the best approaches for: (a) hourly time series, (b) two-hour time series, and (c) three-hour time series, where  $c$  is the coefficient of correlation.

Since the coefficients of correlation were greater than its Fisher’s superior limits, a negative linear relation could not be rejected between validation set residuals and measurements of runoff differences for the time series. Also insights into location of measured discharges on predicted probability density functions are possible, but at this moment this analysis is outside the scope of this work and will be investigated later.

#### 4.3.2. Comparison with the forecast by a comprehensive hydrological model

In this section we compare the results of used nonparametric models with the ones obtained by a comprehensive hydrological model LARSIM (see Section Parametric Modelling). The description of parameterization and input variables of LARSIM model to a meso-scale catchment can be found in Heistermann and Kneis (2011). LARSIM was applied to Ammelsdorf streamgauge’s catchment independently.

An hourly forecasting using LARSIM for Ammelsdorf streamgauge with stream discharge assimilation, i.e. in “prediction mode”, consumes too much computer time and is hardly feasible.

Therefore, the following alternative was formulated: 1.) to apply hourly LARSIM without stream discharge assimilation and any kind of corrections to model states and parameters at intermediate times, i.e. in



“simulation mode”, 2.) then to use the relation

$$\hat{Q}_{t+\Delta t} = Q_t + \Delta \hat{Q}_{i,\Delta t} = Q_t + (Q_{t+\Delta t}^{LARSIM} - Q_t^{LARSIM}) \quad (14)$$

where  $Q_t^{LARSIM}$  and  $Q_{t+\Delta t}^{LARSIM}$  are stream discharge simulated by LARSIM without stream discharge assimilation or any kind of correction to the model states and parameters at intermediate times;  $Q_t$  is the measured stream discharge; and  $\hat{Q}_{t+\Delta t}$  is the predicted stream discharge.

The simulation mode is worse than the prediction mode for operational stream discharge forecasting, but equation (14) has the advantage of not compromising any model uncertainties on stream discharge assimilation.

Furthermore, in a previous investigation on hourly hydrographs and areal hyetographs, it was found that an average catchment reaction time was between 3 and 5 hours. Thus only the observed pre-

cipitation was adopted as LARSIM input to forecast one-, two- and three-hour ahead stream discharge.

The application of LARSIM to the Ammeldorf gauge was carried out from a deterministic point of view only, i.e. *one-discharge-value-per-time-step* forecasting, and, consequently, we were only able to compare the dynamic terms of the non-parametric approaches with LARSIM’s results. We used the common calibration set results of both applications (parametric and nonparametric) from May 2004–January 2008 as the compared set, because it was quite a bit larger than the common validation set results. The mean absolute error, MAE (in %) and the range of relative errors, RE (in %) (see equation (13)) were considered as criteria of goodness of fit. Table III shows the comparison for one-, two- and three-hour time series according to the size of the measured discharge ( $m^3/s$ ).

**Table III. Comparison of LARSIM application and the dynamic terms of the nonparametric models—autoregressive (AR), locally averaged and locally constant model-based approaches—for one-, two- and three-hour time series. The number of compared samples, mean absolute error, MAE (in %), and the range of relative errors, RE (in %), are given according to the amount of measured discharge ( $m^3/s$ ).**

Measured discharge ( $m^3/s$ ) higher than	Number of compared samples	LARSIM's Application		AR		Locally Average		Locally Constant	
		MAE	Range of RE	MAE	Range of RE	MAE	Range of RE	MAE	Range of RE
1 hour									
0.0	892	4.3	[-38; 55]	10.2	[-85; 79]	6.5	[-47; 52]	5.3	[-51; 96]
1.1	762	3.5	[-38; 26]	9.5	[-85; 61]	5.5	[-47; 52]	3.8	[-40; 39]
2.2	596	2.8	[-38; 26]	7.8	[-58; 61]	4.5	[-42; 52]	3.0	[-33; 39]
4.4	391	2.2	[-38; 26]	6.2	[-21; 61]	3.0	[-38; 38]	2.3	[-26; 39]
6.6	218	1.8	[-38; 26]	5.8	[-21; 61]	2.2	[-38; 38]	1.9	[-26; 39]
2 hour									
0.0	2004	7.4	[-67; 376]	11.3	[-101; 177]	10.5	[-96; 159]	10.0	[-100; 203]
1.1	1471	5.4	[-67; 76]	9.4	[-101; 177]	8.6	[-96; 159]	7.6	[-100; 203]
2.2	1045	4.3	[-67; 76]	7.8	[-98; 177]	7.3	[-96; 159]	6.2	[-100; 203]
4.4	639	3.2	[-48.7; 76]	5.5	[-55; 177]	4.8	[-56; 141]	4.4	[-62; 203]
6.6	300	2.9	[-48.7; 25]	4.5	[-55; 67]	3.8	[-56; 45]	3.2	[-62; 99]
3 hour									
0.0	2945	8.9	[-63; 407]	12.6	[-97; 259]	13.7	[-140; 258]	13.6	[-161; 370]
1.1	2111	6.2	[-63; 118]	9.7	[-97; 259]	10.9	[-140; 258]	10.4	[-161; 370]
2.2	1523	5.0	[-63; 118]	8.2	[-97; 259]	9.2	[-97; 258]	8.6	[-161; 370]
4.4	753	3.9	[-51; 75]	6.1	[-70; 144]	6.6	[-69; 144]	6.3	[-86; 207]
6.6	349	3.8	[-51; 14]	5.2	[-69; 32]	5.7	[-62; 35]	5.0	[-86; 39]

It was observed in general that the higher the measured discharge, the smaller the MAE and the range of RE of all approaches. The MAE of the LARSIM application was slightly smaller than the best results of the nonparametric approaches; however, the nonparametric approaches always showed larger ranges of RE for measured discharges higher than  $1.1 \text{ m}^3/\text{s}$ , independently of the lead time of forecast.

## 5. Discussion and Conclusions

We have developed in this paper a non-parametric, stochastic dynamic procedure, which used a qualitative dynamical system-based decision criterion for discharge time series forecasting and dealt with the probabilistic nature of the river discharge data. This approach was based only on the discharge time series itself and needed little computation time.

We assessed our procedure for a meso-scale catchment (about  $49 \text{ km}^2$ ), in which runoff events are induced by either convective rainfall during the summer or snowmelt in the spring, and ascribed probability density functions to 1-, 2- and 3-h ahead predicted discharge.

Instead of the actual runoff measurements (Jayawardena and Lai, 1994; Liu et al., 1998; Jayawardena and Gurung, 2000; Sivakumar et al., 2001; Porporato and Riddolfi, 1997, 2001; Sivakumar et al., 2002; Laio et al., 2003; Tamea et al., 2005), the differences between the runoff measurements were used for application of the regression models, because the last series exhibited short-range dependence and presented similar structure to that of dynamical systems contaminated with noise.

The best approaches for one-, two- and three-hour ahead discharge time series were those, which have the sharpest probability density functions for the stochastic term. The locally averaged model-based approaches were the best ones for one- and two-hour time series and the autoregressive model was the best one for the three-hour time series.

This means that the system shifted from a possible dynamical system contaminated

with noise to a linear random process, when the interval time of time series increased. This is expected even for noise-free dynamical systems (see Kantz and Schreiber, 2004). Therefore, we did not find in this work a best unique formulation among the three assumed approaches (autoregressive model, locally averaged and locally constant models) for the dynamic term, although previous studies (Jayawardena and Lai, 1994; Liu et al., 1998; Jayawardena and Gurung, 2000; Sivakumar et al., 2001; Porporato and Riddolfi, 1997; Sivakumar et al., 2002; Laio et al., 2003) presented cases in which local approaches outperformed global ones.

Moreover, the validation set residuals and the measurements of runoff differences presented a negative linear correlation, meaning that runoff underestimation can be expected for rising limbs and overestimation for falling limbs, and thus some of the dynamics are probably not identified by the nonparametric approaches that we used. This trend is inevitable for our simple models based on the past observations only.

The results of the dynamic terms of nonparametric approaches were compared with an application of the distributed hydrological model LARSIM, in which the above mentioned trend is not necessarily presented. On average, the deterministic evolution of both parametric and best nonparametric approaches gave similar results, but the ranges of relative errors were larger for the nonparametric approaches. The main reason for that is probably that our approaches did not consider any information of precipitation series.

The procedure presented was able to forecast, for previously measured discharges higher than  $5.5 \text{ m}^3/\text{s}$  for one-hour time series, and  $8.8 \text{ m}^3/\text{s}$  for two- and three-hour time series (discharge threshold levels), with 95% confidence interval:

- 1-h ahead discharge probability functions with  $1.20 \text{ m}^3/\text{s}$  of range and relative errors (%) in the range  $[-12; 30]$ ;

- 2-h ahead discharge probability functions with  $1.45 \text{ m}^3/\text{s}$  of range and relative errors (%) in the range  $[-21; 20]$ ; and
- 3-h ahead discharge probability functions with  $1.50 \text{ m}^3/\text{s}$  of range and relative errors (%) in the range  $[-32; 31]$

which can be combined to perform hourly forecasting for 1, 2 and 3 hours ahead. Different confidence intervals could also be used, depending on the demands of users.

Thus the method can be used as an alternative approach for poorly-gauged catchments, in which physical characteristics and reliable precipitation series are not available. Furthermore, a hydrological model should at least outperform the presented univariate nonparametric approaches, if it is to be adopted for flood warning purposes.

## 6. Further Work

When other reliable time series, such as precipitation, soil moisture and discharge series, are available, they should be taken into account too, because they might improve the results based on our univariate analysis and even allow reliable discharge forecasting of more than 3 hours ahead. Porporato and Ridolfi (2001), for example, predicted runoff by a multivariate phase-space reconstruction technique using discharge, rainfall and temperature time series.

A multivariate analysis might overcome the runoff underestimation for rising limbs and overestimation for falling limbs and allow lower discharge threshold levels for reliable forecasting.

Further applications of uni- or multivariate nonparametric approaches should be: (a) focused on large data sets of stream gauges to evaluate the performance of this method under different hydrological and monitoring conditions, and (b) based on multiple approaches for the dynamic term adding possible other approaches such as locally polynomial, since a best unique formulation was not found.

Investigation will be carried out to extend our formulation for hydrological models to enable comparison between predicted probability density functions of stream discharges.

## 7. Acknowledgements

The first author thanks the Brazilian National Council for Scientific and Technological Development (CNPq) for the PhD-scholarship. We thank the Saxony state office for the discharge data. We thank Prof. András Bárdossy for his comments on an earlier version of this paper. We thank very much Udo Schwarz from Institute of Physics and Astronomy at University of Potsdam for valuable discussions and his valuable comments on methodological development of this paper. We thank the OPAQUE project (operational discharge and flooding predictions in head catchments), a project within the BMBF-Förderaktivität “Risikomanagement extremer Hochwasserereignisse” (RIMAX), namely its members Dominik Reusser and Thomas Gräff for valuable discussions and data from Wilde Weisseritz catchment. We thank Francisco Ednilson Alves do Santos from Theoretical Physics at Free University of Berlin for his comments on methodological development of this paper. We are also grateful to the two reviewers and the Prof. Koutsoyiannis for their comments and suggestions, which improved this paper significantly.

## **Chapter V:**

### **Discussion and Conclusion**

## 1. Perceptual Model of Channel Transmission Losses

Chapter II shows how a combination type of three different sources of hydrological data (streamflow series, groundwater level series and multi-temporal satellite data-based river water extension) related to “soft” data, e.g. a hydro-geologic map, enabled the analysis of the hydrology of a large poorly gauged river reach of the Jaguaribe River in NE Brazil. The potentials of different sources of data in hydrological analysis have been already shown by e.g. Wenninger et al. (2008), Tetzlaff et al. (2008), Graeff et al. (2009) and McMillan et al. (2011).

The inter-comparison of channel transmission losses responses of the Jaguaribe River, the Cooper Creel River in Australia (Knighton and Nanson, 1994) and the Kuiseb River in Namibia (Lange, 2005) improved the understanding of the channel transmission losses functioning in the Jaguaribe River. This comparison is an example of the comparative hydrology analysis (Falkenmark and Chapman, 1989; de Araújo and Piedra, 2009). Moreover, the experimental analysis points out possible direct impacts of the channel transmission losses on the water availability of a large surface reservoir which is an important component of the regional water resources management in NE Brazil.

The synthesis of the experimental studies led to a perceptual hydrological model of the channel transmission losses of that river reach. In summary, it shows that the river reach is hydraulically connected with aquifer groundwater, which shifts from being a losing river at the dry and beginning of rainy seasons to become a losing/gaining (mostly losing) river at the middle and end of rainy seasons. This seasonal and hydraulic behaviour favours the application of models developed for sub-humid and temperate conditions, e.g. coupling of distributed river and groundwater flow models (see Engeler et al., 2011; Krause and Bronstert, 2007), instead of the classical models for arid and semi-arid

conditions (e.g. Abdulrazzak and Morel-Seytoux, 1983; Illangasekare and Morel-Seytoux, 1984), because these models for arid and semi-arid conditions do not consider the groundwater flow into the river reach. However, spatial data scarcity discourages the application of distributed river-groundwater flow models.

Therefore, the perceptual model was a useful guide to adjust and apply a simulation model in that river reach, rejecting standard approaches of river-groundwater interaction due to its hydrological behaviour (based on Beven, 2002a; Dunn et al., 2008). Initial and boundary conditions of the river-aquifer system can also be inferred from the perceptual model (see next section). Moreover, the perceptual model is also a guideline for future data collection there and may be the most suitable hydrological behaviour concept for ungauged river reaches which have similar climate and hydro-geologic controls with the river studied (based on Sivapalan et al., 2003b).

## 2. Modelling of Channel Transmission Losses

A new process-orientated and semi-distributed channel transmission losses model was developed, which was based primarily on the capability of simulation in very different dryland environments (based on Bronstert, 2004; Kirchner, 2006; Andréassian et al., 2007, 2009, 2010) and flexible model structures for testing various hypotheses on the dominant hydrological processes of river reaches (Graeff et al., 2009; Savenije, 2009; Andréassian et al., 2010; Buytaert and Beven, 2011; McMillan et al., 2011; Clark et al., 2011a) (see Chapter III), what is called multi-hypotheses modelling.

First, a multi-hypotheses modelling of channel transmission losses was applied to a reach of the Jaguaribe River in NE Brazil (see also Chapter II). The initial conditions of the underlying aquifer wetness and some boundary conditions of the river system, e.g. negligible lateral flow originated from the direct drainage area between the stream gauges, (see Chapter III) were de-

rived from the perceptual model of that reach (see the previous section for its summary). This perceptual model also orientated the build of the hypotheses on the dominant hydrological processes, i.e. the possible model structures.

The multi-hypotheses modelling reduced structural model uncertainties as undertaken similarly by Buytaert and Beven (2011) and Clark et al. (2011a). Moreover, it provided insights into the functioning of the channel transmission losses, which were not reported in the previous perceptual model of the reach, hypothesizing that both lateral (stream-)aquifer water fluxes and groundwater flow in the underlying alluvium parallel to the river course are necessary to predict streamflow and channel transmission losses, the former process being more relevant than the latter. This modelling-based hypothesis may subsequently inform field campaigns targeted to validate it (Dunn et al., 2008).

The channel transmission losses model application to different dryland environments enabled learning about the model itself from differences in channel reach responses (comparative diagnostic analysis, see Li et al., 2010). The parameters related to the unsaturated part of the model, which were active for the small-scale stream reach in the Walnut Gulch Experimental Watershed, presented much higher variation in the sensitivity coefficients than those which drove the saturated part of the channel transmission losses model, which were active for the Jaguaribe River. Moreover, avoiding the one-case-study may be the most appropriate way in hydrological sciences to undertake the repeating experiment procedure (Andréassian et al., 2009, 2010).

It seems that the multi-hypotheses modelling not only improves hydrological knowledge as aforementioned, but also is a way to report modelling *failures* rejecting model structure hypotheses, namely streamflow without river-aquifer interaction and stream-aquifer flow without groundwater flow parallel to the river

course. These modelling failures may be as important as or even more important than modelling successes for advancing hydrological knowledge of large dryland rivers as advocated by Andréassian et al. (2010) and Refsgaard and Hansen (2010).

### 3. Optimized Forecasting of Streamflow

Quite separate from the previous two sections, in which the hydrological knowledge shown to be fundamental for learning about, inferring from and modelling/predicting flow transmission processes in river-systems, this section discusses the results of the time series analysis, which disregards any hydrological process knowledge, carried out to forecast streamflow in a headwater catchment in Germany (Chapter IV).

Traditionally, time series analysis focuses on optimized forecasting of streamflow only, but the nonparametric stochastic dynamic approach developed in this work was based on a qualitative dynamical system-based criterion, which involved a learning process about the structure of the river discharge data, instead of a fitting procedure (Brockwell and Davis, 2003; Kantz and Schreiber, 2004) only. Then, a testing set provided the residual time series used to derive the stochastic term, coloured noise, which ascribes a probability density function (predictive uncertainty) to the predicted river discharge.

This learning-process-based method to derive the nonparametric approaches demonstrated, for example, that the differences between runoff measurements were more suitable than the actual runoff measurements for the application of the regression models. This result would not be able to come from a fitting procedure only. Moreover, the analysis of the residuals time series showed that: a) the catchment runoff system shifted from being a possible dynamical system contaminated with noise to a linear random process, when the interval time of time series increased, and b) runoff underestimation can be expected for rising limbs and overestimation for falling limbs.

The deterministic evolution of a calibrated distributed hydrological model, LARSIM (Ludwig and Bremicker, 2006), was compared with that of the best nonparametric approaches. The parametric and nonparametric approaches presented similar results on average. However, uncertainty analysis was not carried out for the LARSIM model as undertaken for the nonparametric approach developed here. This clearly limited the comparison between the both approaches.

The most popular methods of uncertainty analysis for hydrological models are the GLUE method (Beven and Binley, 1992; Beven, 2002b) and the Bayesian frameworks (e.g. Todini, 2007; Kuczera et al., 2010), although uncertainty analysis for hydrological modelling is under intensive discussion and seems to be far away from a convergent point in the hydrologic community (see e.g. Savenije, 2001; Loague and VanderKwaak, 2004; Beven, 2006; Ebel and Loague, 2006; Mantovan and Todini, 2006; Montanari, 2007; Hall et al., 2007; Andréassian et al., 2007; Todini, 2007; Beven, 2008; Sivapalan, 2009; Hughes, 2010; Beven, 2010).

Recently, the residual time series analysis of hydrological models arose seemingly as an alternative to the GLUE method and the Bayesian frameworks. This was introduced by Abebe and Price (2003) and has rarely been applied. The main rationale of this procedure is the assumption that the residual time series is the best reflection of the difference between the model and the physical process it represents (Abebe and Price, 2003). This assumption is also at the heart of the nonparametric approach developed here and of other nonparametric stochastic approaches (Tamea et al., 2005; Chen and Yu, 2007). Furthermore, Abebe and Price (2003) used the structure presented in the residual time series to derive regression models and coupled them with a conceptual hydrological model in order to improve streamflow forecasts.

The residual time series analysis has the following advantages over the aforementioned popular methods for uncertainty

analysis: a) it may be used to assess model failures and to learn from them straightforwardly as undertaken e.g. for the nonparametric approach developed in this work and b) it may be a link between time series and hydrological models, complementary modelling (Abebe and Price, 2003), which may improve flow forecasts without missing the insights of the hydrological model. Further work will be carried out to apply residual time series analysis to (semi-)distributed hydrological models, in order to improve flow forecasting as done by Abebe and Price (2003) and their comparison with nonparametric approaches.

### **4. A Benchmark for Hydrological Research using Semi-Distributed Modelling**

In this section, a new benchmark for hydrological research is proposed using semi-distributed modelling as based on the previous sections, the works of Buytaert and Beven (2011), McMillan et al. (2011) and Clark et al. (2011a) and suggestions of Savenije (2009), Andréassian et al. (2009, 2010), Li et al. (2010) and Clark et al. (2011b). The aim here is not to describe a blueprint for hydrological modelling design as done e.g. by Freeze and Harlan (1969) and Beven (2002b), but rather to propose a scientific method to improve hydrological knowledge using semi-distributed hydrological modelling.

The elements of this approach are:

a) A semi-distributed hydrological model with a flexible structure as used in this work, which may be a compromise between downward and upward approaches.

b) Perceptual models of the underlying hydrological systems (conceptualization of the main hydrological processes), which can orientate the application of numerical models (see previous sections and e.g. Tetzlaff et al. (2008) and McMillan et al. (2011)).

c) A testing of the hypotheses on the dominant hydrological processes, i.e. building different model structures (see Chapter III, Buytaert and Beven (2011))

and Clark et al. (2011a)), which can generate insights into catchment functioning through comparisons of model performance (Li et al., 2010) and may be a way to report modelling *failures* (Andréassian et al., 2010; Refsgaard and Hansen, 2010) as demonstrated in Section 2.

d) A model application for different case studies, which can provide insights into catchment functioning (or the model itself (see Chapter III)) from differences in catchment responses (Li et al., 2010) and may be the unique way to undertake the repeating experiment procedure (Andréassian et al., 2009, 2010).

e) A *validation* of different simulated variables, which can provide insights into catchment functioning from differences in variable responses (based on Bronstert, 2004; Ebel and Loague, 2006; Kirchner, 2006).

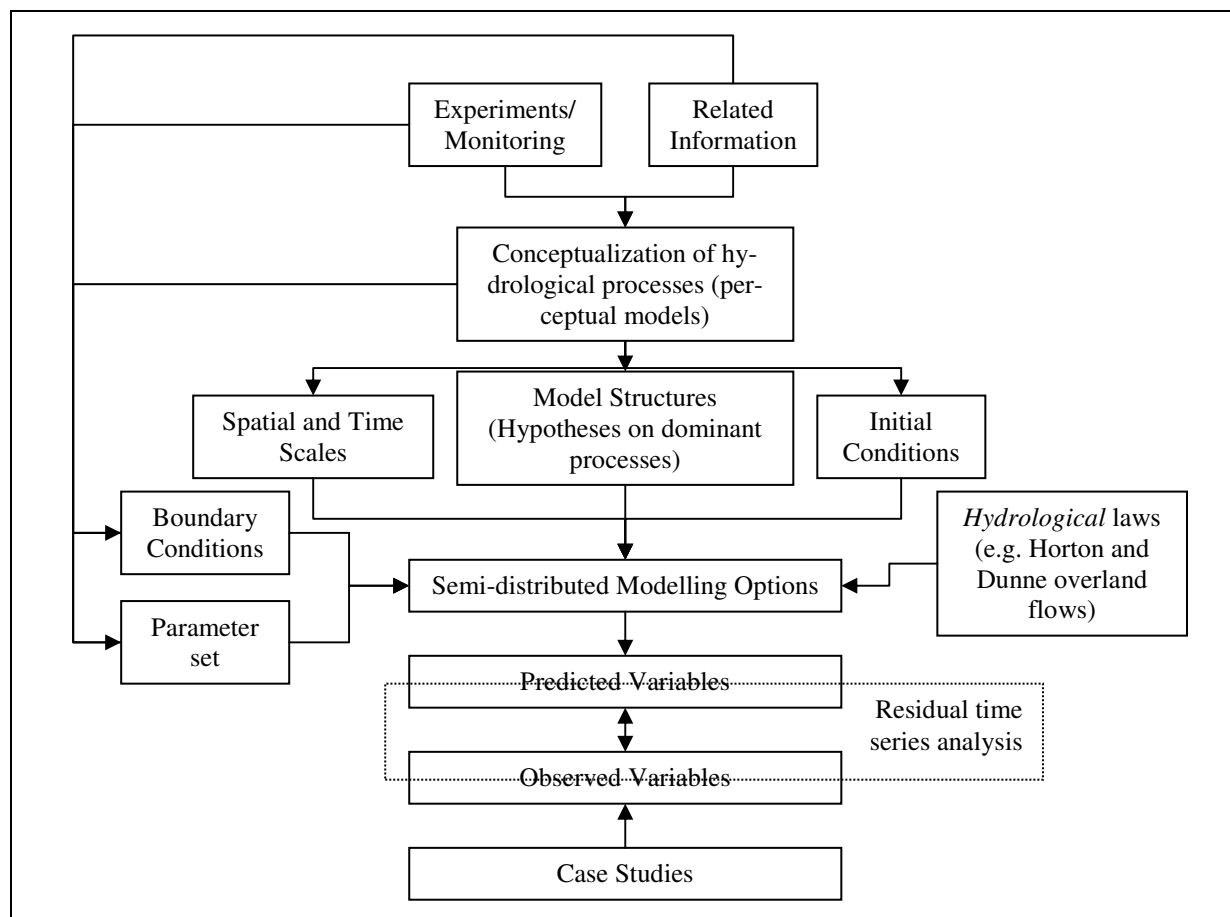
f) A residual time series analysis, which can provide insights into model functioning and assumptions and ascribe a

probability density function to the predictand (predicative uncertainty) based on the distribution of the residuals as suggested in the previous section.

For this multi-hypotheses, -case-studies and -validation investigation considering a residual time series-based uncertainty analysis, the parameter calibration should be abandoned, because it limits insights into model error, making it difficult to discriminate among alternative hypotheses, understand sources of uncertainty, and develop strategies for reducing them (Clark et al., 2011a). For example, Clark et al. (2011a) reported that all five model structures tested, when calibrated, achieved the same performance, but they failed to adequately represent the diagnostic hydrological signatures based on measurements.

The benchmark for hydrological research using semi-distributed modelling based on those elements is illustrated in Fig. 1 below:





**Figure 1. Benchmark for hydrological research using semi-distributed modelling based on a multi-hypotheses, -case-studies and -validation investigation considering a residual time series-based uncertainty analysis.**

The conceptualization of the main hydrological processes (perceptual models) arises as the most important element of this benchmark, which has implications on model structures (hypotheses on dominant processes), initial and boundary conditions, parameter set and model scale. This conceptualization is strengthened by a combination of different sources of hydrological data (e.g. Wenninger et al., 2008; Tetzlaff et al., 2008; McMillan et al., 2011) and a comparative hydrology analysis (Falkenmark and Chapman, 1989; de Araújo and Piedra, 2009) as shown in the section 1.

In the context of this benchmark, the semi-distributed numerical model is the simplest and the most flexible mathematical description of the perceptual model of a hydrological system, which enables the testing of the hypotheses on the dominant hydrological processes of this system. Therefore, the degree of modelling simplification/complexity and flexibility should,

on the one hand, be constrained by the perceptual model of the hydrological system, but on the other hand, it should also be able to approach the hypotheses on the functioning of this system.

Moreover, the semi-distributed modelling developed is based on *hydrological* laws, such as Horton and Dunne overland flows, (bottom-up-based point of view) and empirical laws, which arise directly from the data constraints and the hydrological conceptualization (top-down-based point of view).

The residual time series analysis is based on the differences between predicted and observed variables. In this work, this kind of analysis pointed out model failures and model behaviour throughout temporal scales in a nonparametric approach, as well as ascribing a probability density function to the predictand (predicative uncertainty). Furthermore, it can be useful for better predictions (complementary modelling)

(Abebe and Price, 2003) without missing the insights of the semi-distributed hydrological model.

The benchmark can work as follows:

a) If the number of model structures (hypotheses on the dominant hydrological processes) is greater than one and there is one case study, then the objectives are generating new insights into the functioning of a case study (e.g. Clark et al., 2011a; Li et al., 2010) and report structural modelling failures (Andréassian et al., 2010; Refsgaard and Hansen, 2010) (multi-hypotheses).

b) If there is more than one case study, then the objectives are learning from differences in case-study responses (e.g. Li et al., 2010) and undertaking the repeating experiment procedure (Andréassian et al., 2009, 2010) (multi-case-studies).

c) If the number of predicted and observed variables is greater than one, then a multi-variable validation can be carried out to improve model confidence (based on Bronstert, 2004; Ebel and Loague, 2006; Kirchner, 2006) and maybe rejecting hypotheses (multi-validation).

All procedures aforementioned can lead to a complete rejection of the hypotheses on the dominant hydrological processes, indicating that new experiments and/or monitoring should be implemented in order to investigate further the main hydrological processes. Hypotheses evaluated positively not only ascertain the most possible model structure given the previous hydrological knowledge derived from a perceptual model, but also can add a new element over this knowledge as shown in this work (section 2). This new modelling-based element should naturally be targeted for validation in future field campaigns (Dunne et al, 2008).

The multi-case-studies and multi-validation application strengthen model development and assessment (based on Bronstert, 2004; Ebel and Loague, 2006; Kirchner, 2006; Andréassian et al., 2009, 2010), learning and/or rejecting hypotheses from differences in case-study responses and in multi-variable validation.

This work (Chapters II and III) can be considered an example of multi-hypotheses and multi-case-studies investigation, because hypotheses on the dominant hydrological processes of a large reach of the Jaguaribe River, Ceará, Brazil, were studied and a channel transmission losses model was applied to that river reach and to a small reach in the Walnut Gulch Watershed, Arizona, USA. The multi-hypotheses study improved the hydrological knowledge about the channel transmission losses in the Jaguaribe River and the multi-case-studies application generated insights into the sensitivity of two different parameter sets. Examples of both multi-hypotheses and multi-case-studies reports, which begin with the perceptual model of the experimental areas and do not apply calibration procedures, have been rare and apparently only McMillan et al. (2011) and Clark et al. (2011a) undertook similar work.

## 5. Conclusion

This research dealt with analyzing and modelling flow transmission processes in river-systems with a focus on semi-arid conditions. A perceptual hydrological model was evolved for a large reach of the Jaguaribe River in NE Brazil, which improved the knowledge about channel transmission losses, since reports on channel transmission losses in large dryland rivers are rare in hydrological literature (see e.g. Cooper Creel River in Australia (Knighton and Nanson, 1994) and the Kuiseb River in Namibia (Lange, 2005)), and also became a guideline for data sampling and modelling studies in hydrologically similar rivers.

A process-orientated and semi-distributed channel transmission losses model for different dryland environments was developed and successfully tested in a multi-hypotheses study on the Jaguaribe River in NE Brazil and in a multi-cases-studies application to both it and a small stream reach in the Walnut Gulch experimental Watershed, Arizona, USA. This flexible and simplified model was adapted

to match the perceptual models of the case studies and hypotheses on the dominant hydrological processes. Moreover, a non-parametric approach, which deals with both deterministic evolution and inherent fluctuations in river discharge data, was developed and applied to flood forecasting in a headwater catchment in Germany. This approach presented similar results to those produced by a calibrated distributed hydrological model, but not containing the inherent uncertainties of (semi-)distributed hydrological models arising from initial conditions, spatially distributed parameters, model structure and space-time scale effects.

The observation and analysis of channel transmission losses in a large poorly gauged dryland river, the development of a flexible simplified channel transmission losses model and of a nonparametric approach based only on discharge time series may be useful hydrological knowledge and mathematical tools in order to predict and forecast flow transmission processes in poorly gauged and ungauged watersheds in arid and semi-arid regions. The approaches developed in this research should nevertheless still be targets for post-evaluation in real-world applications for water planning and management (based on Andréassian et al., 2010; Refsgaard and Hansen, 2010).

As a synthesis of Chapters II to IV, a benchmark for hydrological research using semi-distributed hydrological modelling was proposed. It is a multi-hypotheses, -case-studies and -validation investigation considering a residual time series-based uncertainty analysis. After the application of this proposed investigation to a case study, it is hoped that the actual state of its hydrological knowledge and its predicative uncertainty can be determined, based primarily on rejected hypotheses on the dominant hydrological processes and differences in catchment/variable responses. Furthermore, this hydrological knowledge may be a guide to further hydrological research requirements in terms of both data sampling/analysis and model development/assessment in the case study. Also,

this knowledge may be transferable to ungauged catchments, which have similar climate and hydro-geologic controls to those which are studied, in order to undertake field campaigns and/or modelling studies. Further work will be needed to implement and to assess this benchmark.

Finally, the main results of this research are listed as follow:

1. It is expected for regular rainy seasons that the studied Jaguariber River reach recharges and discharges groundwater, but losing on average 30% of the upstream inflow event along 30 km of the reach.

2. Channel transmission losses in the Jaguaribe River reach infiltrate mainly through the streambed and the levees and not through the floodplains; therefore, streamflows might lose water for floodplains only during extreme flood events.

3. A mathematically flexible, but hydrologically complex, modelling of the channel transmission losses can match the most important hydrological processes for streamflow prediction in dryland rivers throughout different scales and controls.

4. A perceptual hydrological model and a test of different model structures enable the application of the channel transmission losses model to a poorly gauged river, without using parameter calibration.

5. Data-driven models, which are based on streamflow series only, present reliable one-, two- and three-hours ahead streamflow forecasting for flood warning in a meso-scale catchment.

6. Data-driven and distributed hydrological models can have comparable streamflow forecasting for meso-scale catchments.

## References

- Abdulrazzak, M.J., and Morel-Seytoux, H.: Recharge from an ephemeral stream following wetting front arrival to water table, *Water Resour. Res.*, 19 (1), 194–200, 1983.
- Abebe, A.J., and Price, R.K.: Managing uncertainty in hydrological models using complementary model, *Hydrol. Sci. J.*, 48, 679–692, 2003.
- Al-Qurashi, A., McIntyre, N., Wheeler, H., and Unkrich, C.: Application of the Kineros2 rainfall-runoff model to an arid catchment in Oman, *J. Hydrol.*, 355, 91–105, doi: 10.1016/j.hydrol.2008.03.022, 2008.
- Andréassian, V., Lerat, J., Loumagne, C., Mathevet, T., Michel, C., Oudin, L., and Perrin, C.: What is really undermining hydrologic science today?, *Hydrol. Process.*, 21, 2819–2822, doi: 10.1002/hyp.6854, 2007.
- Andréassian, V., Perrin, C., Berthet, L., Le Moine, N., Lerat, J., Loumagne, C., Mathevet, T., Ramos, M.-H., and Valéry, A.: Hess Opinions “Crash tests for a standardized evaluation of hydrological models”, *Hydrol. Earth. Syst. Sci.*, 13, 1757–1764, 2009.
- Andréassian, V., Perrin, C., Parent, E., and Bárdossy, A.: The court of miracles of hydrology: can failure stories contribute to hydrological science?, *Hydrol. Sci. J.*, 55, 849–856, 2010.
- Anishchenko, V.S., Astakhov, V.V., Neiman, A.B., Vadivasova, T.E., and Schimansky-Geier, L.: *Nonlinear Dynamics of Chaotic and Stochastic Systems*. 2nd Edn, Springer Series in Synergetics, Heidelberg, 2003.
- Arnold, J.G., and Williams, J.R.: SWRRB – A watershed scale model for soil and water resources management, in: *Computer Models of Watershed Hydrology*, edited by: Singh, V.P., Water Resources Publications, Colorado, USA, 847–908, 1995.
- Bauer, P., Gumbricht, T., and Kinzelbach, W.: A regional coupled surface water/groundwater model of the Okavango Delta, Botswana, *Water Resour. Res.*, 42, W04403, doi:10.1029/2005WR004234, 2006.
- Beven, K.: Changing ideas in hydrology – the case of physically-based models, *J. Hydrol.*, 105, 157–172, 1989.
- Beven, K.J., and Binley, A.M.: The future of distributed models: Model calibration and uncertainty prediction, *Hydrol. Process.*, 6, 279–298, 1992.
- Beven, K.J.: Runoff generation in semi-arid areas, in: *Dryland Rivers: Hydrology and Geomorphology of Semi-Arid Channels*, edited by: Bull, L.J., and Kirkby, M.J., John Wiley & Sons, Chichester, England, 2002a.
- Beven, K.: Towards an alternative blueprint for a physically based digitally simulated hydrologic response modelling system, *Hydrol. Process.*, 16, 189–206, doi: 10.1002/hyp.343, 2002b.
- Beven, K.J.: Prophecy, reality and uncertainty in distributed hydrological modelling, *Adv. in Water Resour.*, 16, 41–51, 1993.
- Beven, K.: On undermining the science?, *Hydrol. Process.*, 20, 3141–3146, doi: 10.1002/hyp.6396, 2006.
- Beven, K.: On doing better hydrological science, *Hydrol. Process.*, 22, 3549–3553, doi: 10.1002/hyp.7108, 2008.
- Beven, K.: Preferential flows and travel time distributions: defining adequate hypothesis tests for hydrological process models, *Hydrol. Process.*, 24, 1537–1547, doi: 10.1002/hyp.7718, 2010.
- Blasch, K., Ferré T.P.A., Hoffman, J., Pool, D., Bailey, M., and Cordova, J.: Process controlling recharge beneath ephemeral streams in Southern Arizona, in: *Groundwater Recharge in a Desert Environment: The Southwestern United States*, Water Science and Application 9, edited by: Hogan J.F., Phillips F.M., and Scanlon, B.R., American Geophysical Union, Washington, 2004.
- Blöschl, G., and Sivapalan, M.: Scale issues in hydrological modelling: a review, *Hydrol. Process.*, 9, 251–290, 1995.
- Bracken, L., and Croke, J.: The concept of hydrological connectivity and its contribution to understanding runoff-dominated geomorphic systems, *Hydrol. Process.*, 21, 1749–1763, 2007.
- Brockwell, P.J., and Davis, R.A.: *Introduction to time series and forecasting*. 2nd Edn., Springer, New York, 2003.
- Bronstert, A.: Capabilities and limitations of detailed hillslope hydrological modelling, *Hydrol. Process.*, 13, 21–48, 1999.
- Bronstert, A.: Rainfall-runoff modelling for assess-

- ing impacts of climate and land-use change, *Hydrol. Process.*, 18, 567–570, doi: 10.1002/hyp.5500, 2004.
- Bronstert, A., Carrera, J., Kabat, P., and Lütkebecher, S. (Eds): *Coupled Models for the Hydrological Cycle: Integrating Atmosphere, Biosphere and Pedosphere*, Springer Verlag, Berlin, 2005.
- Bronstert, A., Creutzfeldt, B., Graeff, T., Hajnsek, I., Heistermann, M., Itzerott, S., Jagdhuber, T., Kneis, D., Lück, E., Reusser, D., and Zehe, E. Potentials and constraints of different type of soil moisture observations for flood simulations in headwater catchments, *Nat. Hazards*, doi: 10.1007/s11069-011-9874-9, 2011.
- Brunner, P., Simmons, C.T., Cook, P.G., and Therrien, R.: Modeling surface water-groundwater interaction with MODFLOW: some considerations, *Ground Water*, 48, 174–180, doi: 10.1111/j.1745-6584.2009.00644.x, 2010.
- Bull, L.J., and Kirkby, M.J.: Dryland river characteristics and concepts, in: *Dryland Rivers: Hydrology and Geomorphology of Semi-Arid Channels*, edited by: Bull, L.J., and Kirkby, M.J., John Wiley & Sons, Chichester, England, 2002.
- Buytaert, W., and Beven, K.: Models as multiple working hypotheses: hydrological simulation of tropical alpine wetlands, *Hydrol. Process.*, 25, 1784–1799, doi: 10.1002/hyp.7936, 2011.
- Cardier, E.: Small watershed hydrology in semi-arid north-eastern Brazil: basin typology and transposition of annual runoff data, *J. Hydrol.*, 182, 117–141, 1996.
- Carle, S.F., and Fogg, G.E.: Transition Probability-Based Indicator Geostatistics, *Math. Geology*, 28, 453–476, 1996.
- Carle, S.F., and Fogg, G.E.: Modeling Spatial Variability with One and Multidimensional Continuous-Lag Markov Chains, *Math. Geology*, 29, 891–918, 1997.
- Carle, S.F., LaBolle, E.M., Weissman, G.S., Van Brocklin, D., and Fogg, G.E.: Conditional simulation of hydrofacies architecture: a transition probability/Markov approach, in: *Hydrologic Models of Sedimentary Aquifers, Concepts in Hydrology and Environmental Geology*, edited by: Fraser, G.S., Davis, J.M.: SEPM (Society for Sedimentary Geology), N 1, Special Publication, 147–170, 1998.
- Carneiro, F.B.: Withdrawal situation for water supply system of Iguatu city–Ceará (In Portuguese), Fundação Nacional de Saúde, Fortaleza, Ceará, Brasil, 1993.
- Clark, M.P., McMillan, H.K., Collins, D.B.G., Kavetski, D., and Woods, R.A.: Hydrological field data from a modeller’s perspective: Part 2: process-based evaluation of model hypotheses, *Hydrol. Process.*, 25, 523–543, doi: 10.1002/hyp.7902, 2011a.
- Clark, M.P., Kavetski, D., and Fenecia, F.: Pursuing the method working hypotheses for hydrological modelling, *Water Resour. Res.*, 47, W09301, doi:10.1029/2010WR009827: 2011b.
- Chen, S.-T., and Yu, P.-S.: Real-time probabilistic forecasting of flood stages, *J. Hydrol.*, 340, 63–77, 2007.
- Chirico, G.B., Grayson, R.B., and Western, A.W.: A downward approach to identifying the structure and parameters of a process-based model for a small experimental catchment, *Hydrol. Process.*, 17, 2239–2258, doi: 10.1002/hyp.1330, 2003.
- Chow, V.T., Maidment, D.R., Mays, L.W.: *Applied Hydrology*, McGraw-Hill, Singapore, 1988.
- Chu, X., and Mariño, M.A.: Determination of ponding condition and infiltration into layered soils under unsteady rainfall, *J. Hydrol.*, 313, 195–207, 2005.
- Costa, A.C., Bronstert, A., and de Araújo, J.C.: A channel transmission losses model for different dryland rivers, *Hydrol. Earth Syst. Sci. Discuss.*, 8, 8903–8962, doi:10.5194/hessd-8-8903-2011, 2011
- Costa, A.C., Förster, S., De Araújo, J.C., and Bronstert, A.: Analysis of channel transmission losses in a dryland river reach in northeastern Brazil using streamflow series, groundwater level series and multi-temporal satellite data, *Hydrol. Process.*, submitted, 2012.
- Costelloe, J., Grayson, R., and McMahon, T.: Modelling streamflow in a large anastosing river of the arid zone, Diamantina River, Australia, *J. Hydrol.*, 323, 138–153, 2006.
- CPRM – Brazilian Geological Service.: *Census of the groundwater use of the State of Ceará: Diagnostic of Iguatu City (In Portuguese)*. CPRM. Fortaleza, Brazil, 1998.
- Dagès, C., Voltz, J.G., Lacas, O., Huttel, O., Negro, S., and Louchart, X.: An experimental study of water table recharge by seepage losses from a ditch with intermittent flow, *Hydrol. Process.*, 22, 3555–

## References

---

3563, doi: 10.1002/hyp.6958, 2008.

Dahan, O., Shani, Y., Enzel, Y., Yechieli, Y., and Yakirevich, A.: Direct measurements of floodwater infiltration into shallow alluvial aquifers, *J. Hydrol.*, 344, 157–170, doi: 10.1016/j.hydrol.2007.06.033, 2007.

Dahan, O., Tatarsky, B., Enzel, Y., Kulls, C., Seely, M., and Benito, G.: Dynamics of flood water infiltration and ground water recharge in hyperarid desert, *Ground Water*, 46, 450–461, doi: 10.1111/j.1745-6584.2007.00414.x, 2008.

De Araújo, J.C., and Piedra, J.I.C.: Comparative hydrology: analysis of a semiarid and a humid tropical watershed, *Hydrol. Process.*, 23, 1169–1178, doi: 10.1002/hyp.7232, 2009.

Dingman, L.S.: *Physical Hydrology*, 2nd Edn., Prentice Hall, Upper Saddle River, USA, 2002.

Dunkerley, D., and Brown, K.: Flow behaviour, suspended sediment transport and transmission losses in a small (sub-bank-full) flow event in an Australian desert stream., *Hydrol. Process.*, 13, 1577–1588, 1999.

Dunn, S.M., Freer, J., Weiler, M., Kirkby, M.J., Seibert, J., Quinn, P.F., Lischeid, G., Tetzlaff, D., and Soulsby, C.: Conceptualization in catchment modelling: simply learning?, *Hydrol. Process.*, 22, 2389–2393, doi: 10.1002/hyp.7070, 2008.

Ebel, B.A., and Loague, K.: Physics-based hydrologic-response simulation: Seeing through the fog of equifinality, *Hydrol. Process.*, 20, 2887–2900, doi: 10.1002/hyp.6388, 2006.

El-Hames, A.S., and Richards, S.K.: An integrated, physically based model for arid region flash flood prediction capable of simulating dynamic transmission loss, *Hydrol. Process.*, 12, 1219–1233, 1998.

Engeler, I., Hendricks-Franssen, H.J., Müller, R., and Stauffer, F.: The importance of coupled modelling of variably saturated groundwater flow-heat transport for assessing river-aquifer interactions, *J. Hydrol.*, 397, 295–305, 2011.

Emmerich, W.E.: *Soil Survey of Walnut Gulch Experimental Watershed, Arizona, Special Report, National Cooperative Soil Survey, USDA-ARS, Tucson, USA, 2008.*

Falkenmark, M., and Chapman, T.: *Comparative Hydrology – An Ecological Approach to Land and Water Resources*. UNESCO, Paris, 1989.

Fenicia, F., Savenije, H.H.G., Matgen, P., and Pfister, L.: Understanding catchment behaviour through stepwise model concept improvement, *Water Resour. Res.*, 44, W06419, doi: 10.1029/2007WR006386, 2008a.

Fenicia, F., McDonnell, J.J., and Savenije, H.H.G.: Learning from model improvement: On the contribution of complementary data to process understanding, *Water Resour. Res.*, 44, W01402, doi: 10.1029/2006WR005563, 2008b.

Fisher, R.A.: The general sampling distribution of the multiple correlation coefficient, *Proc. London Roy. Soc.*, A 121, N787, 654–673, 1928.

Fread, D.L.: *DAMBRK: The NWS DAMBRK Model: Theoretical Background/ User Documentation*, Hydrologic Res. Lab., Off. Hydrology, NWS. NOAA, Silver Spring, 1988.

Fread, D.L.: Flow routing, in: *Handbook of Hydrology*, edited by: Maidment, D.R., McGraw-Hill inc., New York, USA, 1993.

Freeze, R.A., and Harlan, R.L.: Blueprint for a physically-based, digitally-simulated hydrologic response model, *J. Hydrol.*, 9, 237–258, 1969.

Freyberg, D.L.: Modeling the effects of a time-dependent wetted perimeter on infiltration from ephemeral channels, *Water Resour. Res.*, 19, 559–566, 1983.

Freyberg, D.L., Reeder, J.W., Franzini, J.B., and Remson, I.: Application of the Green-Ampt model to infiltration under time-dependent surface water depths, *Water Resour. Res.*, 16, 517–528, 1980.

Gaiser, T., Krol, M., Frischkorn, H., and De Araújo, J.C. (Eds): *Global Change and Regional Impacts*, Springer Verlag, Berlin, 2003.

Gallart, F., Amaxidis, Y., Botti, P., Canè, G., Castiello, V., Chapman, P., Froebrich, J., García-Pintado, J., Latron, J., Llores, P., Lo Porto, A., Morais, M., Neves, R., Ninov, P., Perrin, J., Ribarova, I., Skoulikidis, N., and Tournoud, M.: Investigating hydrological regimes and processes in a set of catchments with temporary waters in Mediterranean Europe, *Hydrol. Sci. J.*, 53, 618–628, 2008.

Gheith, H., and Sultan, M.: Construction of a hydrology model for estimating wadi runoff and groundwater recharge in the Eastern Desert, Egypt, *J. Hydrol.*, 263, 36–55, 2002.

Goodrich, D.C., Williams, D.G., Unkrich, C.L., Hogan, J.F., Scott, R.L., Hultine, K.R., Pool, D.,

- Coes, A.L., Miller, S.: Comparison of methods to estimate ephemeral channel recharge, Walnut Gulch, San Pedro River, in: *Groundwater Recharge in a Desert Environment: The Southwestern United States*, Water Science and Application 9, edited by: Hogan, J.F., Phillips, F.M., and Scanlon, B.R., American Geophysical Union, Washington, 294 pp., 2004.
- Graeff, T., Zehe, E., Reusser, D., Lück, E., Schröder, B., Wenk, G., John, H., and Bronstert, A.: Process identification through rejection of model structures in a mid-mountainous rural catchment: observations of rainfall-runoff response, geophysical conditions and model inter-comparison, *Hydrol. Process.*, 23, 702–718, doi: 10.1002/hyp.7171, 2009.
- Güntner, A., and Bronstert, A.: Representation of landscape variability and lateral redistribution processes for large-scale hydrological modelling in semi-arid areas, *J. Hydrol.*, 297, 136–161, 2004.
- Güntner A., Krol M.S., De Araújo J., and Bronstert A.: Simple water balance modelling of surface reservoir systems in a large data-scarce semiarid region, *Hydrolog. Sci. J.*, 5, 145–164, 2004.
- Gupta, V.H., Wagener, T., and Liu, Y.: Reconciling theory with observations: elements of a diagnostic approach to model evaluation, *Hydrol. Process.*, 22, 3802–3813, doi: 10.1002/hyp.6989, 2008.
- Hall, J., O’Connell, E., and Ewen, J.: On not undermining the science: coherence, validation and expertise. Discussion of Invited Commentary by Keith Beven *Hydrological Processes*, 20, 3141 – 3146 (2006), *Hydrol. Process.*, 21, 985–988, doi: 10.1002/hyp.6639, 2007.
- Hameed, T., Mariño, M.A., and Cheema, M.N.: Time series modelling of channel transmission losses, *Agr. Water Manage.*, 29, 283–298, 1996.
- Hillel, D.: *Fundamentals of Soil Physics*, Academic Press, San Diego, California, 413 pp., 1980.
- Heistermann, M and Kneis, D.: Benchmarking quantitative precipitation estimation by conceptual rainfall-runoff modeling, *Water Resour. Res.*, 47, W06514, doi: 10.1029/2010WR009153, 2011.
- Hughes, D.A.: Modelling semi-arid and arid hydrology and water resources: the southern Africa experience, in: *Hydrological Modelling in Arid and Semi-Arid Areas*, edited by: Wheeler, H., So-rooshian, S., and Sharma, K.D. Cambridge Press, New York, USA, 2008.
- Hughes, D.A.: Hydrological models: mathematics or science?, *Hydrol. Process.*, 24, 2199–2201, doi: 10.1002/hyp.7108, 2010.
- IBGE – Brazilian Institute of Geography and Statistics: *Hydrogeological Map of Iguatu Micro-region (SB24YB)*. Accessed on April 24th 2008: [http://www.ibge.gov.br/home/geociencias/default\\_p rod.shtm#HIDROGEO](http://www.ibge.gov.br/home/geociencias/default_p rod.shtm#HIDROGEO), 2003.
- Illangasekare, T.H., and Morel-Seytoux, H.J.: Design of a physically-based distributed parameter model for arid-zone surface-groundwater management, *J. Hydrol.*, 74, 213–232, 1984.
- Ivkovic, K.M.: A top-down approach to characterise aquifer-river interaction processes, *J. Hydrol.*, 365, 145–155, 2009.
- Jayawardena, A.W. and Lai, F.: Analysis and prediction of chaos in rainfall and stream flow time series, *J. Hydrol.*, 153, 23–52, 1994.
- Jayawardena, A.W., and Gurung, A.B.: Noise reduction and prediction of hydrometeorological time series: dynamical systems approach vs. stochastic approach, *J. Hydrol.*, 228, 242–264 2000.
- Kantz, H., and Schreiber, T.: *Nonlinear Time Series Analysis*, 2nd Edn, Cambridge University Press, Cambridge, 2004.
- Klemeš, V.: Conceptualisation and scale in hydrology, *J. Hydrol.*, 65, 1–23, 1983.
- Kirchner, J.: Getting the right answers for the right reasons: Linking measurements, analyses, and models to advance the science of hydrology, *Water Resour. Res.*, 42, W03S04, doi: 10.1029/2005WR004362, 2006.
- Kite, G., and Pietroniro, A.: Remote sensing of surface water, in: *Remote sensing in hydrology and water management*, edited by Schultz, G., and Engman, E., Springer, Berlin, 2000.
- Knighton, A.D., and Nanson, G.C.: Flow transmission along an arid zone anastomosing river, Copper Creek, Australia., *Hydrol. Process.*, 8, 137–153, 1994.
- Komorník, J., Komorníková, M., Mesiar, R., Szökeová, D., and Szolgay, J.: Comparison of forecasting performance of nonlinear models of hydrological time series, *Physics and Chemistry of the Earth*, 31, 1127–1145, 2006.
- Konrad, C.P.: Location and timing of river-aquifer exchanges in six tributaries to the Columbia River

## References

---

- in the Pacific Northwest of the United States, *J. Hydrol.*, 329, 444–470, 2006.
- Koutsoyiannis, D., Yao, H., and Georgakakos, A.: Medium-range flow prediction for the Nile: a comparison of stochastic and deterministic methods, *Hydrolog. Sci. J.*, 53, 142–164, 2008.
- Koutsoyiannis, D.: On the quest for chaotic attractors in hydrological processes, *Hydrolog. Sci. J.*, 51, 1065–1091, 2006.
- Koutsoyiannis, D.: The Hurst phenomenon and fractional Gaussian noise made easy, *Hydrolog. Sci. J.*, 47, 573–595, 2002.
- Krause, S., and Bronstert, A.: The impact of groundwater-surface water interactions on the water balance of a mesoscale lowland river catchment in northeastern Germany, *Hydrol. Process.*, 21, 169–184, doi: 10.1002/hyp.6182, 2007.
- Kuczera, G., Renard, B., Thyler, M., and Kavetski, D.: There are no hydrological monsters, just models and observations with large uncertainties!, *Hydrol. Sci. J.*, 55, 980–991, 2010.
- Laio, F., Porporato, A., Revelli, R., and Ridolfi, L.: A comparison of nonlinear flood forecasting methods, *Water Resour. Res.*, 39, 1129, doi: 10.1029/2002WR001551, 2003.
- Lane, L.J.: Transmission losses, in: *National Engineering Handbook Section NEH-4: Hydrology*, chap. 19, 1–21, edited by: Soil Conserv. Serv., US Dep. of Agric., Washington, D.C., 1983.
- Lange, L., Leibundgut, Ch., Schwartz, U., Grodek, T., Lekach, J., and Schick, A.P.: Using artificial tracers to study water losses of ephemeral floods in small arid streams, *IAHS Publ.*, 247, 31–40, 1998.
- Lange, J., Leibundgut, C., Greenbaum, N., and Schick, A.P.: A noncalibrated rainfall-runoff model for large, arid catchments, *Water Resour. Res.*, 35, 2161–2173, 1999.
- Lange, J.: Dynamics of transmission losses in a large arid stream channel, *J. Hydrol.*, 306, 112–126, 2005.
- Li, H., Sivapalan, M., and Tian, F.: Comparative diagnostic analysis of runoff generation processes in Oklahoma DMIP2 basins: The Blue River and Illinois River, *J. Hydrol.*, doi: 10.1016/j.jhydrol.2010.08.005, in press, 2010.
- Lima, C.H.R., Frischkorn, H., and Burte, J.: Assessing river-aquifer interaction from experimental data and an analytical model (In Portuguese), *Revista Brasileira de Recursos Hídricos*, 12, 217–230, 2007.
- Liu, Q., Islam, S., Rodriguez-Iturbe, I., and Le, Y.: Phase-space analysis of daily streamflow: characterization and prediction, *Adv. in Water Resour.*, 21, 463–475, 1998.
- Littlewood, I.G., Croke, B.F.W., Jakeman, A.J., and Sivapalan, M.: The role of ‘top-down’ modelling for Prediction in Ungauged Basins (PUB), *Hydrol. Process.* 17, 1673–1679, doi: 10.1002/hyp.5129, 2003.
- Loague, K., and Van der Kwaak, J.E.: Physics-based hydrologic response simulation: platinum bridge, 1958 Edsel, or useful tool, *Hydrol. Process.*, 18, 2949–2956, doi: 10.1002/hyp.5737, 2004.
- Lorenz, E.N.: Deterministic non-periodic flows, *J. Atmos. Sci.*, 20, 130, 1963.
- Ludwig, K., and Bremicker, M. (Eds): *The water balance model LARSIM – Design, Content and Applications*, Freiburger Schriften zur Hydrologie, Freiburg, 2006.
- Malveira, V.T.C., De Araújo, J.C., and Guentner, A.: Hydrological impact of a high-density reservoir network in the semiarid north-eastern Brazil, *J. Hydrol. Eng.*, doi: 10.1061/(ASCE)HE.1943-5584.0000404, 2011.
- Mantovan, P., and Todini, E.: Hydrological forecasting uncertainty assessment: Incoherence of the GLUE methodology, *J. Hydrol.*, 330, 368–381, 2006.
- Marwan, N., Romano, M.C., Thiel, M., and Kurths, J.: Recurrence plots for the analysis of complex systems, *Physics Reports*, 438, 237–329, 2007.
- McMillian, H.K., Clark, M.P., Bowden, W.B., Duncan, M., and Woods, R.A.: Hydrological field data from a modeller’s perspective: Part 1. Diagnostic tests for model structure, *Hydrol. Process.*, 25, 511–522, doi: 10.1002/hyp.7841, 2011.
- Milewski, A., Sultan, M., Yan, E., Becker, R., Abdeldayem, A., Soliman, F., and Gelil, K.A.: A remote sensing solution for estimating runoff and recharge in arid environments, *J. Hydrol.*, 373, 1–14, doi: 10.1016/j.jhydrol.2009.04.2002, 2009.
- Miller, S.N., Guertin, D.P., and Goodrich, D.C.: Deriving stream channel morphology using GIS-based watershed analysis, in: *GIS for Water Resources and Watershed Management*, edited by:



- Lyon, J.G., Taylor and Francis, New York., 2003.
- Milzow, C., Kgotlhang, L., Bauer-Gottwein, P., Meier, P., and Kinzelbach, W.: Regional review: the hydrology of the Okavango Delta, Botswana – processes, data and modeling, *Hydrogeol. J.*, 17, 1297–1328, 2009.
- Morin, E., Grodek, T., Dahan, O., Benito, G., Kulls, C., Jacoby, Y., Van Langenhove, G., Seely, M., and Enzel, Y.: Flood routing and alluvial aquifer recharge along the ephemeral arid Kuiseb River, Namibia, *J. Hydrol.*, 368, 262–275, 2009.
- Montanari, A.: What do we mean by ‘uncertainty’? The need for a consistent wording about uncertainty assessment in hydrology, *Hydrol. Process.*, 21, 841–845, doi: 10.1002/hyp.6623, 2007.
- Mudd, S.M.: Investigation of the hydrodynamics of flash floods in ephemeral channels: scaling analysis and simulation using a shock-capturing flow model incorporating the effects of transmission losses, *J. Hydrol.*, 324, 65–79, 2006.
- Niu, G.-Y., Yang, Z.-L., Dickinson, R.E., Gulden, L.E., and Su, H.: Development of a simple groundwater model for use in climate models and evaluation with Gravity Recovery and Climate Experiment data, *J. Geophys. Res.*, 112, D07103, doi:10.1029/2006JD007522, 2007.
- Osterkamp, W.R.: Geology, soils and geomorphology of the Walnut Gulch Experimental Watershed, Tombstone, Arizona, *J. Arizona-Nevada Acad. Sci.*, 40, 136–154, 2008.
- Parissopoulos, G.A., and Wheater, H.S.: Experimental and numerical infiltration studies in a wadi stream bed, *Hydrolog. Sci. J.*, 37, 27–37, 1992.
- Porporato, A., and Ridolfi, L.: Nonlinear analysis of river flow time sequences, *Water Resour. Res.*, 33, 1353–1367, 1997.
- Porporato, A., and Ridolfi, L.: Multivariate nonlinear prediction of river flows, *J. Hydrol.*, 248, 109–122, 2001.
- Rapideye AG: Rapideye Standard Image Product Specifications, Rapideye AG, Germany, version 3.0; 54, 2010.
- Rawls, W.J., Ahuja, L.R., Brakensiek, D.L., and Shirmohammadi, A.: Infiltration and soil water movement, in: *Handbook of Hydrology*, edited by: Maidment, D.R., McGraw-Hill inc., USA, 1993.
- Refsgaard, J.C., and Hansen, J.R.: A good-looking catchment can turn into a modeller’s nightmare, *Hydrol. Sci. J.*, 55, 899–912, 2010.
- Renard, K.G.: The hydrology of semiarid rangeland watersheds, Rep. ARS-41-162, Agric. Res. Serv., US Dep. of Agric., Washington, D.C., 1970.
- Renard, K.G., Nichols, M.H., Woolhiser, D.A., and Osborn, H.B.: A brief background on the U.S. Department of Agriculture Agricultural Research Service Walnut Gulch Experimental Watershed, *Water Resour. Res.*, 44, W05S02, doi:10.1029/2006WR005691, 2008.
- Reusser, D.E., Blume, T., Schaeffli, B., and Zehe, E.: Analysing the temporal dynamics of model performance for hydrological models, *Hydrol. Earth Syst. Sci.*, 13, 999–1018, 2009.
- Rushton, K.R., and Tomlinson, L.M.: Possible mechanisms for leakage between aquifers and rivers, *J. Hydrol.*, 40, 49–65, 1979.
- Savenije, H.H.G.: Equifinality, a blessing in disguise?, *Hydrol. Process.*, 15, 2835–2838, doi: 10.1002/hyp.494, 2001.
- Savenije, H.H.G.: HESS Opinions “The art of hydrology”, *Hydrol. Earth Syst. Sci.*, 13, 157–161, 2009.
- Schmugge, T.J., Kustas, W.P., Ritchie, J.C., Jackson, T.J., Rango, A.: Remote sensing in hydrology, *Adv. Water Res.*, 25, 1367–1385, 2002.
- Semmens, D.J., Goodrich, D.C., Unkrich, C.L., Smith, R.E., Woolhiser, D.A., and Miller, S.N.: KINEROS2 and the AGWA modeling framework, in: *Hydrological Modelling in Arid and Semi-Arid Areas*, Wheater, H., Sorooshian, S., and Sharma, K. D., Cambridge Press, New York, 2008.
- Shannon, J., Richardson, R., and Thornes, J.: Modelling Event-based Fluxes in Ephemeral Streams, in: *Dryland Rivers: Hydrology and Geomorphology of Semi-Arid Channels*, edited by: Bull, L.J., and Kirkby, M.J., John Wiley & Sons, Chichester, England, 2002.
- Sharma, K.D., and Murthy, J.S.R.: Estimating transmission losses in an arid region – a realistic approach, *J. Arid Environ.*, 27, 107–113, 1994.
- Sharma, K.D., Murthy, J.S.R., and Dhir, R.P.: Streamflow routing in the Indian Arid zone, *Hydrol. Process.*, 8, 27–43, 1994.
- Shentsis, I., and Rosenthal, E.: Recharge of aquifers by flood events in an arid region, *Hydrol. Process.*,

## References

---

- 17, 695–712, doi: 10.1002/hyp.1160, 2003.
- Shentsis, I.: Increasing transmission losses from flood events due to groundwater extraction, *Hydrol. Process.*, 17, 713–725, doi: 10.1002/hyp.1161, 2003.
- Sivakumar, B., Berndtsson, R., and Persson, M.: Monthly runoff prediction using phase space reconstruction, *Hydrol. Sci. J.*, 46, 377–387, 2001.
- Sivakumar, B., Jayawardena, A., and Fernando, T.M.K.G.: River flow forecasting: use of phase-space reconstruction and artificial neural networks approaches, *J. Hydrol.*, 265, 225–245, 2002.
- Sivapalan, M., Blöschl, G., Zhang, L., and Vertessy, R.: Downward approach to hydrological prediction, *Hydrol. Process.*, 17, 2101–2111, doi: 10.1002/hyp.1425, 2003a.
- Sivapalan, M., Takeuchi, K., Franks, S.W., Gupta, V.K., Karambiri, H., Lakshmi, V., Liang, X., McDonnell, J.J., Mendiondo, E.M., O’Connell, P.E., Oki, T., Pomeroy, J.W., Schertzer, D., Uhlenbrook, S., and Zehe, E.: IAHS Decade on Predictions in Ungauged Basins (PUB), 2003–2012: Shaping an exciting future for the hydrological sciences, *Hydrol. Sci. J.*, 48, 857–880, 2003b.
- Sivapalan, M.: The secret to ‘doing better hydrological science’: change the question!, *Hydrol. Process.*, 23, 1391–1396, doi: 10.1002/hyp.7242, 2009.
- Smith, R.E., Goodrich, D.C., Woolhiser, D.A., and Unkrich, C.L.: KINEROS - A kinematic runoff and erosion model, in: *Computer Models of Watershed Hydrology*, Water Resources Pub., edited by: Singh, V.J., Highlands Ranch, Colorado, 1995.
- Sophocleous, M.: Interactions between groundwater and surface water: the state of the science, *Hydrogeol. J.*, 10, 52–67, doi: 10.1007/s10040-001-0170-8, 2002.
- Soulsby, C., Neal, C., Laudon, H., Burns, D.A., Merot, P., Bonell, M., Dunn, S.M., and Tetzlaff, D.: Catchment data for process conceptualization: simply not enough?, *Hydrol. Process.*, 22, 2057–2061, doi: 10.1002/hyp.7242, 2008.
- Spangler, D.P.: A geophysical study of the hydrology of the Walnut Gulch Experimental Watershed, Tombstone, Arizona, PhD Dissertation, Dept. of Geology, Univ. of Arizona, Tucson, 103 pp., 1969.
- Stone, J.J., Nichols, M.H., Goodrich, D.C., and Buono, J.: Long-term runoff database, Walnut Gulch Experimental Watershed, Arizona, United States, *Water Resour. Res.*, 44, W05S05, doi: 10.1029/2006WR005733, 2008.
- Takens, F.: Detecting Strange Attractors in Turbulence, in: *Lecture notes in Mathematics*, edited by: Rang, D., and Young, L.S., Springer, Berlin, 1980.
- Tamea, S., Laio, F., and Ridolfi, L.: Probabilistic nonlinear prediction of river flows, *Water Resour. Res.*, 41, W09421, doi: 10.1029/2005WR004136, 2005.
- Tetzlaff, D., Uhlenbrook, S., Eppert, S., and Soulsby, C.: Does the incorporation of process conceptualization and tracer data improve the structure and performance of a simple rainfall-runoff model in a Scottish mesoscale catchment?, *Hydrol. Process.*, 22, 2461–2474, doi: 10.1002/hyp.6841, 2008.
- Todini, E.: Role and treatment of uncertainty in real-time flood forecasting, *Hydrol. Process.*, 18, 2521–2746, 2004.
- Todini, E.: Hydrological catchment modelling: past, present and future, *Hydrol. Earth Syst. Sc.*, 11, 468–482, 2007.
- Van Dam, J.C., and Feddes, R.A.: Numerical simulation of infiltration, evaporation and shallow groundwater levels with the Richards equation, *J. Hydrol.*, 233, 72–85.
- Van Oel, P., Krol, M., Hoekstra, A., de Araújo, J.C.: The impact of upstream water abstractions on reservoir yield: the case of the Orós Reservoir in Brazil, *Hydrol. Sci. J.*, 53, 857–867, 2008.
- Von Dijk, A.I.J.M., Renzullo, L.J.: Water resource monitoring systems and the role of satellite observations, *Hydrol. Earth Syst. Sc.*, 15, 39–55, 2011.
- Van Kampen, N.G.: *Stochastic Processes in Physics and Chemistry*, 2nd Edn, North Holland, Amsterdam, 1992.
- Wenninger, J., Uhlenbrook, S., Lorentz, S., and Leibundgut, C.: Identification of runoff generation processes using combined hydrometric, tracer and geophysical methods in a headwater catchment in South Africa, *Hydrol. Sci. J.*, 53, 65–80, 2008.
- Werner, P.C., and Gerstengarbe, F-W.: The climate of Piauí and Ceará, in: *Global Change and Regional Impacts* edited by: Gaiser, T., Krol, M., Frischkorn, H., De Araújo, J.C., Springer Verlag, Berlin, 81–86, 2003.

Wheater, H., Sorooshian, S., and Sharma, K.D. (Eds): *Hydrological Modelling in Arid and Semi-Arid Areas*, Cambridge Press, New York, 2008a.

Wheater, H.: Modelling hydrological processes in arid and semi-arid areas: an introduction, in: *Hydrological Modelling in Arid and Semi-Arid Areas*, Wheater, H., Sorooshian, S., and Sharma, K. D., Cambridge Press, New York, 2008b.

Xavier, T.M.B.S.: *Time for Rainfall: Climatological and Forecasting Studies for Ceará and Northeast* (In Portuguese), ABC Editora: Fortaleza, Ceará, Brazil, 2001.

Xie, Z., and Yuan, X.: Prediction of water table under stream-aquifer interactions over an arid region, *Hydrol. Process.*, 24, 160–169, doi: 10.1002/hyp.7434, 2010.

Young, P.: Top-down and data-based mechanistic modelling of rainfall-flow dynamics at the catchment scale, *Hydrol. Process.*, 17, 2195–2217, doi: 10.1002/hyp.1328, 2003.

## Acknowledgements

First of all, I would like to thank very much my main supervisor Axel Bronstert for the valuable scientific discussion, the indispensable advice during my PhD, the necessary funding and the very pleasant work environment since my first day at the University of Potsdam.

My sincerely thanks to my second supervisor José Carlos de Araújo, who provided me with all facilities to carry out this research in Brazil and contributed significantly to the improvement of this thesis.

I would also like to express my gratitude to Saskia Förster, Boris Schröder, Udo Schwarz, David Kneis, Eunice M. de Andrade, Helba Araújo, Ana Célia, Till Francke and Thomas Graeff for the scientific cooperation during this PhD.

I profoundly thank for the technical support of Andreas Bauer, Daniel Bazant, Markus Morgner, Hauke Sattler, Jocasta Bezerra, Júnior, Júlio César, Marcos, Mário, Efraim, Eliakim and Carlos Alexandre. I must also not forget to thank Sabine Schrader, Steffi Zarnack and Mrs. Horst (Uni Potsdam), Mrs. Salgado (German Academic Exchange Service) and Mrs. Rocha, Mrs. Mendes and Mrs. Krohn (Brazilian National Council for Scientific and Technological Development) for the necessary bureaucratic issues during this PhD. And many thanks to Celia Kirby for proof-reading my manuscripts!

My special thanks to SESAM and the Hydrological-Processes-AG people Andreas Güntner, Ramón Batalha, José López-Tarazón, Susanna Werth, Sandra Werb, Arlena Brosinsky and Christoph Kormann for their close co-operation.

A lot of thanks also should go to my friends and colleagues, many already aforementioned, for the enjoyable moments at the University of Potsdam: Ingmar, Peter B., Philip, Christian M., Christian G., Jan W., Stephan, Katherine, Damaris, Frank, Rubben, Loes, Theresa, Maik, Torsten, Carlos, Gabriele, Hanna, Nicole, Jan B., Cathy, Jana, Juliane, Anett, Anne-Kathrin, Jennifer, Flor, Peter V., Beate,

Alex, Sibylle, Dominik, Jenny, Nada, Frauke, Mr. Tschochner, Mr. Blumenstein and Mr. Kaden.

Special thanks to Mr. Aurino Barreto and his family for the accommodation in Iguatu City.

The experience with Gameleira community in Ceará, Brazil, was unforgettable. They provided me not only all the support necessary for the field work, but also a valuable experience of life. Therefore, I thank Sir Antônio (Tico), Hosana, Mrs. Socorro, Mrs. Leontina (*in memoriam*) and Mrs. Irací.

I thank the RapidEye Science Archive (RESA) of the German Aerospace Center (DLR) for providing the RapidEye images, also the Brazilian Geological Service (CPRM), the Brazilian Water Agency (ANA), the Meteorological and Water Resources Foundation of the State of Ceará (FUNCEME) and the Water Resources Agency of the State of Ceará (COGERH) for the data provided. Datasets were also provided by the USDA-ARS Southwest Watershed Research Center. Funding for these datasets was provided by the United States Department of Agriculture, Agricultural Research Service.

I thank the Federal Institute of Education, Science and Technology (IFCE) and the Brazilian Institute of Environment and Renewable Natural Resources (IBAMA) for the facilities during the field work in Iguatu city and in Aiuaba City, respectively.

I thank the Brazilian National Council for Scientific and Technological Development (CNPq) for the PhD-scholarship.

Finally, I would like to express my very special thanks to my wife Keylane, who patiently encouraged me to carry out this PhD and shared with me the happiness and the difficulties of living in Germany. Certainly, she and our son, Heitor, motivated me extremely during this PhD.